ΕΛΛΗΝΙΚΗ ΓΕΩΛΟΓΙΚΗ ΕΤΑΙΡΙΑ

ΕΠΙΤΡΟΠΗ ΤΗΛΕΠΙΣΚΟΠΗΣΗΣ ΚΑΙ ΔΙΑΣΤΗΜΙΚΩΝ ΕΦΑΡΜΟΓΩΝ

http://etde.space.noa.gr/

1η ΗΜΕΡΙΔΑ ΤΗΛΕΠΙΣΚΟΠΗΣΗΣ ΚΑΙ ΔΙΑΣΤΗΜΙΚΩΝ ΕΦΑΡΜΟΓΩΝ

Τετάρτη 21 Φεβρουαρίου 2018, Χαροκόπειο Πανεπιστήμιο, Ελ. Βενιζέλου (Θησέως) 70, Αθήνα

ΠΡΟΓΡΑΜΜΑ

09:00-09:30	**ΧΑΙΡΕΤΙΣΜΟΙ**
09:30-10:30	**ΟΜΙΛΙΑ ΠΡΟΣΚΕΚΛΗΜΕΝΟΥ ΟΜΙΛΗΤΗ: *Dr. Salvatore Stramondo*** *Instituto Nazionale di Geofisica e Vulcanologia (INGV), Roma, Italy* **Ground motion effects of natural disasters and anthropogenic activities from Remote Sensing: state of art, limits and perspectives**
10:30-10:50	ΔΙΑΛΕΙΜΜΑ ΓΙΑ ΚΑΦΕ - POSTER

ΕΝΟΤΗΤΑ 1 : ΕΥΡΩΠΑΪΚΕΣ - ΕΘΝΙΚΕΣ ΔΡΑΣΕΙΣ
Προεδρείο: Α. Γκανάς, Β. Χαραλαμποπούλου

10:50:11:05	**ESA's Thematic Exploitation Platforms initiative and the GEP** *Papadopoulou T., Bally P., Pacini F., Patruno J. and Foumelis M.*
11:05-11:10	**EU Earth Observation initiatives: The EuroGeoSurveys perspective** *Herrera, G., Przylucka M. and Kopackova V.*
11:10-11:20	**The Excelsior Horizon 2020 Teaming project as a tool for the Eratosthenes Research Centre to become a Centre of Excellence in Cyprus and Eastern Mediterranean region** *Hadjimitsis D.*
11:20-11:35	**Application of remote sensing methods and techniques in the Hellenic cadastre** *Lolonis P.*

ΕΝΟΤΗΤΑ 2Α : ΦΥΣΙΚΕΣ ΚΑΤΑΣΤΡΟΦΕΣ – ΓΕΩΚΙΝΔΥΝΟΙ – RADAR
Προεδρείο: Ι. Παρχαρίδης, Ο. Συκιώτη

11:35-11:50	**The July 20, 2017 M6.6 Kos (Gulf of Gökova, SE Aegean Sea) earthquake. Fault constraints exploiting space geodesy and seismology** *Elias P., Ganas A., Kapetanidis V., Valkaniotis S., Briole P., Kassaras I., Argyrakis P., Barberopoulou A., and Moshou A.*
11:50-12:05	**2003-2015 deformation history of the central Ionian islands, Greece, mapped by InSAR** *Ganas A., Elias P., Ilieva M., Dimitrov D., Briole P., Parcharidis I., Valkaniotis S., Papathanassiou G., Papastergios A., Argyrakis P., Mendonidis E. and Kollia E.*
12:05-12:20	**UAV application in documenting earthquake environmental effects and mapping geological structures. The case of November 17th 2015 M6.5 earthquake, Lefkada, Greece** *Valkaniotis S., Papathanassiou G., Grendas N., Kollia E. and Ganas A.*
12:20-13:00	ΔΙΑΛΕΙΜΜΑ – ΓΕΥΜΑ - POSTER

ΕΝΟΤΗΤΑ 3 : ΕΤΑΙΡΙΚΕΣ ΠΑΡΟΥΣΙΑΣΕΙΣ
Προεδρείο: Π. Τυρολόγου, Π. Κρασάκης

13:00-13:45	• **Tsunami monitoring technologies -** *METRICA S.A. (H. Pappas)* • **How satellite data ensure safety (TerraSAR-X, Pleiades, SPOT 6-7, WorldDEM) -** *TerraSpatium S.A.* • **SARSCAPE & OPTICALSCAPE: A real operational context for geological remote sensing applications -** *Inforest O.C.* • **Very high resolution Optical, SWIR and SAR. Single images and Platforms, in Geology and Natural disasters applications -** *Total View (V. Giavi)* • **Innovative MEMS Solutions for Space Applications -** *European Sensor Systems (E.S.S) (P. Broutas)* • **Geotech – Παρουσίαση προϊόντων** - *Geotech A.E. (I. Sofiou)*

ΕΝΟΤΗΤΑ 2Β : ΦΥΣΙΚΕΣ ΚΑΤΑΣΤΡΟΦΕΣ – ΓΕΩΚΙΝΔΥΝΟΙ – RADAR
Προεδρείο: Ι. Παρχαρίδης, Ο. Συκιώτη

13:45-14:00	**Advanced earth observation techniques applied for the study of land subsidence phenomena. The case of the Kalochori region, Thessaloniki Greece** *Loupasakis C., Raspini F., Svigkas N., Papoutsis I., Rozos D., Tsangaratos P., Moretti S., Kiratzi An., Kontoes Ch. and Adam N.*
14:00-14:15	**Multi-temporal DinSAR to detect surface deformation of the Evinos dam** *Papastergios A. and Parcharidis I.*
14:15-14:30	**Geological validation of selected InSAR results carried out by Institute of Geology and Mineral Exploration** *Stefouli M.*
14:30-14:45	**Landslide mapping using Sentinel-1 and Sentinel-2 data** *Maltezos E. and Charalampopoulou V.*
14:45-15:00	**Rheticus®: Monitoring from space geological transformations of earth surface for detecting instabilities of critical infrastructure** *Spastra Y., Bollanos S., Sykas D., Ioannou I., Lamantia C., Massimi V., Samarelli S. and Casaburi M.*
15:00-15:15	**Operational Use of Sentinel satellite and Copernicus data for Monitoring, Prevention and Restoration of Natural Hazards** *Symeonidis P., Vakkas T. and Taskaris S.*
15:15-15:35	ΔΙΑΛΕΙΜΜΑ ΓΙΑ ΚΑΦΕ - POSTER

ΕΝΟΤΗΤΑ 4 : ΧΑΡΤΟΓΡΑΦΗΣΗ - ΟΠΤΙΚΟΙ ΔΕΚΤΕΣ – ΤΕΧΝΙΚΕΣ ΕΠΕΞΕΡΓΑΣΙΑΣ
Προεδρείο: Μ. Στεφούλη, Π. Ηλίας

15:35-15:50	**Mineral mapping using Sentinel-2 imagery: the case study of the "Nisi" Fe-Ni open mine (Voiotia, Greece)** *Anifadi A., Sykioti O., Vassilakis E. and Stamatakis M.*
15:50-16:05	**Planetary Mineral Mapping using Advanced Hyperspectral Image Spectral Unmixing. Case study: the Syrtis Major area on planet Mars** *Sykioti O., Giampouras P., Rontogiannis A. and Koutroumbas K.*
16:05-16:20	**Camera Spatial Distortions in UAV-Photogrammetry: A New Correction Workflow and Software Implementation** *Argyropoulos N., Nikolakopoulos K. and Koukouvelas I.*
16:20-16:35	**Advancing ocean colour retrieval for the Hellenic Seas. *Joint efforts of Research Institutes and Academia*** *Karageorgis A., Drakopoulos P., Iona S., Kapsimalis V., Psarra S., Sofianos S., Spyridakis N., Topouzelis K. and Zervakis V.*

POSTERS

Π.1	**Mapping of the Historic "1536-1669" volcanic products of Mt. Etna through Spectral Unmixing of Hyperion Hyperspectral data** *Daskalopoulou L., Sykioti O., Koutroumbas K. and Rontogiannis A.*
Π.2	**Land cover monitoring through spectral unmixing, classification and clustering on multispectral Sentinel-2 data of Southern Pindos** *Boutsi A.Z., Daskalopoulou V. and Bouskou E.*
Π.3	**Benchmarking Supervised methods for Hyperspectral data classification** *Fokeas K.*
Π.4	**Mapping distribution and investigation of correlation between Surface Sea Temperature and Chlorophyll-a in the Mediterranean Sea** *Vasiliou N.*
Π.5	**Lake Monitoring Using State of the Art Remote Sensing Technologies** *Stefouli M. and Charou E.*
Π.6	**UAV photogrammetry for coastal areas monitoring** *Kogkas S., Kozarski D. and Nikolakopoulos K.G.*
Π.7	**Mapping terrain changes using interferometric DSM from Sentinel-1 data** *Kyriou A. and Nikolakopoulos K.*
Π.8	**Assessment of landslide susceptibility using geospatial analysis and interferometry data, in the mountainous municipalities of Nafpaktia and Karpenisi** *Krassakis P. and Loupasakis C.*
Π.9	**Investigating land subsidence phenomena by using remote sensing techniques and ground truth engineering geology investigation methods** *Tsangaratos P. , Loupasakis C. and Ilia I.*
Π.10	**A feasability study to estimate vertical deformation in the central southern margin of the Gulf of Corinth Using Digital Elevation Models** *Panoutsopoulos G., Sykioti O., Kranis H., Skourtsos Em. and Elias P.*
Π.11	**Ionospheric Anomalies prior to Recent Strong Earthquakes in Greece observed by CGPS Data** *Vlachou K.*
Π.12	**Investigation Land Susidence phenomena of the Thriassio Basin using Radar Interferometry techniques** *Kaitantzian A., Loupasakis C. and Parcharidis I.*
Π.13	**Flood Susceptibility Index (FSI). *(A new Index for mapping Flood Susceptibility via RS & GIS)*** *Stathopoulos N., Kalogeropoulos K., Polykretis Ch., Skrimizeas P., Louka P., Karymbalis E. and Chalkias Ch.*
Π.14	**Synergy of Sentinel-2 satellite data with an Unmanned Airctaft System (UAS) for Precision Agricutlture: A pilot vineyard in Greece** *Vlachopoulos O.*

Ground motion effects of natural disasters and anthropogenic activities from Remote Sensing: state of art, limits and perspectives

Stramondo S.
National Earthquake Center
Istituto Nazionale di Geofisica e Vulcanologia
salvatore.stramondo@ingv.it

Abstract

The aim of this talk is to provide an overview about the most recent outcomes in Earth Sciences, describe the role of satellite remote sensing, together with GPS, ground measurement and further data, for geophysical parameter retrieval in well known case studies where the combined approach dealing with the use of two or more techniques/datasets have demonstrated its effectiveness. Remote Sensing is a reliable technique in case of detection, investigation, analysis of surface effects due to natural and manmade activities. This is the case of mining, fluid extraction, water table exploitation, nuclear tests, urban subsidence due to urbanization.

Today the Earth Sciences have a wide availability of such remote instruments and sensors able to provide scientists with an unprecedented capability to study the physical processes driving earthquakes, volcanic eruptions, landslides, and other dynamic Earth systems. Indeed measurements from satellites allow systematic observation of the Earth surface covering large areas, over a long time period and characterized by growing sample intervals. An additional variable to put effective constraints to the role of "remote sensing" is the available satellite system. Today we may exploit the capabilities of VHR (very high resolution) SAR (Synthetic Aperture Radar) systems (COSMO-SkyMed, TerraSAR-X). Additionally, we may exploit the past generation of satellite SAR systems (from ERS to Envisat) as a "time machine" to go back and reanalyze the past; on the other side, Sentinel 1A-B missions, that are specifically addressed to the investigation of surface effects of major and medium size natural disasters, together with VHR SAR systems open new perspectives and unprecedented applications.

Some examples are shown. State of art, together with limits and perspectives making continuous progress are also discussed.

ΕΝΟΤΗΤΑ 1

ΕΥΡΩΠΑΪΚΕΣ - ΕΘΝΙΚΕΣ ΔΡΑΣΕΙΣ

Προεδρείο: Α. Γκανάς, Β. Χαραλαμποπούλου

ESA's Thematic Exploitation Platforms initiative and the GEP

Papadopoulou T.[1], Bally P.[2], Pacini F.[3], Patruno J.[4], Foumelis M.[5]

[1] *ARGANS Limited, Plymouth, UK, tpapadopoulou@argans.co.uk*
[2] *European Space Agency (ESA), Frascati, Italy, philippe.bally@esa.int*
[3]*Terradue, Roma, Italy, fabrizio.pacini@terradue.com*
[4]*RHEA Group, Frascati, Italy, j.patruno@rheagroup.com*
[5]*BRGM - French Geological Survey, Orleans, France, m.foumelis@brgm.fr*

ABSTRACT

In 2014, the European Space Agency (ESA) has started the Thematic Exploitation Platforms (TEPs) initiative, a set of R&D activities to support the use of Earth Observation (EO) by creating an ecosystem of interconnected processing environments on European footing. The Geohazards Exploitation Platform (GEP, geohazards-tep.eo.esa.int) is an activity originated by ESA in November 2015 and led by Terradue to support the geohazards community exploiting satellite EO data to assess geohazard risks. The GEP supports data storage, access and processing of many different EO resources (e.g. Synthetic Aperture Radar missions, High and Very High Resolution Optical missions); it provides hosted processing (e.g. terrain motion monitoring based on radar interferometry and stereo-optical data); it promotes and strengthens collaborative work (e.g. sharing results with the community) and community building.

The GEP has six partners engaged in pilot services with TRE Altamira, CNR-IREA, DLR, INGV, ENS-CNRS/NOA and EOST-CNRS. In particular, the Corinth Rift Laboratory pilot run by ENS-CNRS and NOA concentrates on the validation of cloud services for interferogram generation, unwrapping and multi-temporal InSAR processing, active fault characterization and terrain motion mapping. Conventional InSAR services (e.g. DIAPASON service of CNES, StaMPS service of the University of Leeds and the GAMMA service), advanced InSAR services (e.g. InSAR SBAS of CNR-IREA) and the Optical MPIC OPT service of the University of Strasbourg have been made available to the team for validation. In addition, a number of users have been granted the Early Adopter status to test the platform services or to integrate their processing chains.

The GEP primarily focuses on expert EO specialists from scientific institutes and end-users from organisations such as geological surveys or mandated Disaster Risk Management (DRM) organisations. Today, there are 62 users from more than 50 organisations, primarily Europe, and some from Asia, Africa and the Americas. Furthermore, users of the Committee on Earth Observation Satellites (CEOS) Working Group on Disasters (http://ceos.org/ourwork/workinggroups/disasters/) and the Geohazard Supersites and Natural Laboratories (GSNL http://www.earthobservations.org/gsnl.php) community have been testing and using the GEP to access or process EO data.

The GEP has been selected as the gateway for the Satellite Data Thematic Core Service of the European Plate Observing System (EPOS) and will contribute to the CEOS Geohazards Lab initiative, which is a platform with federated resources from CEOS agencies (e.g. ASI, CNES, DLR and ESA) and community partners (e.g. CNR IREA) that provides data delivery mechanisms, on-line processing tools and services and an e-collaboration environment to exploit EO data to assess geohazards and their impact. The Geohazards Lab will support primarily the CEOS and GSNL users, but also users from the entire geohazards community.
Following the successful Acceptance Review completion, the new version of the GEP is now being deployed. It offers access to on-demand hosted services (20+ chains), systematic services (8 services monitoring extended targets in a continuous fashion) and scalable infrastructure allowing parallel massive data processing. It is accessible to a base of 100 Early Adopters from user organizations involved with geohazard risk assessment.

EU Earth Observation initiatives: The EuroGeoSurveys perspective

Herrera G.[1], Przylucka M.[2], Kopackova V.[3]

[1]IGME SPA, [2] Geohazards EO,PGI, [3] Raw Materials EO, CZH

Earth Observation and Geohazards Expert Group (EOEG) is an entity of the EuroGeosurveys - EGS. The mission of EOEG is to bridge the gap between Earth Observation (EO) technological and scientific capabilities and the **delivery of harmonized pan-european information on geo-sciences** improving the operational capacity and economic capabilities of governments, institutions, organizations, businesses and individuals. EuroGeoSurveys through its members (28 Geological Surveys and 80 scientists) have a broad expertise and experience on applied EO to geo hazards, geo resources exploration, mining and environment impact assessment.

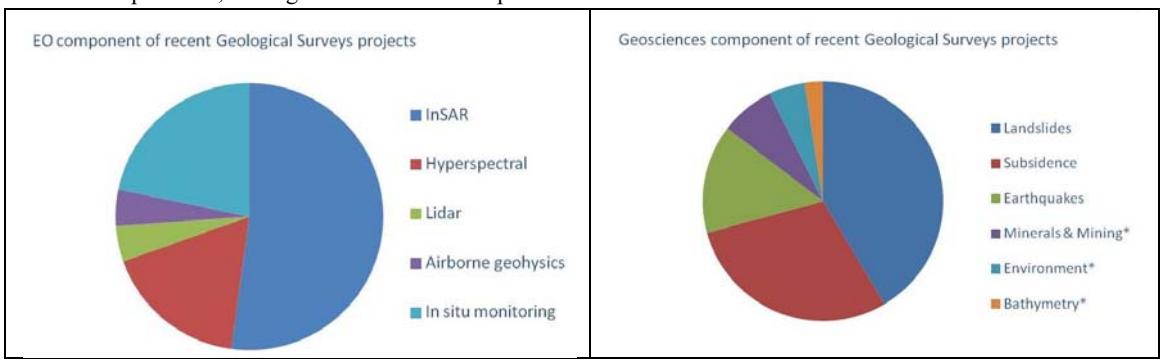

Figure 1. EO and Geosciences component within EGS project

The EOEG group shares common interest with the Committee of Remote Sensing and Space applications of the Hellenic Geological Society as both groups have as an objective to promote Earth Observation Geoscientific data and applications to all interested parties. Within this context and after the invitation by the acting as Chairman of the CRSSA-GSG IGME-GR, the Chairman of EOEG and Deputy Chairs colleagues have summarized some key activities which are of interest to the Earth Observation Community.

1. The White paper for the European Ground Motion Service (EU-GMS) that is under development within the Copernicus framework. This white paper provides an overview of the proposed European Ground Motion Service (EU-GMS). It is written primarily for the European Commission, the Copernicus Committee and User Forum and the eventual Entrusted Entity that will be entrusted with the implementation of the service. Potential end users of the service may also find this paper to be an interesting guide to the products.
2. Applications for deformation mapping and monitoring using SAR data , Figure 2.
3. Multi hazard monitoring and in situ monitoring systems, Figure 3
4. EO Mining related activities: Geological mapping, mineral mapping in mining areas, monitoring mining activities, mining risk assessment, Figure 4.

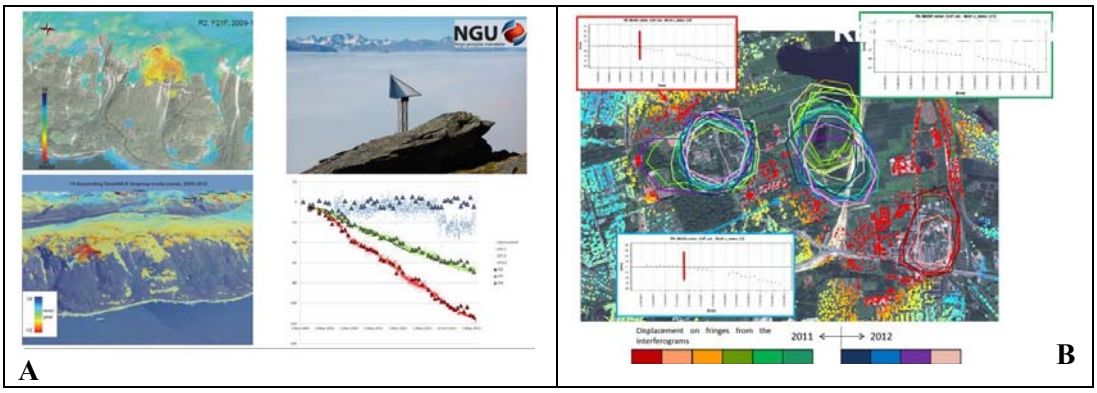

Figure 2. **A**. NGU for monitoring the state of activity of landslide phenomena **B.** Evaluating the activity of subsidence phenomena obtained within the Doris EU project

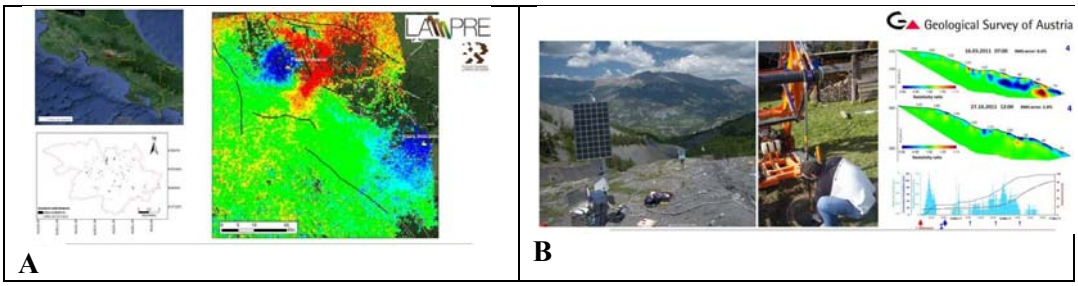

Figure 3. **A.** Multi-hazard monitoring:earthquake coseismic deformation, volcanic inflation and landslides in Costa Rica LAMPRE EU project. **B.** Coordinated in situ monitoring systems (geoelectric monitoring, inclinometric permanent displacement monitoring (DMS), GPS, piezometric sensors, soil humidity sensors, video monitoring

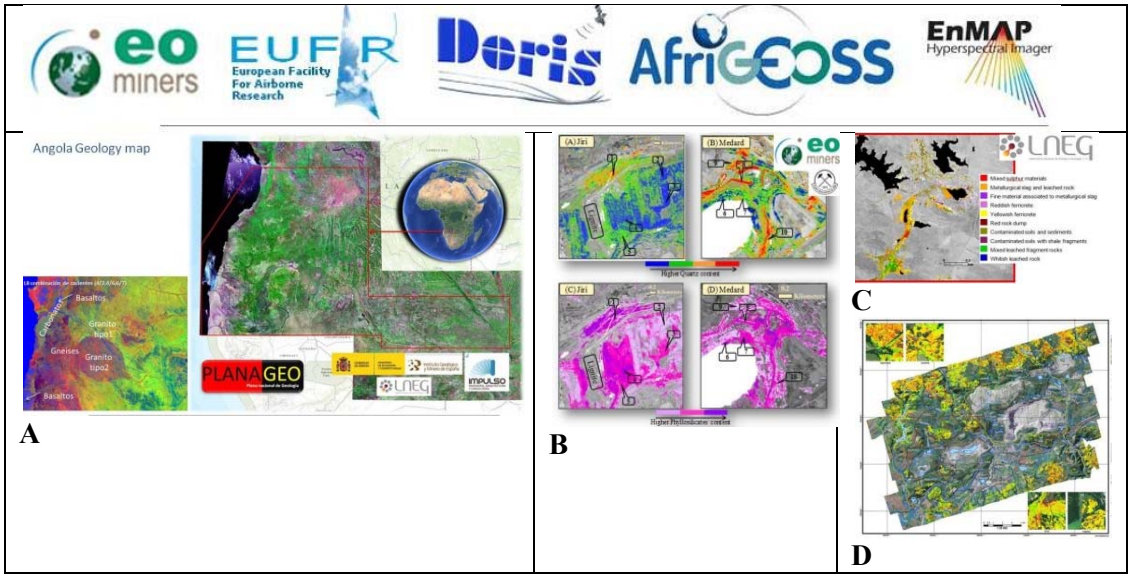

Figure 4. **A.** Angola Geolgoy map, **B.** Mineral thematic map from hyperspectral data **C.** Mining waste mapping derived from hyperspectral data **D.** Vegetation health

EOEG under EGS is also currently running other projects like GeoCradle http://geocradle.eu/en/ . Further projects are promoted as the final goal of EOEG is to develop services for the European citizens.

APPLICATION OF REMOTE SENSING METHODS AND TECHNIQUES IN THE HELLENIC CADASTRE

Lolonis P.

Hellenic Cadastre, 288 Mesogion Ave., 15562 Holargos-Athens, GREECE, plolonis@ktimatologio.gr

ABSTRACT

Although the initial design of the development and operation of the Hellenic National Cadastre was based mainly on topographic and photogrammetric data collection methods, yet, through time, there was a shift towards remote sensing methods. Indeed, even from the initial (pilot) cadastral surveying projects, topographic and photogrammetric methods gave way to remote sensing methods. In fact, orthophotomaps, black-and-white in the beginning, color later, became the main cartographic background on which the boundaries of the cadastral parcels were delineated, particularly for parcels situated in rural and mountainous areas. This approach has been used since then in all subsequent cadastral surveying projects and, in fact, has been enhanced by use of improved accuracy and quality orthophotomaps (color orthophotomaps having GSDs of 20, 25, and 50 cm). Consequently, the remote sensing methods have comprised the core methodology for the collecting the necessary cadastral spatial data and integrating them subsequently into the corresponding cadastral databases.

Besides the delineation of cadastral parcels, the aforementioned methods have been used in an extended range of large-scale projects that were directly related to the development of the Hellenic Cadastre. Specifically, those methods have been used for the compilation of "forest maps" and the determination of "forests" and "forest-like" areas in the country. Those maps, besides spatial planning, environmental protection, and natural resource exploitation, have been used as evidence in determining the land ownership status in the areas at hand. Something similar has been the case for the "shore", where the "preliminary shore line" has been delineated by the Hellenic Cadastre Authority for the entire country using photointerpretation methods on very high resolution (25 cm GSD) color orthophotomaps. That line is, currently, in the process of being administratively ratified in order to comprise the official "shore line" of the country.

In all above cases, aerial-photographic material has been used as the main input in the processes because the corresponding satellite imagery did not exist (e.g. for the case of delineating the "forests" and "forest-like" areas for the 1945 period), the available satellite images did not meet the cadastral specifications (e.g. cadastre of urban areas), or the cost of acquiring and obtaining the satellite images was higher than the corresponding cost of aerial images (e.g. cadastre of rural and mountainous areas). The only cases in which satellite imagery has been used in the Hellenic Cadastre context was the development of the system in border areas in which, due to national security issues, aerial photography was not possible.

Besides the development of the cadastre, the Hellenic Cadastral Agency has used remote sensing methods and technologies in a variety of tasks and activities on its domain. Specifically, the Agency has used satellite images to compile the CORINE Land Cover database of Greece for the years 2006 and 2012, while, currently, it is in the process of compiling that database for 2018. In addition to the CORINE Land Cover, the Agency has undertaken the task to inform regularly the competent public authorities in Greece about all new construction that takes place in the region of Eastern Attica in order to combat illegal construction and prevent infringement of public land. The detection of new construction is made through aerial photography photointerpretation and the outcomes are reported on a bi-monthly basis to the competent authorities. Finally, the Hellenic Cadastre Agency has been involved in the implementation of a Large-Scale-Demonstrator project in Athens (LDA) that aimed to examine the suitability of GNSS and Copernicus data and technologies in developing useful mobile device applications to support day-to-day operations and needs of the society.

It must be noted that use of remote sensing data and methods is not restricted only to the aforementioned applications of the cadastral domain but it extends to other related tasks and activities. Such tasks and activities are pertinent particularly after the completion of the development of the cadastre and may involve use of the widely available EU Copernicus Program to enrich and update the cadastral databases with respect to land uses and land use change. All these prospects and potential, as well as the aforementioned real large-scale implementations, would comprise the core subject of the proposed presentation and would be illustrated using examples in the conference.

ΕΝΟΤΗΤΑ 2

ΦΥΣΙΚΕΣ ΚΑΤΑΣΤΡΟΦΕΣ – ΓΕΩΚΙΝΔΥΝΟΙ – RADAR

Προεδρείο: Ι. Παρχαρίδης, Ο. Συκιώτη

The July 20, 2017 M6.6 Kos (Gulf of Gökova, SE Aegean Sea) earthquake. Fault constraints exploiting space geodesy and seismology

Panagiotis Elias(1), Athanassios Ganas(1), Vasilis Kapetanidis(2), Sotirios Valkaniotis(3), Pierre Briole(4), Ioannis Kassaras(2), Panagiotis Argyrakis(1), Aggeliki Barberopoulou(5) and Alexandra Moshou(1)

1. *National Observatory of Athens, Greece, pelias@noa.gr*
2. *National and Kapodistrian University of Athens, Greece*
3. *42131, Trikala, Greece*
4. *Ecole Normale Supérieure, Paris, France*
5. *AIR Worldwide, Boston, USA*

ABSTRACT

On July 20, 2017 22:31 UTC, a strong Mw = 6.6 earthquake occurred at shallow depth between Kos (Greece) and Bodrum (Turkey). It is the largest event in the area since the destructive April 23, 1933 Kos earthquake [3] of magnitude M_w = 6.5 [4]. The epicentre was determined near the uninhabited islet of Karaada (offshore Bodrum, SW Turkey) by the main seismic networks in the region. The focal parameters of the mainshock indicate normal faulting with nearly E-W strike, moderate dip angles and small sinistral component of slip (reported by the majority of the solutions).

We processed GNSS data (30-s sampling interval) from the following permanent networks: NOA [1], TREE (commercial provider in Greece), METRICA (commercial provider in Greece), HEPOS [2] and three CORS from Turkey (DATC, DIDI, MUG1). Additional GNSS data were provided by [5] acquired at GEOTEKNIK and other CORS-Turkey permanent stations and campaign stations. We used IW swath mode SLC images from ESA (Sentinel 1A/1B satellite data; C-band; one fringe corresponds to half wavelength, i.e. 28 mm). The SAR data were acquired every six days between June 30, 2017 and October 10, 2017 along the ascending track 131 and the descending tracks 36 and 138 of Sentinel-1. Using the ESA SNAP software and the SRTM DEM at 90 m, we produced approximately 20 pre-seismic, 70 co-seismic, and 220 post-seismic interferograms (Fig. 1). The seismic slip at depth generated up to 20 cm of ground deformation, well observed by GNSS at several stations distributed around the fault, and mapped by InSAR, especially on Karaada islet.

Additionally we proceeded first by modelling the fault parameters separately from GNSS and InSAR (ascending and descending) observations and then we derived a co-seismic fault model (Fig. 1) from joint inversion (GNSS and InSAR). According to our joint-inversion model the seismic fault activated during the 2017 earthquake dips towards North at a moderate angle of 37°, with a slip of 2.1 m, being normal with a small component of left-lateral strike-slip (Fig. 1). Our geodetic model is in agreement with published seismological data (MT solutions) and with relocated seismicity spatial distribution (about 1160 events) of aftershocks following a rigorous relocation procedure. Subsidence mapped near Bodrum coast from InSAR is consistent with the flooding observed at coastal localities according to field survey. Post-earthquake field observations mention a first negative wave motion (receding wave) also visible on the Intergovernmental Oceanographic Commission (IOC) of UNESCO tide gauge. This also agrees with the fault model proposed herein, where the dip-direction of the normal fault is pointing towards Bodrum at the north, which is located upon the hanging-wall side of the fault.

Both fault size and geometry indicate that this is a relatively young structure developed during Quaternary and represents the main source of seismic hazard in this region.

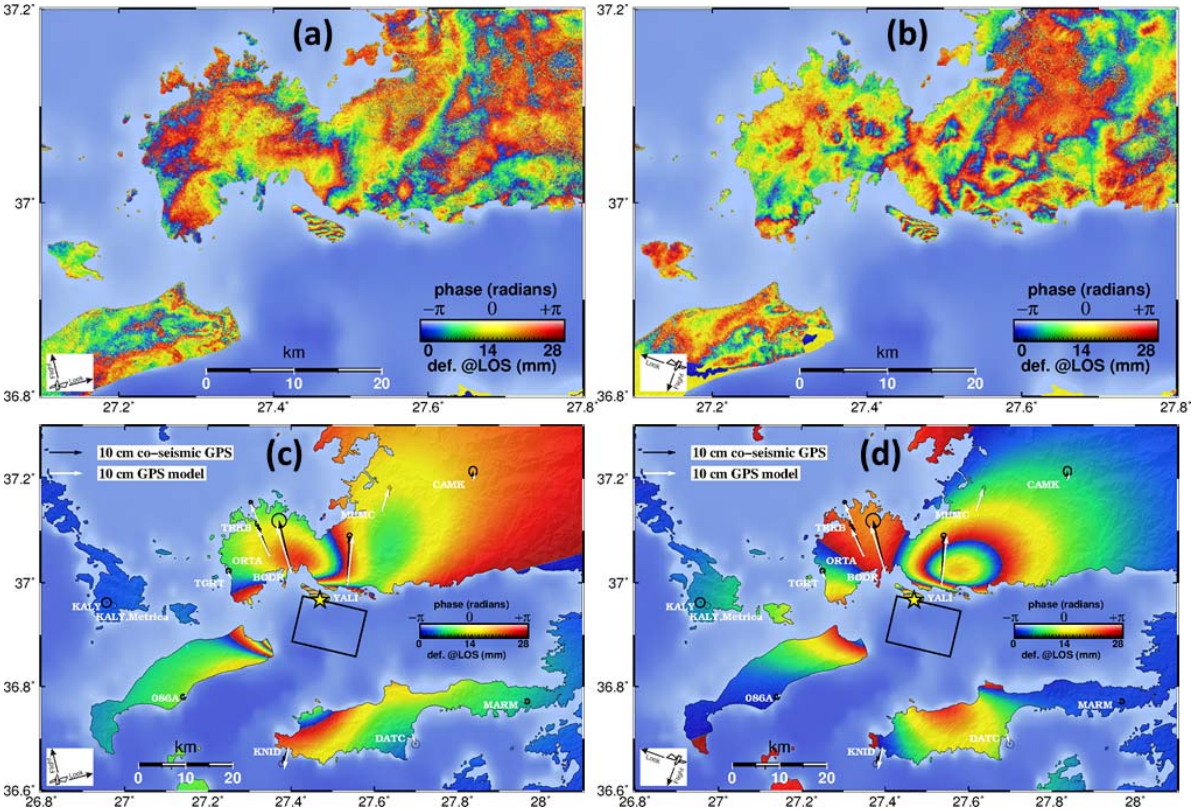

Fig. 1. (a) Best co-seismic ascending (Track 36, dated 18/7/2017 – 24/7/2017) and (b) descending (track 131, dated 12/7/2017 – 24/7/2017) interferograms and (c) and (d) the corresponding synthetic ones calculated from the modelled fault parameters. The GPS observed and modelled deformation vectors are shown. The black rectangle indicates the projected to the surface modelled fault plane. With star the earthquake epicentre (NOA) is located.

ACKNOWLEDGEMENTS

We would like to thank TREE, Metrica and CORS for the GPS data they provided and ESA for the provision of SNAP software and SENTINEL-1 acquisitions.

REFERENCES

[1] Ganas, A., Drakatos, G., Rontogianni, S., Tsimi, C., Petrou, P., Papanikolaou, M., ... & Stavrakakis, G. (2008). NOANET: the new permanent GPS network for Geodynamics in Greece. In Geophysical Research Abstracts (Vol. 10).

[2] Gianniou, M. (2015). Detecting permanent displacements caused by earthquakes using data from the HEPOS network. EUREF 2011 Symposium.

[3] Kouskouna, V., Sesetyan, K. & Stucchi, M. (2017). The Kos Earthquake of 1933: a Preliminary Study. Gruppo Nazionale di Geofisica della Terra Solida 36o Convegno Nazionale, 14-16/11/2017, TriesteGanas, A., Elias, P., Bozionelos, G., Papathanassiou, G., Avallone, A., Papastergios, A., Valkaniotis, S., Parcharidis, Is.,

[4] Makropoulos, K., Kaviris, G., & Kouskouna, V. (2012). An updated and extended earthquake catalogue for Greece and adjacent areas since 1900. Natural Hazards and Earth System Sciences, 12(5), 1425.

[5] Tiryakioğlu, İ., Aktuğ, B., Yiğit, C. Ö., Yavaşoğlu, H. H., Sözbilir, H., Özkaymak, Ç., ... & Özener, H. (2018). Slip distribution and source parameters of the 20 July 2017 Bodrum-Kos earthquake (Mw6. 6) from GPS observations. Geodinamica acta, 30(1), 1-14.

2003-2015 deformation history of the central Ionian islands, Greece, mapped by InSAR

Ganas A.[1], Elias P.[1], Ilieva M.[2], Dimitrov D.[2], Briole P.[3], Parcharidis I.[4], Valkaniotis S.[5], Papathanassiou G.[6], Papastergios A.[4], Argyrakis P.[1], Mendonidis E.[1], Kolia E.[1]

[1.] *National Observatory of Athens, Greece, aganas@noa.gr*
[2.] *Bulgarian Academy of Sciences, Sofia, Bulgaria*
[3.] *Ecole Normale Supérieure, Paris, France*
[4.] *Harokopio University, Athens, Greece*
[5.] *42131, Trikala, Greece*
[6.] *Department of Civil Engineering, Democritus University of Thrace, Greece*

ABSTRACT

During the last 15 years, four M6+ shallow, strike-slip earthquakes occurred in central Ionian Sea, one of the most seismically active areas in Europe. In chronological order, the earthquakes occurred in NW Lefkada (2003 August 14) **[1]**, in western Cephalonia (2014 January 26, 2014 February 3) **[2,3]** and SW Lefkada (2015 November 17) **[4]**. The availability of space geodesy data provided an unprecedented detail in mapping ground deformation due to seismicity in this plate boundary region. In particular, the geodetic data contributed to identifying that a) the 2003 & 2015 seismic faults run parallel to the west coast of Lefkada (along the Aegean – Apulia plate boundary) b) the 2014 seismic faults run through the Argostoli Gulf, western Cephalonia.

The earthquakes caused permanent ground deformation (mainly co-seismic), extensive damages in the central Ionian islands, and multiple ground failures, especially along their western coasts **[5,6]**. The dominant type of ground failure was a) landslides and b) liquefaction phenomena. No surface breaks due to seismic faulting were observed.

In all events, ENVISAT/ASAR, RADARSAT and SENTINEL images were used to process co-seismic interferograms. Standard SAR processing packages (*ROI-PAC, SNAP, GAMMA* etc.) were used for interferogram generation with the SRTM DEM applied in a two-pass method. Temporal decorrelation affects the signal processing because a) dense vegetation covers the central Ionian islands and b) hundreds of landslides occurred due to strong ground shaking. Vegetation is an obstacle in getting good coherence, since C-band images are used. Ground deformation, of several fringes in the line of sight of the SAR satellites, was mapped on tens of co-seismic interferograms. By inversion of the data from the observed fringes, best fitting models of the activated, strike-slip faults were calculated assuming rectangular dislocations in an elastic half space. The dislocation models also fit observed displacements of permanent GNSS stations of NOA, CNRS and private networks.

We present the fault models responsible for the observed surface deformation and discuss model limitations and constraints. Our dataset highlights the significance of space geodesy in understanding the earthquake cycle along the Cephalonia-Lefkada transform fault (CTF). In particular, it is suggested that the 2003–2015 deformation history in the Ionian Sea region indicates a) the segmented nature of the CTF b) the co-seismic uplift of Paliki Peninsula (western Cephalonia) and c) the existence of a 15-km seismic gap offshore NW Cephalonia, as well as a 8-km gap along the western coast of Lefkada (between Komilio and Kalamitsi).

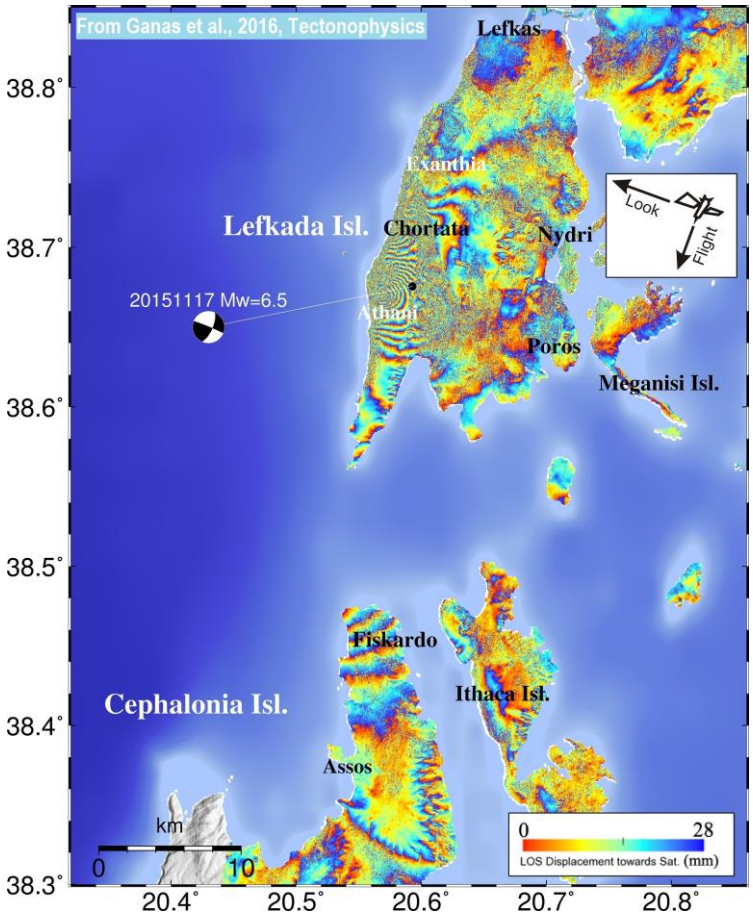

Fig. 1. Sentinel 1 A wrapped interferogram (descending orbit) of the 2015 Lefkada earthquake. Beachball indicates focal mechanism of the earthquake (GCMT solution; http://www.globalcmt.org/).

ACKNOWLEDGMENTS

This research was funded by the GSRT project INDES-MUSA http://www.indes-musa.gr/ FP6 project PREVIEW, FP7 project RASOR http://www.rasor-project.eu/, by CNRS-INSU and by ESA project (TERRAFIRMA).

REFERENCES

[1] Ilieva, M., P. Briole, A. Ganas, D. Dimitrov, P. Elias, A. Mouratidis, R. Charara, 2016. Fault plane modelling of the 2003 August 14 Lefkada Island (Greece) earthquake based on the analysis of ENVISAT SAR interferograms, Tectonophysics, 693, A, 47-65, https://doi.org/10.1016/j.tecto.2016.10.021 .

[2] Boncori Merryman John Peter, Ioannis Papoutsis, Giuseppe Pezzo, Cristiano Tolomei, Simone Atzori, Athanassios Ganas, Vassilios Karastathis, Stefano Salvi, Charalampos Kontoes, and A. Antonioli, 2015. The February 2014 Cephalonia Earthquake (Greece): 3D Deformation Field and Source Modeling from Multiple SAR Techniques Seismological Research Letters, January/February 2015, doi:10.1785/0220140126

[3] Briole, P. et al. 2015. The seismic sequence of January-February 2014 at Cephalonia Island (Greece): constraints from SAR interferometry, and GPS. Geophys. J. Int. 203, 1528–1540, doi:10.1093/gji/ggv353.

[4] Ganas, A., Elias, P., Bozionelos, G., Papathanassiou, G., Avallone, A., Papastergios, A., Valkaniotis, S., Parcharidis, Is., Briole, P. 2016. Coseismic deformation, field observations and seismic fault of the 17 November 2015 M=6.5, Lefkada Island, Greece earthquake, Tectonophysics, 687, 210–222. http://doi:10.1016/j.tecto.2016.08.012

[5] Valkaniotis S., Ganas A., Papathanassiou, G., and Papanikolaou M., 2014. Field observations of geological effects triggered by the January-February 2014 Cephalonia (Ionian Sea, Greece) earthquakes, Tectonophysics, 630, 150-157, DOI:10.1016/j.tecto.2014.05.01

[6] Papathanassiou, G., Valkaniotis S., Ganas A., Grendas, N., Kollia, El. 2017. The November 17th, 2015 Lefkada (Greece) strike-slip earthquake: Field mapping of generated failures and assessment of macroseismic intensity ESI-07, Engineering Geology, Vol. 220 pp. 13–30 http://doi:10.1016/j.enggeo.2017.01.019

UAV application in documenting earthquake environmental effects and mapping geological structures

The case of November 17th 2015 M6.5 earthquake, Lefkada, Greece

Valkaniotis S.[1], Papathanassiou G.[2], Grendas N.[3], Kolia E.[4], and Ganas A.[4]

[1.] *42131, Trikala, Greece*
[2.] *Department of Civil Engineering, Democritus University of Thrace, Greece*
[3.] *Departments of Geology, Aristotle University of Thessaloniki, Greece*
[4.] *Geodynamic Institute, National Observatory of Athens, Greece*
valkaniotis@yahoo.com, gpapatha@gmail.com, ngrendas@gmail.com, kolliaelisavet@gmail.com, aganas@noa.gr

ABSTRACT

Documentation of earthquake environmental effects (surface ruptures, landslides etc.) is a very critical issue, since based on the accuracy of the provided information, protection and mitigation measures can be designed. UAVs provide a convenient remote sensing platform for post-earthquake surveys given their ability to collect ultra-high resolution imagery in short time over terrain that is often difficult to access. Using the Structure from Motion (SfM) image processing technique, a 3D point cloud can be created by intersecting the matched features between the overlapping, offset images. Point clouds from optical images enable detailed representation of complex 3D surfaces, better editing and classification of the dataset and creation of further products like orthophotos, DSMs, DTMs, textured models etc. Comparison between different point cloud sets enables highly accurate change detection analysis, using recently developed matching algorithms.

Following the Mw=6.5 earthquake of November 17, 2015 at Lefkada island, Greece [1], we conducted a field survey in order to document earthquake environmental effects [2,3]. In addition to field measurements, we used a DJI Phantom 3 quadcopter to perform an aerial survey over specific areas of interest: Tsoukalades, Pefkoulia, Gialos, Egremnoi and Okeanos sites were surveyed in order to assess landslide damage, as well as several sites inside Athani-Dragano basin towards the study of neotectonic fault structures.

At the Okeanos site (Fig. 1; southwest of Athani village), a large landslide removed a large part of the coastal steep slope and affected a luxury villas complex. Using the point cloud dataset, we mapped in detail the landslide area and its effects inside and around the main body, such as ground fractures, plane measurements, secondary landslides and damages inside the villas complex [4]. The UAV was useful in the survey of Okeanos site, as most of the area was inaccessible. In order to perform a calculation of the volume removed as result of seismic shaking, we used a point cloud extracted from aerial stereo imagery and the two datasets were compared using CloudCompare software and the M3C2 algorithm. The Okeanos landslide covers an area of 35.000 m2 and the calculated volume of was ~90.000 m3.

The results validate the usefulness and accuracy of UAV surveys for low cost and rapid documenting and mapping earthquake environmental effects and geological structures. Accuracy and detail achieved is sufficient for most geological applications, even without the use of survey-grade ground control points. In addition, usage of point clouds and high resolution texture models can provide an accurate alternative in obtaining structural measurements along fault planes and other major structural surfaces.

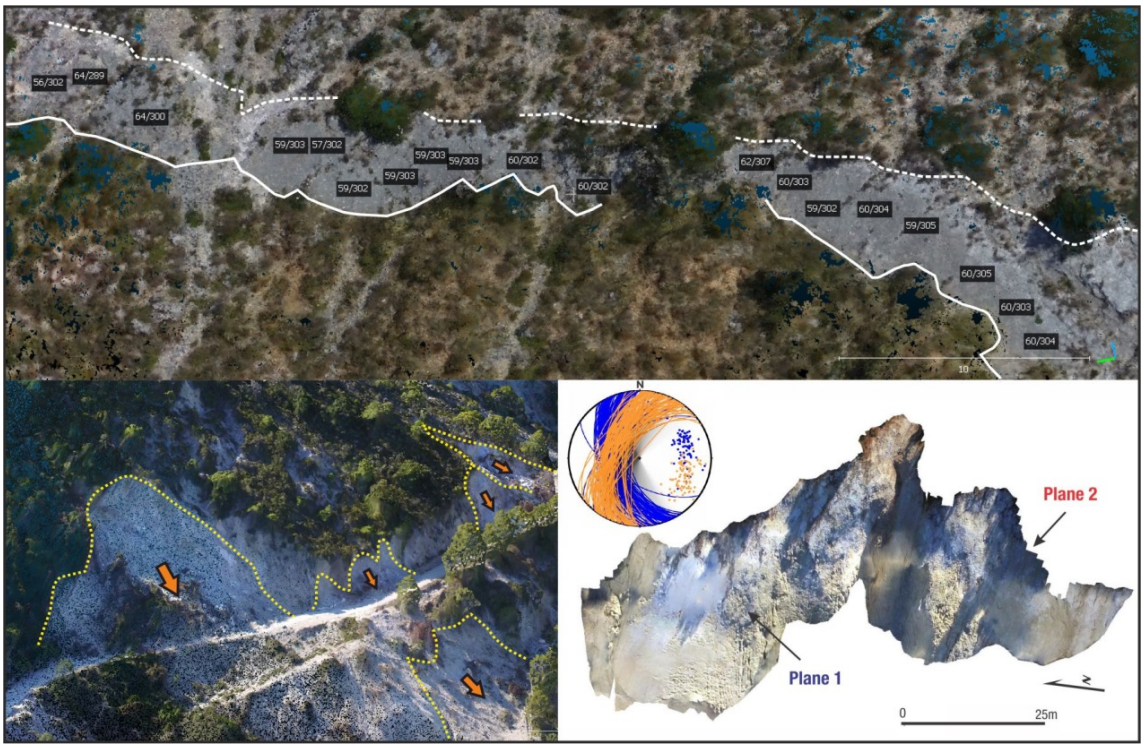

Fig. 1. Top: multiple structural measurements of the fault plane surface (dip, dip direction) using a point cloud dataset. Bottom left: a detailed point cloud dataset showing in detailed co-seismic landslides along the road to Gialos beach. Bottom right: Exposed surface of the Okeanos landslide that follows a pre-existing fault plane. A point cloud dataset obtained from a UAV survey enabled a detailed structural mapping of the slip surface that was inaccessible for field measurements.

REFERENCES

[1] Ganas, A., Elias, P., Bozionelos, G., Papathanassiou, G., Avallone, A., Papastergios, A., Valkaniotis, S., Parcharidis, Is., Briole, P. 2016. Coseismic deformation, field observations and seismic fault of the 17 November 2015 M=6.5, Lefkada Island, Greece earthquake, Tectonophysics, 687, 210–222. http://doi:10.1016/j.tecto.2016.08.012

[2] Papathanassiou, G., Ganas, A., Moshou, A. and Valkaniotis, S. 2016. Geoenviromental effects of the M=6.4 17 November 2015 earthquake on south Lefkada, Ionian Sea, Greece, Proc. of the 14th International Conference of The Geological Society of Greece, Bulletin of the Geological Society of Greece, 25-27 May 2016 Thessaloniki, http://dx.doi.org/10.12681/bgsg.11753

[3] Papathanassiou, G., Valkaniotis S., Ganas A., Grendas, N., Kollia, El. 2017. The November 17th, 2015 Lefkada (Greece) strike-slip earthquake: Field mapping of generated failures and assessment of macroseismic intensity ESI-07, Engineering Geology, Vol. 220 pp. 13–30 http://doi:10.1016/j.enggeo.2017.01.019

[4] Valkaniotis S., Ganas A. & Papathanassiou G. 2017. Using a UAV for collecting information about a deep-seated landslide in the island of Lefkada following the 17 November 2015 strike-slip earthquake (M=6.5). 19th EGU General Assembly 2017, Vienna, Austria.

Advanced earth observation techniques applied for the study of land subsidence phenomena. The case of the Kalochori region, Thessaloniki Greece

Loupasakis C.[1], Raspini F. [2], Svigkas N. [3,4], Papoutsis I.[3], Rozos D. [1], Tsangaratos P.[1], Moretti S. [2], Kiratzi An. [4], Kontoes Ch. [3], Adam N.[5]

[1] *National Technical University of Athens, Athens, Greece, cloupasakis@metal.ntua.gr, rozos@metal.ntua.gr, ptsag@metal.ntua.gr.*
[2] *University of Firenze, Italy, federico.raspini@unifi.it, sandro.moretti@unifi.it*
[3] *National Observatory of Athens, Athens, Greece, ipapoutsis@noa.gr, kontoes@noa.gr.*
[4] *Aristotle University of Thessaloniki, Thessaloniki, Greece, svigkas@geo.auth.gr, kiratzi@geo.auth.gr.*
[5] *German Aerospace Center (DLR), Bonn, Germany, Nico.Adam@dlr.de.*

ABSTRACT

Land subsidence caused by the overexploitation of the aquifers manifest with an increasing frequency in several regions of Greece. In the broader Kalochori village region, at the west side of Thessaloniki, the first signs of subsidence were recorded in 1965 in the form of a progressive marine invasion [1]. In 1969, during a period of intensive rainfall, the seawater reached the southern houses of the village, forcing the construction of embankments along the entire coastline [2]. As a result of the continuous subsidence, reaching next to the coastline maximum values of 3–4 m, the embankments were destroyed and reconstructed several times (Fig. 1A). The land subsidence phenomena continue taking place since 2004 [3,4], when sudden changes at the economic activities lead to the reduction of the water pumping and the gradual recharge of the aquifers. The aquifer recharge impressively changed the motion trend, from subsidence to uplift [5] (Fig. 1C).

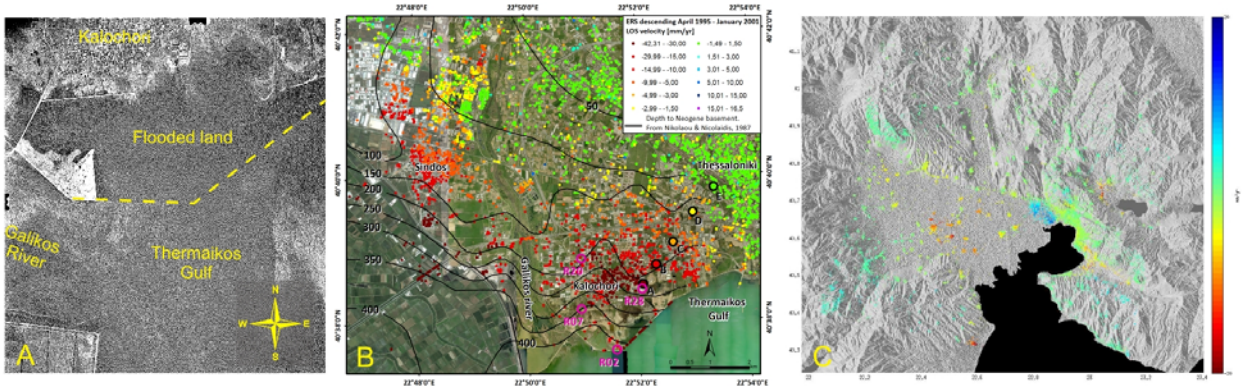

Fig. 1 A) Aerial photograph presenting the flooded area after the collapse of the embankment in 1973. B) land subsidence LOS deformation rates from ERS1/2 data (1995- 2001), C) PS results from Envisat data (2002-2010) indicating uplift due to ground water recharge.

Beside ground truth data the land subsidence trends have been also identified via multi-temporal InSAR techniques. In the framework of Terrafirma project, a set of SAR images acquired in 1995–2001 by the ESA satellites ERS1, 2 were processed with PSI technique, identifying subsiding deformation rates of roughly 4.5 cm/year [3,4] (Fig. 1B). Following research, using PSI and SBAS multi-temporal Interferometric approach, was also applied for the analysis of a 2 decades long ERS 1, 2 and ENVISAT dataset (1992 - 2010). The velocities estimated for the ERS dataset are in excellent agreement with previous studies. The intriguing output of the ENVISAT data archive (2003 - 2010) was an uplift motion trend, during the second decade (Fig. 2).

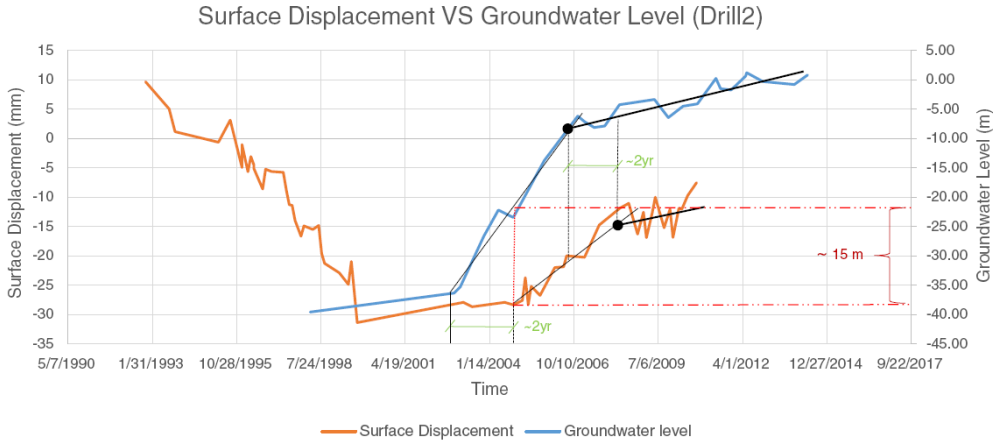

Fig.2 Graph comparing the ground water level variations at a Drill (Drill 2) with the surface deformation time series at a nearby data point produced by the SAR analysis.

REFERENCES

[1] Andronopoulos V., Rozos D., Hatzinakos I. (1991). Subsidence phenomena in the industrial area of Thessaloniki, Greece. In: Johnson, A. (Ed.). Land Subsidence, vol. 200. IAHS Publishers, pp. 59-69.

[2] Loupasakis C. & Rozos D. (2009). Finite - element simulation of land subsidence induced by water pumping in Kalochori village, Greece. Quarterly Journal of Engineering Geology and Hydrogeology, Geological Society of London, v. 42, No. 3; pp. 369-382.

[3] Raspini F., Loupasakis C., Rozos D., Adam N. and Moretti S. (2014) Ground subsidence phenomena in the Delta Municipality region (Northern Greece): geotechnical modelling and validation with Persistent Scatterer Interferometry. International Journal of Applied Earth Observation and Geoinformation, Elsevier 28: 78–89.

[4] Raspini, F., Bianchini, S., Moretti, S., Loupasakis, C., Rozos, D., Duro, J., Garcia, M., (2016) Advanced interpretation of interferometric SAR data to detect, monitor and model ground subsidence: outcomes from the ESA-GMES Terrafirma project. Natural Hazards, 83:S155–S181, DOI 10.1007/s11069-016-2341-x

[5] Svigkas N., Papoutsis I., Loupasakis C., Tsangaratos P., Kiratzi An., Kontoes Ch. (2016) Land subsidence rebound detected via multi-temporal InSAR and ground truth data in Kalochori and Sindos regions, Northern Greece. Engineering Geology, Elsevier, 209(2016): 175-186.

Multi-temporal DinSAR to detect surface deformation of the Evinos dam

Papastergios A.[1,2], Parcharidis I.[1]

[1]*Harokopio University of Athens, Department of Geography, Athens, Greece*
[2]*School of Rural and Surveying Engineering, National Technical University of Athens, Greece*

Ground motion is the surface expression of different physical phenomena like subsidence, earthquakes, landslides etc. In many cases the deformation is of anthropogenic cause (water and oil pumping, slopes undercut by roads, mining et.). Construction and operation of engineering structures and specifically of infrastructures in urban or in rural areas can be seriously affected by ground conditions leading to casualties and financial losses. Prevention, mitigation and management of these risks are of great importance.

In the last decade the detection, mapping and monitoring of ground deformation at centimeter to millimeter resolution with spaceborne SAR interferometry reached some maturity and the technique has become a very useful remote sensing tool. Interferometric SAR techniques exploit the phase difference between two or more coherent complex-valued images in order to derive path-length differences in the scale of the carrier wavelength and bellow. Moving from DInSAR to Persistent Scatterers Interferometry (Ferretti et al. 2001, Werner et. al 2003), in late nineties, obstacles related to the so-called temporal and geometric decorrelation as well as atmospheric artifacts have been overcome allowing a considerably wider spectrum of applications. This last achievement was mainly due to the plethora of data contained in the ESA-ERS and ENVISAT archive. Now days the general trend of the aerospace industry is towards SAR sensors featuring an ever increasing spatial resolution and shorter temporal sampling. Since 2014 Copernicus SAR images of Sentinel -1 offers sustainable data in terms of systematic acquisitions (temporal resolution of 6 days over Europe), open and free as well.
The Evinos Dam on the River Evinos is located close to the Agios Dimitrios (Central Greece). The Dam crest is at +516 m, 104 m above the river bed, with Full Supply Level (FSL) at +505 m. The Max Flood Level is set at 512.1 m. The Evinos Dam is an embankment dam, comprising a central vertical impermeable core with slopes 3:1, filters upstream and downstream of the core and sand -gravel shoulders with slopes of 1:2.3 upstream and 1:2 downstream. The significance of the Evinos dam concerns that water from Evinos Dam is been transferred to the Mornos Dam (some 29 km away), which is the main water supply source for Athens metropolitan area (Kotsovinos et al 2001).
During the last years, research teams apply SAR interferometry to detect and measure potential surface deformation over critical infrastructures and in this frame the earth Observation Application Team at Harokopio University/Dep. of Geography (Drakatou et al. 2014, Parcharidis et al. 2015, Neokosmidis et al. 2016).

The main objective of this study is the application of high resolution SAR interferometry in order to detect and measure the differential displacement over the Evinos dam critical infrastructure.
The data used, in order to estimate potential deformation occurred along the structure, were C band SAR scenes in ascending and descending orbits from Sentinel-1 Copernicus satellite covering the period 09/2014-12/2017. The method used is the MT-DInSAR of Permanent Scatterers. A non-linear model was applied and the results show the cumulative displacement during the previous mentioned period. The results show a maximum cumulative displacement of ~ - 9 mm in the ascending acquisition time series and a maximum cumulative displacement of ~ -13.6 mm in the descending acquisition time series along the line of sight for the whole period.

REFERENCES

Ferretti, A.; Prati, C.; Rocca, F. (2001) Permanent scatterers in SAR interferometry. IEEE Trans. Geosci. Remote Sens., 39, 8–20.

Kotsovinos N.E., Andreakou D.and Angelidis P.B., (2001). Dam break analysis of evinos earth dam: forecasting the characteristics of the downstream flood wave, XXIX IAHR Congress September 17-21, 2001, Beijing, China.

Maria-Louiza Drakatou, Christian Bignami, Salvatore Stramondo, Issaak Parcharidis (2014) Ground deformation observed at Kozloduy (Bulgaria) and Akkuyu (Turkey) NPPS by means of multitemporal SAR interferometry. Proceedings of 10th International Geographical Congress, i-xvi, 1-1866, 1337-1355.

Neokosmidis, S., Elias, P., Parcharidis, I., & Briole, P. (2016). Deformation estimation of an earth dam and its relation with local earthquakes, by exploiting multi-temporal synthetic aperture radar interferometry: Mornos dam case (central Greece). Journal of Applied Remote Sensing, 10(2) doi: 10.1117/1.JRS.10.026010.

Parcharidis, I., Foumelis, M., Benekos, G., Kourkouli, P., Stamatopoulos, C., & Stramondo, S. (2015). Time series synthetic aperture radar interferometry over the multispan cable-stayed Rio-Antirio Bridge (central Greece): Achievements and constraints. Journal of Applied Remote Sensing, 9(1) doi: 10.1117/1.JRS.9.096082

Werner, C., Wegmüller, U., Strozzi, T., Wiesmann, A., (2003). Interferometric point target analysis for deformation mapping. Proceedings of IGARSS '03 7, 4362–4364.

Geological validation of selected InSAR results carried out by Institute of Geology and Mineral Exploration

Stefouli M.
Institute of Geology and Mineral Exploration, Athens, Greece, Email: stefouli@igme.gr

In the 2000s, the development of the SAR-based interferometry allowed to observe various subsiding cases, previously not or poorly known because of low spatial resolution of the national leveling network or the too long time span between the surveys. There is an increasing interest within the geohazard community for mapping deformation e.g. slow landslides, mining, coastal subsidence, peat loss, as operational processing techniques to measure ground motion are now available (e.g. PSI, SBAS). After 2010 a lot of new case studies emerged mainly because of the development of SAR-based interferometry and the availability of free images and software. Evaluation of ground motion data by IGME started since the projects of Terrafirma and Pangeo.

In the framework of the Community Support Framework 2007-2014 - GEOCHART research project with *Title: Collection, codification and documentation of geo-thematic information for urban and suburban areas in Greece / pilot applications on Volos & Igoumenitsa cities,* a methodology for evaluating radar deformation maps has been applied. The main objective of the study is the "Geoscientific validation" of obtained radar deformation maps.

Deformation time series have been obtained for the time span 1992 – 2010 using two data sets:

- ERS 1992 – 2000 for Volos city *
- ENVISAT 2013-2010 for both Volos and Igoumentisa cities**.

In particular, ground velocities have been estimated for the cities of Volos and Igoumenitsa, Greece, as obtained from the analysis of Synthetic Aperture Radar (SAR) imagery. The displacement rates have been measured using two frames, one for each city, via the processing of ASAR/ENVISAT time series data. The data have been processed with the Persistent Scatterrers (PS) and Small Baseline Subset (SBAS) techniques using the StaMPS software. Image processing / GIS techniques have been applied using the TNTgis software. The potential correlation of InSAR measurements with results obtained by detailed geological, geophysical, hydrogeological and multi-temporal land cover change surveys is evaluated. This is essential both for the validation and the comprehensive interpretation of the underlying processes, anthropogenic or natural.
The studies reveal areas with a deformation rate above 15 mm / year in the coastal areas of both cities while deformation anomalies of smaller size occur on the mountainous area, Figure 1. The local deformation patterns are associated with both anthropogenic and natural processes. Analysis reveals that highest rates are detected on clay materials. Clayed materials could be responsible of the subsidence due to ground water level changes and or the pumping of ground waters for port extensions, or the overexploitation of aquifers, as land subsidence rates are localized in the industrial areas of both Volos / Igoumenitsa ports.

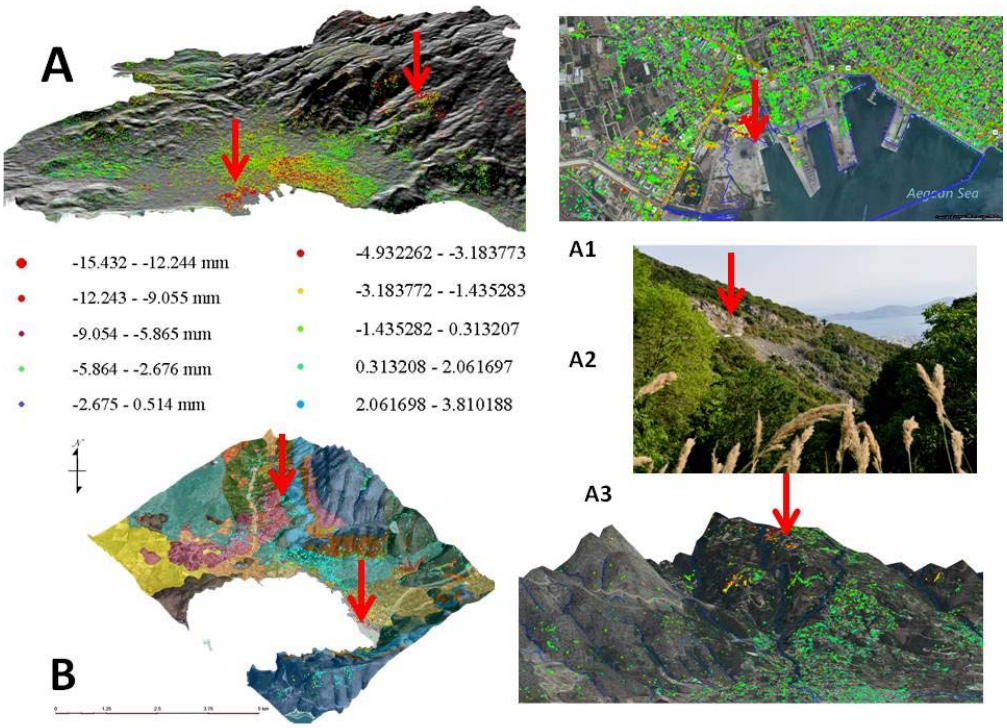

Figure 1 ***A*** *Pilot project area of Volos city. A1 Subsidence at the coastline – port area. A2 & A3 subsidence on the mountainous area of Portaria road.* ***B*** *Igoumenitsa pilot area – arrows show the location where subsidence has been mapped.*

Time series analysis of Radar data is suitable for mapping deformation in urban environments with millimeter level accuracy. Measures can be proposed for mitigation of risks for assets and the local population. Main advantages of the methodology refer to:

- A much wider and accurate quantification (space/time) of ground dynamics.
- An improvement on the various factors driving land subsidence
- Successive update of the datasets

It is indicated that collaboration needs to be established with both Geodetic Surveys for CGNSS calibration and responsible authorities for definition application of 'specific products'. It is also indicated that there is a need for more in depth studies to be carried out so as to improve the "knowledge of the underlying processes" responsible for the mapped on the SAR data deformations. It is expected the Copernicus / Sentinel data will improve the results obtained.

ACKNOWLEDGMENT

The time series data have been obtained by the *European Space Agency, the Terrafirma Project Prime, the PanGeo Coordinator and the PSI SUPLIERS and after the processing by the team of **BEYOND project of the National Observatory of Athens, Institute of Space Applications and Remote Sensing, (M. Kaskara , I.Papoutsis, H. Kontoes)

Landslide mapping using Sentinel-1 and Sentinel-2 data

Maltezos E.[1] and Charalampopoulou V.[1]

[1]*Geosystems Hellas S.A., Athens, Greece, {e.maltezos, b.charalampopoulou}@geosystems-hellas.gr*

ABSTRACT

Landslides can be triggered by natural occurrences, such as rain or earthquakes, or manufactured causes, including deforestation or excavation. Having an accurate, rapid and automated detection system can mean the difference between the ability to base decision-making on timely information or simply guessing at the level of damage resulting from the incident. For example, landslides are a constant threat in open pit mines. Monitoring the slope of mine walls and thresholds can not only aid in verifying landslides, but can also assist in predicting if and when they will occur. Timely and accurate analysis of the landslide can be invaluable in planning and executing all rescue and reparation activities in the affected areas. Such information is invaluable to anyone who monitors or makes decisions concerning mine activity.

Landslides can happen without warning, and having the data to decide next steps after they occur is imperative. With the continued emergence of free-use data such as that from the Copernicus/ESA program, decision-making has become easier. This data, with its high temporal frequency, spatial accuracy and broad coverage, provides a solid base to work from. Multimodal approaches, such as combining information from optical and radar sensors like the Sentinel-1 and Sentinel-2 satellites, can lead to improved accuracy, detection and verification of landslide phenomena. Despite the constant technological development of computer vision and space technology, the automatic landslide detection still remains challenging.

The main goal of this research is the rapid and automatic detection of large landslide phenomena using Sentinel-1 and Sentinel-2 data applying several change detection algorithms. As case study, the big landslide of the Amyntaio's mine in Greece at 10/6/2017 was selected. Four (4) change detection techniques were adopted to map the large landslide of the Amyntaio's mine. The used time series data from Copernicus/ESA program, i.e., before the landslide and after the landslide, were: 2 SAR images type IW/SLC from Sentinel-1 (4/6/2017 and 10/6/2017) and 2 optical images type MSIL2A from Sentinel-2 (1/6/2017 and 21/6/2017) (Figure 1). Concerning the Sentinel-1 data, change detection maps were extracted using the magnitude and the phase layer. On the other hand, concerning the Sentinel-2 data, change detection maps were extracted through direct image processing and machine learning using spectral information and annotated data. Figure 2 shows the workflow of the proposed processing procedure.

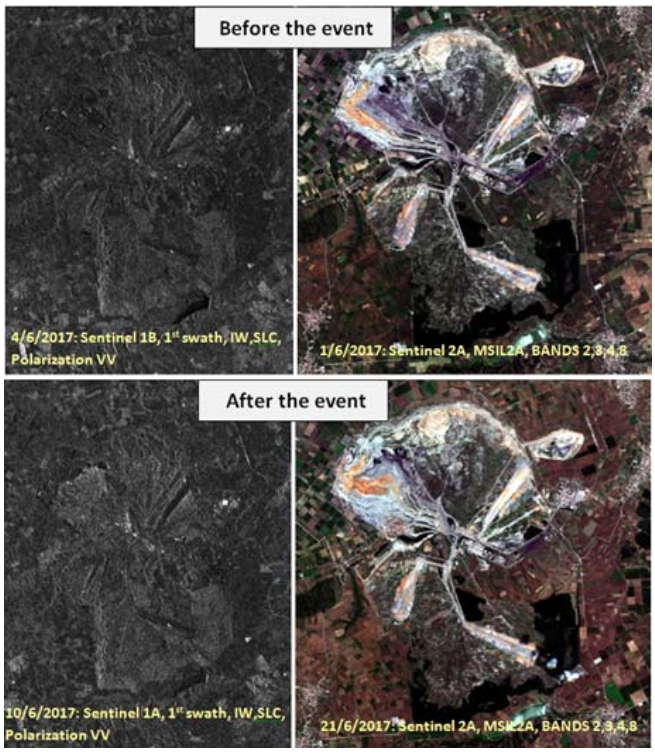

Figure 1. Used time series data from Sentinel-1 and Sentinel-2.

The landslide detection was performed via change detection techniques at ERDAS IMAGINE software (Imagine SAR Feature tool, Imagine SAR Interferometry tool, Imagine Objective tool, and Change Detection tools). The landslide was rapidly and effectively detected through operational and automatic processes. Thus, rapid and reliable conclusions can be extracted for decision making and risk monitoring.

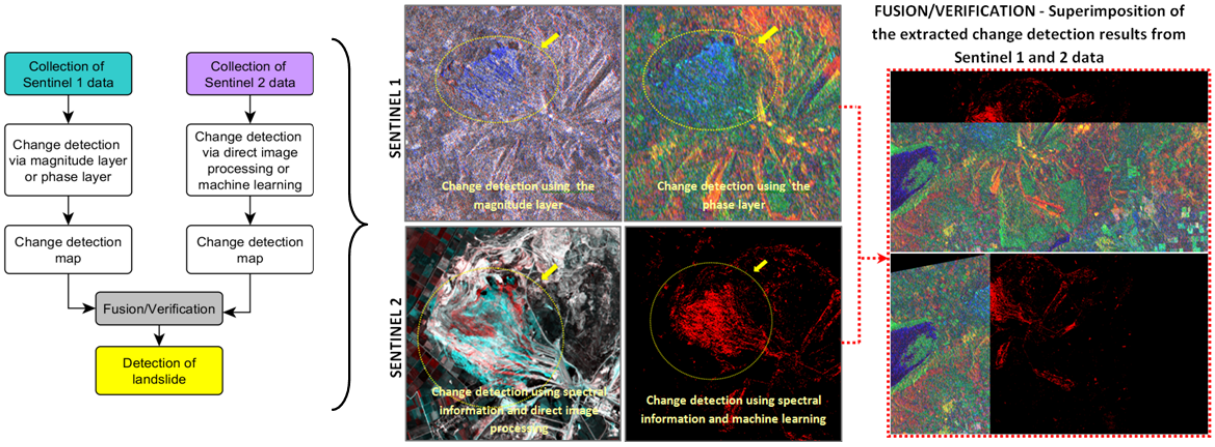

Figure 2. Change detection strategy and results using Sentinel-1 and Sentinel-2 data.

keywords: *Landslide detection, Sentinel-1, Sentinel-2, Fusion, Multi-temporal*

Rheticus®: Monitoring from space geological transformations of earth surface for detecting instabilities of critical infrastructure

Yiota Spastra*, Stelios Bollanos*, Dimitrios Sykas*, Ilias Ioannou*,
Claudio Lamantia**, Vincenzo Massimi**, Sergio Samarelli**, Mauro Casaburi**

*Planetek Hellas, 44 Kifisias Avenue, 15125 Marousi, Athens, Greece, e-mail: info@planetek.gr
**Planetek Italia s.r.l., Via Massaua 12, I-70132 Bari, Italy, e-mail: info@planetek.it

ABSTRACT

Rheticus® is the Planetek cloud-based data and services hub able to process radar and optical data from multiple open-data satellite constellations designed to continuously deliver updated geoanalytics information through complex automatic processes and minimum interaction with human beings.

"Rheticus® displacement" represents a revolutionary model concept (through subscription) in monitoring Critical Infrastructure (roads, bridges dams, water networks, pipelines etc) with the use of SAR data and the permanent scatter technique (PS), designed for users with high expectations in the value of information and its user friendliness provision.

More specifically, Rheticus® Displacement provides accurate information to monitor over time, through Multi-Temporal SAR Interferometry (MTInSAR) techniques, movements occurring across landslide features or structural weaknesses that could affect buildings or infrastructures. The availability of open data radar images acquired by the Sentinel-1 (S1) satellite mission (designed by the European Space Agency in the framework of the Copernicus programme) has fostered the implementation of a fully automatic MT-InSAR processing chain. In particular, Rheticus® browses and accesses the products of the rolling archive of ESA S1 Scientific Data Hub; S1 data are then handled by a mature running processing chain, which is responsible of producing displacement maps immediately usable to measure with sub-centimetric precision movements of coherent Persistent Scatterers.

Smart M.App 'Water Network Monitoring' is a tool of Rheticus Displacement to monitor Infrastructure stability. It was developed to simplify the analysis of the Persistent Scatterers provided by Rheticus® Displacement for a water and sewage networks providing a support to the customer for a management of the maintenance activity and inspection priority, based on ground movements measured with the Multi Temporal SAR Interferometry techniques.

In the framework of this paper will also be presented Greek and international case studies where satellite monitoring via Rheticus® was applied.

OPERATIONAL USE OF SENTINEL SATELLITE AND COPERNICUS DATA FOR MONITORING, PREVENTION AND RESTORATION OF NATURAL HAZARDS

Symeonidis P.[1], Vakkas T.[1], Taskaris S.[1]

[1] *GEOSPATIAL ENABLING TECHNOLOGIES, Athens, Greece*
[psymeonidis@getmap.gr, tvakkas@getmap.gr, *staskaris@getmap.gr]*

ABSTRACT

Aim of this paper is to present the basic functional and technological specifications of GETOPENDATA platform, a geospatial and satellite data sharing and visualization platform that was developed by GET in order to provide easy and near real time access to the Sentinel and Copernicus information and datasets. The platform can be used in different areas like precision agriculture, environmental monitoring, urban planning and safety. In this study, we focus on the use of the platform for monitoring, prevention and restoration of natural hazards like forest fires, floods and landslides.

The GETOPENDATA platform is an online web application developed using the GET SDI PORTAL, an open source software that provides rich cartographic functionalities for visualization and analysis of spatial data. The application utilizes the OGC services like WMS, WFS, WCS, CSW available in different open data repositories in order to provide catalog, view and download services.

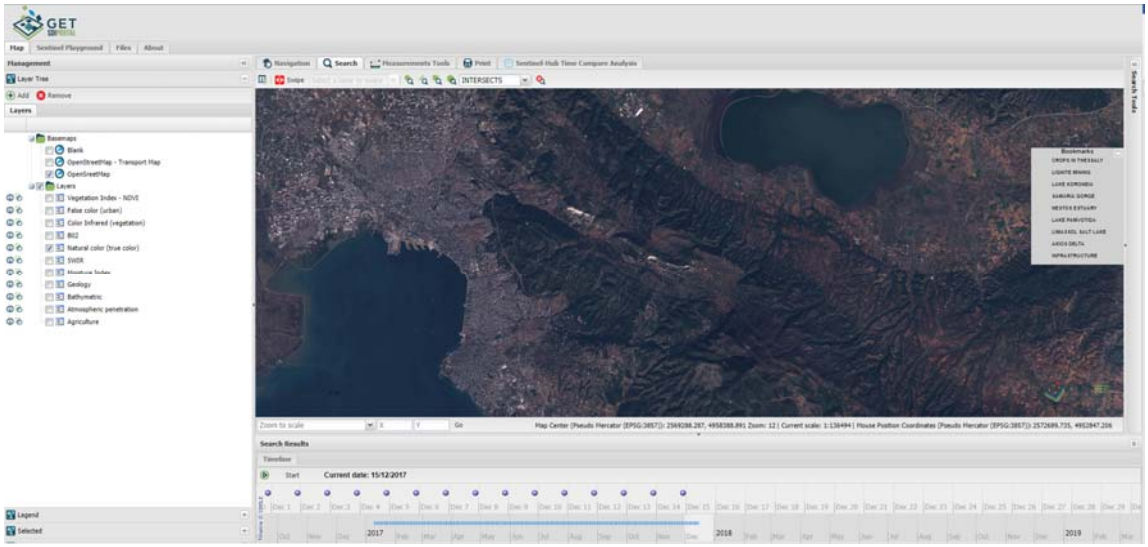

Fig. 1. The user interface of GETOPENDATA

The application provide access to satellite data using the Sentinel-Hub services by Sinergise. Among the data that are available using this service are: Sentinel 1 (GRD), Sentinel 2 (L1C, L2A), Sentinel 3 (OLCI), Landsat 5, Landsat 7, Landsat 8, MODIS, and Envisat Meris. Users can select the acquisition date for any date from the beginning of data capture until now. The platform can visualize the data as RGB composites images (true color, false color etc.) or as remote sensing indices like NDVI, EVI, LAI etc. A unique feature of the application is that the satellite data service automatically creates image mosaic from multiple satellite images / scenes based on the maximum cloud coverage parameter, provided by the user.

The platform can be used for the prevention, monitoring and restoration of natural hazards like forest fires, floods and landslides. The following images presents examples of these cases from events that occurred recently in Greece.

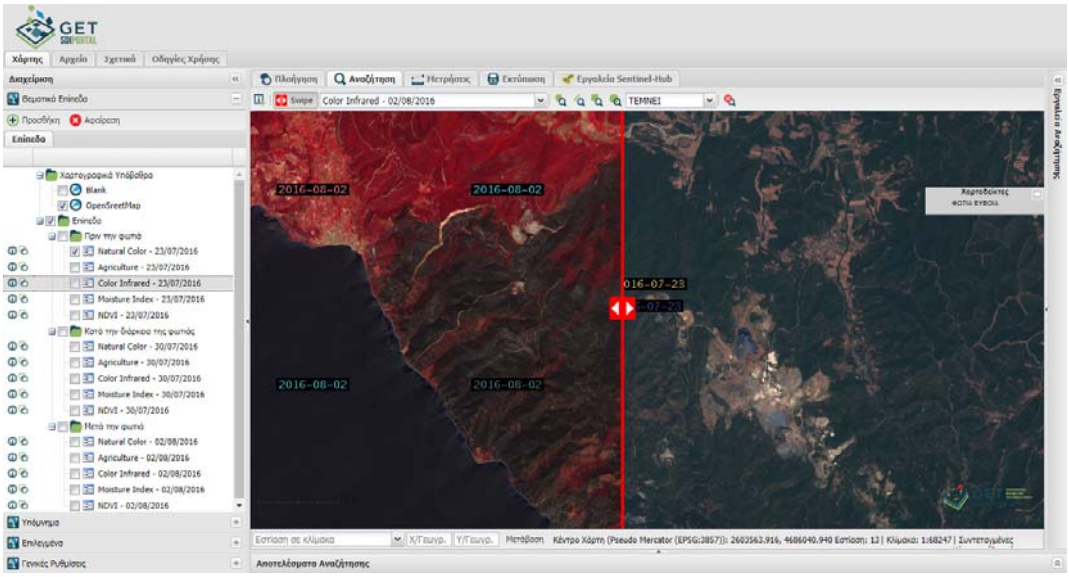

Fig. 2. Monitoring burned areas in Evia island after a forest fire occurred during the summer of 2017 (http://fires.getopendata.eu/)

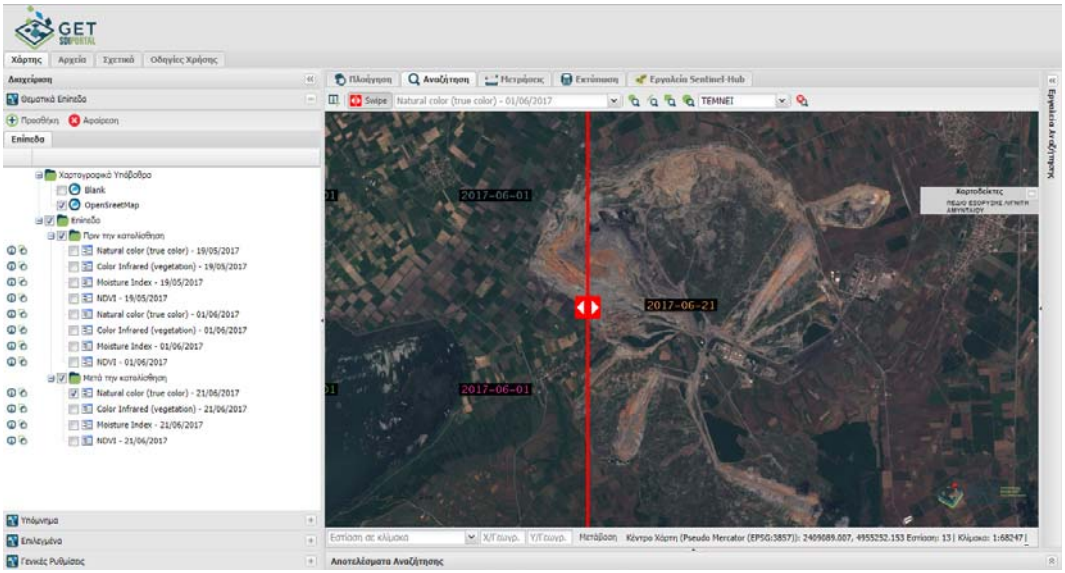

Fig. 3. Monitoring the landslide effects in the lignite center in Amyntaio, Greece (http://landslides.getopendata.eu/)

ΕΝΟΤΗΤΑ 3

ΕΤΑΙΡΙΚΕΣ ΠΑΡΟΥΣΙΑΣΕΙΣ

Προεδρείο: Π. Τυρολόγου, Π. Κρασσάκης

PLANETEK HELLAS (PKH)

Planetek Hellas is a company of the Planetek Group that since 1994, operates in the field of Science Data Exploitation, Software Development for the On Board and the Ground Segment, Earth Observation and INSPIRE compliant Spatial Data Infrastructures.

The company's applications and solutions are developed within the most important European programs in the field of space related applications and integrated satellite systems for the management, analysis and sharing of coastal and land-related information.

Planetek Hellas is based in the premises of the newly born Space Cluster in Athens, which permits to the company to have access to the most advanced technological infrastructure of now days.

Planetek Hellas has in its portfolio a variety of successful contracts with the European Commission and the European Space Agency, which allow an excellent knowledge of the European procedures and high quality requirements.

The expertise of Planetek Hellas has led the company to strengthen specific skills related to:

- Science and earth observation data management and processing for both on-board and ground deployments
    - Satellite based Near Real Time Sea Water Quality Monitoring (Chlorophyll-a concentration, Sea Surface Temperature, Water Transparency)
    - Water Turbidity at high resolution
    - Harmful Algae Bloom (Red Tide) monitoring
    - Satellite Seabed and Sea Grass Mapping (Posidonia Oceanica)
    - Shallow Waters bathymetry
    - Satellite Coastline Monitoring
    - Coastal erosion and Restoration
    - Coastal Land Use (Mangrove mapping)
    - Census and classification of Coastal Work
    - Oil and Gas Implantation monitoring
    - Near-shore dredging / excavation works
    - Pipeline movement detection (Sewage and Water pipe network monitoring)
- Data fusion procedures for Science/EO added value products and service deliveries

ΘΕΜΑ : Η πορεία της εταιρίας και τα συναφή ενδιαφέροντα σε θέματα Τηλεπισκόπησης
Ομιλητής : Σοφία Φυδάνη

GEOSYSTEMS HELLAS (GSH): Η Geosystems Hellas A.E., www.geosystems-hellas.gr, ιδρύθηκε το Νοέμβριο του 2009 και είναι το πιο πρόσφατο μέλος του Ευρωπαϊκού ομίλου GEOSYSTEMS EU GROUP, www.geosystems-group.eu. Δραστηριοποιείται στην Ελλάδα και στην Κύπρο ως Sole Authorized Distributor των λογισμικών λύσεων της Hexagon Geospatial σε desktop και Enterprise Solutions και σε εφαρμογές Smart M.Apps®, ως Sole Reseller COMNAV GPS solutions και intergraded systems και σαν σύμβουλος σε έργα γεωγραφικών πληροφοριακών συστημάτων, φωτογραμμετρίας, τηλεπισκόπησης και έρευνας και ανάπτυξης. Η GSH έχει επίσης και την εμπορική δραστηριότητα και δραστηριότητα υπηρεσιών λήψης δεδομένων αερομεραφερόμενων εικόνων και LiDAR στο επίπεδο συνεργασίας της με την Hexagon Geosystems - Airborne Systems. Η εταιρία έχει τρία τμήματα : α) εμπορικό, β) ανάπτυξη εφαρμογών και υπηρεσιών, γ) R & D.
Η Geosystems Hellas έχει αποκτήσει σημαντική εμπειρία σε συστήματα διαχείρισης γης και έχει επεκταθεί σε τεχνολογίες Decision Support Systems και Geospatial Smart/Safe Cities solutions με πελατολόγιο στην Ελλάδα. Με τη συμμετοχή της στην υλοποίηση έργων με έμφαση στην ανάπτυξη εφαρμογών φωτογραμμετρίας, τηλεπισκόπησης, στη συλλογή και επεξεργασία γεωγραφικών δεδομένων, στη διαχείριση δεδομένων airborne LiDAR και ψηφιακών αεροφωτογραφιών, στο σχεδιασμό γεωγραφικών βάσεων δεδομένων και στη συλλογή δεδομένων πεδίου έχει αναπτύξει εκτενές πελατολόγιο στην Ελλάδα και στην Κύπρο. Εστιάζοντας σε Remote Sensing και photogrammetry applications, Big Data, Data Fusion και Data Analytics techniques, Airborne Lidar 3D monitoring techniques και συναφή applications, GIS/WebGIS, Imagery data production και standardization και έχει χαράξει μια επιτυχή πορεία βασιζόμενη στην τεχνογνωσία του ανθρώπινου δυναμικού της, το οποίο έχει παρουσία στον χώρο πάνω από 20 χρόνια και εστιάζει στις ανάγκες του επαγγελματία, παρέχοντας ποιοτικές, σύγχρονες και αποδοτικές λύσεις προσθέτοντας αξία στο έργο του.
Η Geosystems Hellas είναι μέλος της ΕΒΙΔΙΤΕ και χρηματοδοτούμενο μέλος της πρώτης φάσης του του si-cluster. Είναι ενεργό μέλος του EARSC και στελέχη της εταιρίας συμμετέχουν σε διάφορα working groups του EARSC αλλά και της ESA.
Συνεργάζεται με εταιρίες και Ινστιτούτα / Εκπαιδευτικά Ιδρύματα εκτός και εκτός χώρας, αξιοποιώντας έτσι την τεχνογνωσία της στους τομείς της φωτογραμμετρίας, τηλεπισκόπησης, WebGIS, ανώτερης γεωδαισίας και του περιβάλλοντος. Η εταιρία θεωρεί ότι οι υγιείς συνεργασίες αποτελούν μοχλό ανάπτυξης και εξέλιξης.

GEOSYSTEMS-HELLAS A.E.: 88A Ginossati – GR 14452 Metamorfosi – Athens – Greece

Branch : 48 Konstantinoupoleos str., HELLAS SAT Building, Nisiza Place, Karelas, Koropi, GR 19400, T. +30 210 2846144 -145 | F. +30 211 7801508

E-mail : mail@geosystems-hellas.gr – web : www.geosystems-hellas.gr

- Spatial Data Infrastructure Platform for delivery, dissemination and exploitation of geospatial products with a strong competence in INSPIRE compliant web deployments.

The experience in providing Geoinformation solutions (Earth Observation & Spatial Data Infrastructure) and the collaboration with ESA and EC, makes the company a provider of specific technologies, needed to receive and process the satellite data acquired by the spacecrafts instruments.

The company is able to provide solutions and systems to archive, disseminate, publish and share the generated products as well as engineering consulting services for new missions definition, feasibility studies, and definition and implementation of software system architecture, requirements specification and design.

Very high resolution Optical, SWIR and SAR. Single images and Platforms, in Geology and Natural Disasters applications.

Giavi Vasiliki[1]

TotalView, Athens, Greece, vgiavi@totalview.gr

Current achievements in satellite technology provides scientific and business community, unique and unprecedented tools to explore and create more-better-faster results. More satellites, better sensors, shorter revisit time, easier access, faster and richer processing, easier and simpler delivery, collaboration and integration are the driving forces in today's demanding environment.

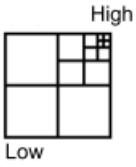

Advances in **spatial resolution** brings **30cm resolution** at reception in nadir from DigitalGlobe's WorldView 3 & 4 satellites. These are the only commercially available satellites that can achieve Zoom Level 19, as defined from Bing Maps and Google Earth.

DigitalGlobe's WorldView3 satellite is the first very high spatial resolution, **super-spectral satellite**, with **16 bands covering Visible, NIR, and SWIR** parts of the sun spectrum.

- Eight Multispectral bands: Coastal Blue, Red, Green, Blue, Red Edge, Near Infrared 1, Near Infrared 2, Yellow
- Eight Shortwave Infrared bands (SWIR)
- Twelve CAVIS (Cloud, Aerosol, Water-Vapor, Ice, Snow, Atmospheric Calibration Instrument)

WorldView-3's spectral bands allow for unique mineral identification and chemical measurements. While the geology and mining industries spend millions of dollars to identify potential mining sites during their exploration phase, WorldView-3 SWIR data can cut costs and increase efficiency by narrowing the potential area before field verification is planned. Non-visual imagery (i.e. what humans cannot see) will become a new standard for imagery information extraction and insight derivation.

The current focus in satellite imagery tasking is collaboration. Creating satellite constellations, combining sensors from the same company, or from other providers (free or commercial) under a common platform is the best way to achieve the **more and faster** target. Planet has more than 175 micro satellites that provides new images of the whole planet every day. Digitalglobe plans to launch the Legion constellation of 6 to 12 satellites with 30cm resolution and 4 bands and Scout constellation with 30min revisit time at 80cm minimum resolution. In cases of natural disasters, the benefits could be enormous.

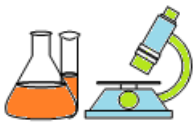

One of the side-effects of this data-plethora is the new horizons opening from exploitation tools and techniques such as big-data and machine learning. More than 100 TB soon will be the daily amount of data collected from satellite providers. Only DigitalGlobe's data are close to 100PB (PetaBytes) and increase 10PB every year. Amazon Web Services (AWS) is a key enabler in this model. The current best practice is to process and extract actionable insights at the source of data. **Platforms** from Planet and Digitalglobe gives the ability to process data with prebuild algorithms or upload yours. A marketplace is expected to be formed in the next years. Surface geology mapping, Land use classification, Flood mapping, Coastal change monitoring without downloading a single image, is possible with platforms like GBDX.

Investments (current and announced) in the commercial sector of remote sensing satellites, start-ups, emerging technologies and business models, gives a hint for the near future.

ΕΝΟΤΗΤΑ 4

ΧΑΡΤΟΓΡΑΦΗΣΗ - ΟΠΤΙΚΟΙ ΔΕΚΤΕΣ – ΤΕΧΝΙΚΕΣ ΕΠΕΞΕΡΓΑΣΙΑΣ

Προεδρείο: Μ. Στεφούλη, Π. Ηλίας

Mineral mapping using Sentinel-2 imagery: the case study of the "Nisi" Fe-Ni open mine (Greece)

Anifadi A.[1,2], Sykioti O.[3], Vassilakis E.[1], Stamatakis M.[1]

[1]*National & Kapodistrian University of Athens, Department of Economic Geology & Geochemistry, Faculty of Geology & Geoenvrionment, University Campus- Zografou Athens, GR-15784, aanyfant@geol.uoa.gr, stamatakis@geol.uoa.gr, evasilak@geol.uoa.gr*
[2] *LARCO G.M.M. S.A. alexandra.anifanti@larco.gr*
[3]*Institute for Astronomy, Astrophysics, Space Applications & Remote Sensing, National Observatory of Athens, Vas. Pavlou & I. Metaxa, Penteli, GR-15 236, sykioti@noa.gr*

The aim of this study is to investigate the potential of Sentinel-2 imagery in mineral mapping and in particular, suitability for identifying and mapping laterization minerals at the "Nisi" Fe-Ni open mine (Greece).

The Nisi open mine is located in Neo Kokkino (Boiotia, Greece) as shown in Fig.1. The area has been investigated for laterite ores by LARCO GMM S.A. and currently operates as a Ni laterite open mine. The laterization develops in the form of lenses on the paleokarst surface of Jurassic limestones. The Ni laterite ore is conformably overlain, by Cretaceous limestone and is characterized, by alternating layers of iron ore with a wide range of stone blocks. The Nisi deposit has lenticular form, composed of bauxite and/or Fe-Ni laterite ore. The eastern lens of the field is characterized by the presence of Ni laterite in the lower part and bauxite in the upper part. This particular form is present only in the specific deposit in which bauxite coexists with Fe-Ni ore [1], [5].

Figure1. Digitized geological map of the study area (red rectangle) extracted from [2]. On the upper left inset, the red circle indicates the location of the study area in mainland Greece.

A Sentinel-2A image of 28 June 2017 was used for the purpose of this study. The image was atmospherically corrected using ESA's SNAP toolbox. After the correction, ten spectral bands with 10m spatial resolution were retained for further processing. An additional georeferencing accuracy control was performed by using GPS measurements in the field.

The image was classified by using the Spectral Angle Mapper (SAM) method. This is a physically-based spectral classification that generally uses an n-D angle to match pixels to reference spectra. The algorithm determines the spectral similarity between two spectra by calculating the angle between the spectra and treating them as vectors in a space with dimensionality equal to the number of bands. SAM compares the angle between the endmember spectrum vector and each pixel vector in n-D space. Smaller angles represent closer matches to the reference spectrum. Pixels further away than the specified maximum angle threshold are not classified. In this study, the same maximum angle threshold of 0.1rad was imposed for all spectra in order to ensure that only high matches to reference spectra are retained (Fig. 2a). As reference spectra, we used selected spectra from the USGS mineral spectral library [3]. The selected minerals are compliant to the geology of the area and in particular the laterization phase namely clay minerals (smectite, chlorite, nontronite, and montmorillonite/illite), hematite, goethite and calcite. Prior to SAM, the reference spectra were re-sampled to the Sentinel-2 spectral bands. Finally, the classification map, along with the produced SAM map of each individual mineral, was imported to a GIS platform in order to produce the final detailed mining map (Fig. 2b).The final mining map depicts the presence of all classified minerals in the area.

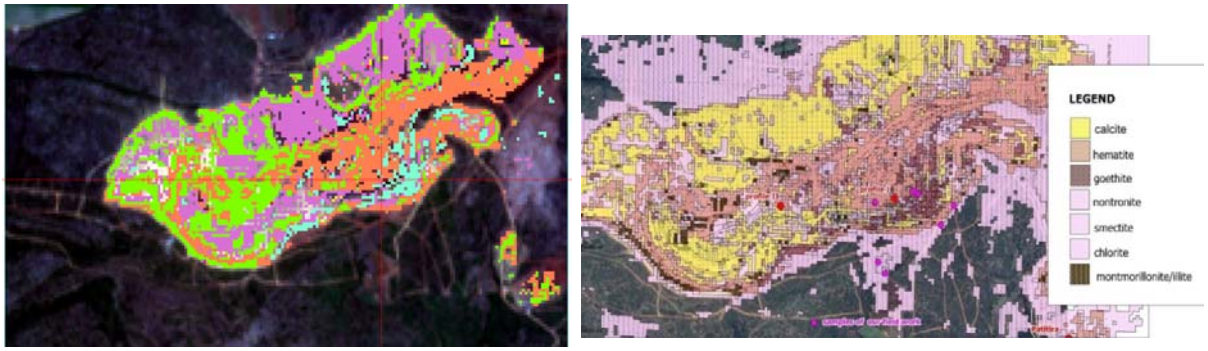

(a) (b)

Figure2. (a) SAM classification result. The mineral classes are: calcite (green), clays (smectite, chlorite, nontronite, and montmorillonite/illite) (purple), hematite (orange) and goethite (light blue). (b) The produced new mining map. The red points show locations where the phases of the ore are identified as hematite.

The classification results were successfully validated with field in situ investigations and they are in good agreement with previous studies in the area [4].

The result of this study shows the promising potential of Sentinel-2 satellite in detailed mineral mapping despite the sensor's lack of detailed spectral information, especially in the SWIR region. Further investigations will be conducted in order to assess the full potential of Sentinel-2 satellite imagery in mineral detection and mapping.

Key words: *Sentinel-2, remote sensing, Spectral Angle Mapping, mineral map, mine, laterite ores*

REFERENCES

[1] Apostolikas, A., Nickel deposit .Ioannina. Ed. Efyra, ISBN 978-960-6886-08-9, Greece, 2009.
[2] IGME, Geological Map, Sheet "VAGIA", 1:50.000, 1967.
[3] Kokaly, R.F., Clark, R.N., Swayze, G.A., Livo, K.E., Hoefen, T.M., Pearson, N.C., Wise, R.A., Benzel, W.M., Lowers, H.A., Driscoll, R.L., and Klein, A.J., USGS Spectral Library Version 7: U.S. Geological Survey Data Series 1035, 61 p., 2017. (https://doi.org/10.3133/ds1035)
[4] Kalatha, S., Economou-Eliopoulos. M., Framboidal pyrite and bacterio-morphic goethite at transitional zones between Fe–Ni-laterites and calcites: Evidence from Lokris, Greece. *Ore Geology Reviews*, 65, 413–425, 2015.
[5] Economou-Eliopoulos.M, Eliopoulos D.G., Geochemical and mineralogical characteristics of Fe-Ni and bauxitic-laterite deposits of Greece. *Ore Geology Reviews*, 16, 41-58, 2000.

Planetary Mineral Mapping using Advanced Hyperspectral Image Spectral Unmixing. Case study: the Syrtis Major area on planet Mars

Sykioti O.[1], Giampouras P.[1], Rontogiannis A.[1], Koutroumbas K.[1]

[1]*Institute for Astronomy, Astrophysics, Space Applications & Remote Sensing, National Observatory of Athens, Vas. Pavlou & I. Metaxa, GR-15 236 Penteli, Greece, sykioti@noa.gr, paris@noa.gr, tronto@noa.gr, koutroum@noa.gr*

During the last decade, hyperspectral imaging (HSI) has been extended to the field of planetary exploration. Investigating the geochemical composition and evolution of a planet is a challenging task of high scientific importance. Spectral unmixing (*SU*) is one of the most challenging problems in HSI processing. *SU* is the process of indentifying (a) pure material spectra (endmembers) that are present in an image, and (b) their corresponding fractional proportions within each pixel (abundances). This study aims to contribute to mineral mapping using *SU*, with the development of a new efficient algorithm. For this purpose, planetary HSI data were used from the OMEGA imaging spectrometer onboard ESA's Mars Express mission. The mineral mapping of the planet's surface was selected for the evaluation of the performance of the algorithm, its efficiency assessment and overall robustness. One of the areas that were used as case studies is the Syrtis Major area presented here below.

The low albedo Syrtis Major Planum is located in the boundary between the northern lowlands and southern highlands of Mars (Fig.1a). It is a Hesperian (3.7-3.0 Mya) low-relief shield volcano, [1]. The dark color comes from the basaltic volcanic composition of the region and the relative lack of dust. Recent studies show that there is a significant presence of mafic minerals (pyroxenes, olivines) and phyllosilicates, [2, 3], mainly high-Ca pyroxene (HCP) (Fig.2a). Low-Ca pyroxene (LCP) also occur in association with HCP but in the more recent volcanic deposits in Syrtis Major These occurrences are directly associated with volcanic activity of mafic, ultramafic, to perhaps picritic composition.

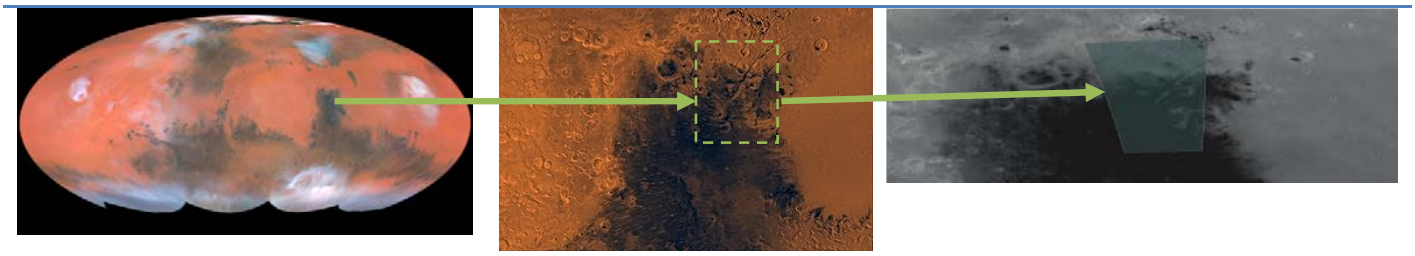

Figure 1. Location of the study area: (a) Syrtis Major Planum location on Mars, (b) study area (green rectangle), (c) footprint of the OMEGA/MEx ORB422_4 datacube.

The OMEGA/MEx ORB0422_4 datacube used in this study depicts part of the NE Syrtis Major area (Fig. 1b-c). The observation time is 20-5-2004, the scene center is Lat 20.245, Lon 74.335, the spatial resolution is 300m and the dimensions of the image are 183 x 63 pixels. The initial datacube includes two channels: (a) 128 spectral planes from 0.93 to 2.73 μm (spectral resolution 14nm) and (b) 128 spectral planes from 2.55 to 5.11 μm (spectral resolution 21nm). After exclusion of noisy bands and radiometric calibration, in order to avoid the thermal emission spectral range only 110 bands covering 0.93 to 2.73 μm were retained for further processing (Fig. 3a) The endmembers' dictionary consists of 32 spectra of minerals that are known to be present on the surface of Mars and the Moon (Fig.2b).

We assume that the measured pixel spectra are linear combinations of the 32 endmembers. We focus then on the inverse problem of abundance estimation, subject to the physical constraint of non-negativity. Besides non-negativity, recent novel studies have put forth the exploitation of sparse representations, as well as the spatial correlation in HSIs [4-6]. Sparsity implies that usually only a few endmembers contribute to each pixel's spectrum. As a result, abundance vectors shall have only a few non-zero entries. On the other hand, it has recently been shown that the *SU* results can be improved by taking advantage of the spatial correlation that inherently exists among pixels lying in homogeneous regions of an image. Hence, it is logically assumed that neighboring pixels share the same support set of contributing materials and, thus, their corresponding abundance vectors form a matrix that can be well approximated by a low-rank one, [7]. Focusing on the aforementioned notions i.e., sparsity and spatial correlation, we next perform SU in order to explore and detect chemical components lying on the Martian surface. To this end, based on the alternating direction method of multipliers (ADMM), an unmixing algorithm has been developed named Alternating Direction Sparse and Low-Rank Unmixing algorithm (ADSpLRU). ADSpLRU exploits the aforementioned properties by suitably incorporating sparsity and low-rankness in a newly derived constrained optimization problem, [8, 9].

Examples of the resulting mineral abundance maps after the application of the ADSpLRU estimator are displayed in Fig.3b-e. The abundance maps reveal the presence of three areas with distinct mineral characteristics. In the middle part of the image, LCP prevails (hypersthene) (Fig.3c). In the upper part of the image, where low reflectances occur, HCP (diopside) prevails with low abundances though (Fig. 3b). The lower part of the image is characterized by the presence of iron oxides, such as goethite (Fig. 3e), accompanied by clay minerals such as nontronite. Finally, olivines are detected with low abundances in limited regions where LCP is also observed (Fig. 3d). Phyllosilicates such as muscovite are detected with low abundances in the whole image. The aforementioned results are in accordance to the corresponding maps presented in [10, 11]. However, the overall low mineral abundances is an indication that the endmembers' library used in the process may be insufficient to effectively describe the full mineral composition of the scene, as also noted in [11].

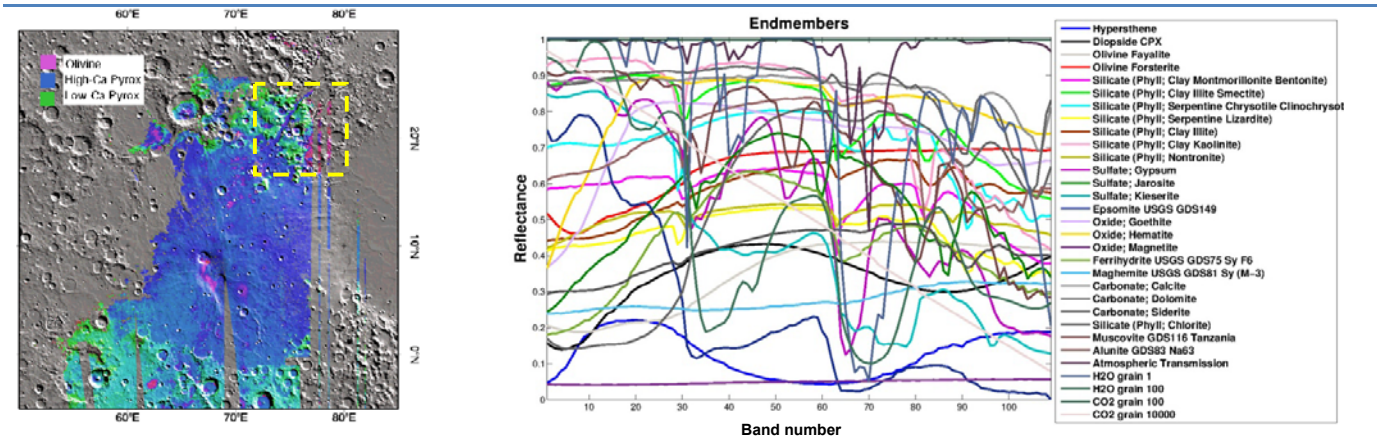

(a) (b)

Figure 2. Mineralogy of the Syrtis Major area. (a) Distribution map of the main iron-bearing mafic minerals HCP, LCP and olivines, [3]. The yellow rectangle shows the study area; (b) Spectral signatures of the 32 spectral signatures of the endmember minerals used in this study.

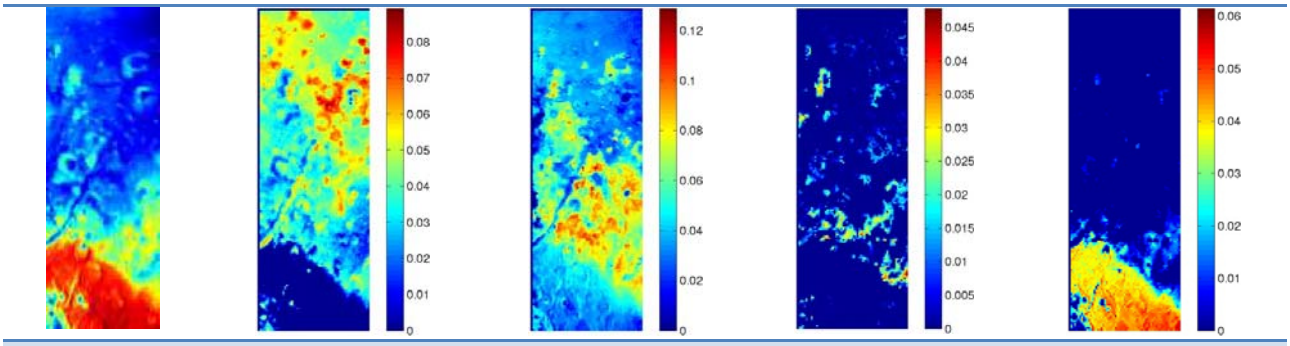

(a) (b) (c) (d) (e)

Figure 3. (a) First PC of the OMEGA dataset; (b-e) Mineral abundance maps resulting from ADSpLRU algorithm: (b) diopside, (c) hypersthene, (d) fosterite, (e) goethite. Color bars (for b-e) correspond to abundance ranges.

Keywords: *Hyperspectral, Spectral Unmixing, Direction Sparse and Low-Rank Unmixing algorithm OMEGA, Mars Express, Mars, Syrtis Major*

ACKNOWLEDGMENTS

This research was supported by the EXCELLENCE (ΑΡΙΣΤΕΙΑ) Programme entitled "HSI-MARS- Advancing Hyperspectral Image Processing for Planetary Mineral Exploration and Thematic Mapping: the Case of Planet Mars" conducted in IAASARS/NOA.

REFERENCES

[1] Hiesinger H., and J. W. Head III J.W., The Syrtis Major volcanic province, Mars: Synthesis from Mars Global Surveyor data, *J. Geophys. Res.*, 109, E01004, 1-37, 2004.
[2] Bramble, M.S., Mustard, J.F., Mark A., Salvatore, R., The geological history of Northeast Syrtis Major, Mars, *Icarus*, 293, 66-93, 2017.
[3] J.F. Mustard, S. Erard, J.-P. Bibring, J. W. Head, S. Hurtrez, Y. Langevin, C. M. Pieters, and C. J. Sotin, The surface of Syrtis Major: Composition of the volcanic substrate and mixing with altered dust and soil, *J. Geophys. Res.*, 98, 3387 – 3400, 1993.
[4] K.E. Themelis, A.A. Rontogiannis, and K.D. Koutroumbas, Semisupervised hyperspectral unmixing via the weighted lasso. in *Proc. ICASSP*, 1194-1197, 2010.
[5] J. M. Bioucas-Dias and M. A. Figueiredo, Alternating direction algorithms for constrained sparse regression: Application to hyperspectral unmixing, Hyperspectral Image and Signal Processing: Evolution, in *Proc. 2nd Workshop IEEE WHISPERS,* 1-4, 2010.
[6] K. Themelis, A. Rontogiannis, and K. Koutroumbas, A novel hierarchical, bayesian approach for sparse semisupervised hyperspectral unmixing, *IEEE Transactions on Signal Processing*, 60(2), 585-599, Feb. 2012.
[7] Q. Qu, N. Nasrabadi, and T. Tran, Abundance estimation for bilinear mixture models via joint sparse and low-rank representation, *IEEE Transactions on Geoscience and Remote Sensing*, 52, 7, 4404-4423, 2014.
[8] P. V. Giampouras, K. E. Themelis, A. A. Rontogiannis, and K. D. Koutroumbas, Hyperspectral image unmixing via silultaneously sparse and low rank abundance matrix estimation, in *Proc. 7th Workshop on Hyperspectral Image and Signal Processing: Evolution in Remote Sensing (WHISPERS)*, June 2015.
[9] P. Giampouras, K. Themelis, A. Rontogiannis, and K. Koutroumbas, Simultaneously sparse and low-rank abundance matrix estimation for hyperspectral image unmixing, *IEEE Transactions on Geoscience and Remote Sensing*, 54(8), 4775-4789, Aug. 2016.
[10] A.A. Rontogiannis, K.E. Themelis, O. Sykioti, K.D. Koutroumbas, A Fast Variational Bayes Algorithm for Sparse Semi-Supervised Unmixing of OMEGA Mars Express Data, in *Proc. 5th Workshop IEEE WHISPERS*, Gainsville, Florida, June 2013.
[11] F. Schmidt *et al.*, Accuracy and performance of linear unmixing techniques for detecting minerals on OMEGA/Mars Express, in *Proc. 3rd Workshop IEEE WHISPERS*, 1-4, June 2011.

Camera Spatial Distortions in UAV-Photogrammetry: A New Correction Workflow and Software Implementation

Argyropoulos N.*†, Nikolakopoulos K.**, Koukouvelas I.***

* Dept. of Geology, Univ. of Patras, Patras, Greece, n.argiropgeo@gmail.com
** Dept. of Geology, Univ. of Patras, Patras, Greece, knikolakop@upatras.gr
*** Dept. of Geology, Univ. of Patras, Patras, Greece, iannis@upatras.gr

ABSTRACT

Since the very first UAVs where made commercially available, there was an interest in using them for photogrammetric purposes. Nowadays, continuous advancements in UAV technology allow for easier to use, smaller and cheaper products. The main factor in which the smaller, cheaper UAVs lack in comparison to larger, photogrammetric UAVs, are the cameras they are equipped with.

Most of these cameras have a very small focal length in the order of up to 10mm, low quality lenses and sensors with very small pixel pitch. All these parameters play an important role in the 3D reconstruction of the photographed area, since they can significantly degrade the geometric accuracy of the 3D models by introducing different types of distortion. In addition to the above, the electronic or rolling shutter most of these have, causes further spatial distortion by introducing artifacts when there is a relative motion between the photographed scene and the camera. The rolling shutter effect -as it is called- is discussed and a mathematical rolling shutter camera model is proposed to, á posteriori, deal with the artifacts that it causes on the images.

A software package -named ImageCor- was created to incorporate the correction of the aforementioned spatial distortions. Specifically, it allows for camera calibration using two techniques -in order to estimate the intrinsics, extrinsics and lens distortion parameters of the camera- with a complementary lens distortion correction module. ImageCor also allows for correction of the rolling shutter effect which is also the novelty of this thesis. The rolling shutter correction proposed here assumes the general case of imagery with unknown exterior orientation.

The effect of the rolling shutter effect correction is investigated, using data from multiple flights performed under different conditions, and it is shown that even those cheap, low quality cameras can be used to create 3D models with extremely high geometric fidelity.

Keywords: rolling shutter; rolling shutter correction; spatial distortion; UAVs; uav-photogrammetry; visual sfm; 3d reconstruction; bundle adjustment;

† Oral presentation

Advancing ocean colour retrieval for the Hellenic Seas

Joint efforts of Research Institutes and Academia

Karageorgis A.[1*], Drakopoulos P.[2], Iona S.[1], Kapsimalis V.[1], Psarra S.[1], Sofianos S.[3], Spyridakis N.[1], Topouzelis K.[4], Zervakis V.[4]

[1*] *Hellenic Centre for Marine Research-Institute of Oceanography, ak@hcmr.gr; sissy@hcmr.gr; kapsim@hcmr.gr; spsarra@hcmr.gr*

[2] *Athens University of Applied Sciences, Laboratory of Optical Metrology, pdrak@teiath.gr*

[3] *National and Kapodistrian University of Athens, Ocean Physics and Modeling Group, sofianos@oc.phys.uoa.gr*

[4] *University of the Aegean, Dept. of Marine Sciences, topouzelis@marine.aegean.gr; zervakis@marine.aegean.gr*

ABSTRACT

Global primary production exceeds 100 billion tons of carbon per annum, out of which 50% originates in marine plants –phytoplankton– with prime importance for life in planet Earth. A common proxy for determining net primary productivity and phytoplankton biomass is chlorophyll-*a*, routinely determined through laboratory methods, optical field measurements and remote sensing techniques [1]. Chlorophyll-*α* is a fundamental parameter regulating biogeochemical cycles and marine trophic interactions [2], therefore its quantitative determination in marine waters is of prime importance in describing and monitoring marine ecosystems' state. Moreover, chlorophyll-*a* constitutes one of the core parameters of Descriptor 5 of the EU Marine Strategy Framework Directive, aiming to achieve Good Environmental Status –GES– until the year 2020. Both ocean colour and phytoplankton are considered 'Oceanic' Essential Climate Variables, for which the provision of information is essential to implement climate information services that contribute to sustainable national economic development and public wellbeing.

For many countries, monitoring of the marine environment through earth-observation is widely used because it provides a synoptic view of the ocean with high spatial and temporal resolution [3]. This should be also the case for Greece, a country characterized by extensive and complex marine sectors. Moreover, new space-born ocean colour radiometry sensors, coupled with increasingly adopted free and open data policies, offer a variety of products far more cost-effective than expensive oceanographic cruises. However, global semi-analytical or empirical algorithms employed in remote sensing, though often with satisfactory performance over the oceans, exhibit large uncertainties in the Hellenic seas and Eastern Mediterranean pelagic waters because of the peculiarities of these systems, such as very low productivity and high transparency [4-10]. Therefore, a strategic National target for Greece would be to formulate/develop novel regional algorithms, taking into account the specific optical properties of seawater in the region by carefully estimating water-leaving radiance, the primary quantity captured by satellite sensors [8]. Although satellites provide global coverage of ocean colour and high-resolution depictions, the linkage between ocean colour and ecosystem variables, including chlorophyll-α and its distribution with depth, remains limited [11]. Therefore, the sound scientific and technically feasible way forward, in order to obtain estimates at large scales, is to link discrete *in situ* measurements of apparent and inherent optical properties (AOPs & IOPs) and biogeochemical parameters, with the synoptic and repetitive satellite observations. This linkage involves the development of various models/semi-analytical or empirical algorithms [8, 12].

Over the last few years the Institute of Oceanography of the Hellenic Centre for Marine Research, through national and EU funding, managed to acquire several instruments for measuring optical properties of seawater (AOPs: TriOS submersible radiance and irradiance, and reference sensor; IOPs: WETLabs ac-s, transmissometer C-Star 660 nm, CDOM fluorometer, ECOBB3B 470, 532, and 650 nm, Chelsea transmissometer 470 nm, chlorophyll-*a* fluorometer, Sequoia particle-sizer LISST-Deep) coupled with Seabird CTD integrated systems [13, 14]. Moreover, a prototype submersible platform (0-250 m depth) was designed and constructed *in-house* providing power supply, frame orientation information, and data acquisition/internal storage from the various sensors, employing 2 mini-PCs, a motion sensor, and wireless data transmission. The prototype platform was used in research cruises in the Eastern Mediterranean (NE Aegean, S. Aegean and NW Levantine / Libyan Seas) and the Black Sea.

We propose an integrated approach to tackle the problem of delivering improved algorithms for the assessment of chlorophyll-*α* from satellite products based upon available data sets, as well as new field data. The correction, calibration and overall management of *in situ* bio-optical data will feed the exclusive numerical model Hydrolight [15] that assures the optimum estimation of ocean colour remote sensing reflectance from the available IOPs and AOPs. To the best of our knowledge similar experiments have not been conducted in the proposed study area, whereas very few have been conducted in the Eastern Mediterranean [5, 16]. The ultimate goal, which is the formulation of regional empirical algorithms for the assessment of chlorophyll-*α*, constitutes a top scientific challenge in the global scale and has attracted the attention of the scientific community over the last decades.

Such challenges are certainly better tackled through close collaboration between scientists occupied at research institutes and university departments, by exchanging ideas, experience and knowledge, and together with bright young students who will boost research in new grounds. The present contribution is an initial statement of the authors originating from HCMR, AUAS, UoA, and NKUA, who share the common vision of joining forces to achieve the promotion of science in the highly complex and competitive field of bio-optics and ocean colour.

REFERENCES

[1] Behrenfeld, M.J., Boss, E., 2006. Beam attenuation and chlorophyll concentration as alternative optical indices of phytoplankton biomass. Journal of Marine Research 64, 431–451.

[2] Catlett, D., Siegel, D.A., 2017. Phytoplankton pigment communities can be modeled using unique relationships with spectral absorption signatures in a dynamic coastal environment. Journal of Geophysical Research, DOI 10.1002/2017JC013195
[3] Palialexis, A., Tornero, V., Barbone, E., Gonzalez, D., Hanke, G., Cardoso, A.-C. et al., 2014. In-Depth Assessment of the EU Member States' Submissions for the Marine Strategy Framework Directive under articles 8, 9 and 10. European Union, 149 p., doi: 10.2788/64014.
[4] Bricaud, A., Bosc, E., Antoine, D., 2002. Algal biomass and sea surface temperature in the Mediterranean Basin. Intercomparison of data from various satellite sensors, and implications for primary production estimates. Remote Sensing of Environment 81, 163– 178.
[5] Sancak, S., Besiktepe, S.T., Yilmaz, A., Lee, M., Frouin, R., 2005. Evaluation of SeaWiFS chlorophyll-a in the Black and Mediterranean Seas. International Journal of Remote Sensing 26(10), pp 2045-2060.
[6] Berthon, J-F., Melin, F., Zibordi, G., 2008. Ocean Colour Remote Sensing of the Optically Complex European Seas. In: Barale, V. and Gade, M. (eds.), Remote Sensing of the European Seas (Springer, Berlin).
[7] Psarra, S., Lagaria, A., Pagou, P., Assimakopoulou, G., Drakopoulos, P.G., Petihakis, G., et al., 2014. Assessing phytoplankton dynamics in the Aegean Sea: combining field data and remote sensing. PERSEUS Scientific Workshop, Marrakesh, p. 9.
[8] Lee, Z., Marra, J., Perry, M.-J., Kahru, M., 2015. Estimating oceanic primary productivity from ocean color remote sensing: A strategic assessment. Journal of Marine Systems 149, 50–59.
[9] Drakopoulos, P.G., Petihakis, G., Valavanis, V., Nittis, K., Triantafyllou, G., 2003. Optical variability associated with phytoplankton dynamics in the Cretan Sea during 2000 and 2001. In: "Building the European Capacity in Operational Oceanography", Elsevier Oceanography Series No 69, Elsevier BV, 69, 554-561.
[10] Drakopoulos, P.G., Banks, A.C. Kakagiannis, G. Karageorgis, A.P. Lagaria, A. Papadopoulou, A. et al., 2015. Estimating chlorophyll concentrations in the optically complex waters of the North Aegean Sea from field and satellite ocean colour measurements, Proc. SPIE 9535, Third International Conference on Remote Sensing and Geoinformation of the Environment (RSCy2015), 95351I (June 19, 2015); http://dx.doi.org/10.1117/12.2192571.
[11] GCOS, 2015. Status of the Global Observing System for Climate. World Meteorological Organization, 2015, pp. 373.
[12] IOCCG, 2006. Remote Sensing of Inherent Optical Properties: Fundamentals, Tests of Algorithms, and Applications. Edited by ZhongPing Lee, pp. 126.
[13] Karageorgis, A.P., Georgopoulos, D., Kanellopoulos, T.D., Mikkelsen, O.A., Pagou, K., Kontoyiannis, H. et al., 2012. Spatial and seasonal variability of particulate matter optical and size properties in the Eastern Mediterranean Sea. Journal of Marine Systems, 105–108, 123–134. doi:10.1016/j.jmarsys.2012.07.003.
[14] Karageorgis, A.P., Drakopoulos, P.G., Psarra, S., Pagou, K., Krasakopoulou, E., Banks, A.C. et al., 2017. Particle characterization and composition in the NE Aegean Sea: combining optical methods and biogeochemical parameters. Continental Shelf Research, 149, 96-111.
[15] Mobley, C.D., Sundman, L.K., 2013. HYDROLIGHT 5.2, ECOLIGHT 5.2 Users' guide. Sequoia Scientific, Inc.
[16] Bricaud, A., Morel, A., Babin, M., Allali, K., Claustre, H., 1998. Variations of light absorption by suspended particles with chlorophyll a concentration in oceanic (case 1) waters: Analysis and implications for bio-optical models. Journal of Geophysical Research 103(C13), pp 31,033-31,044.

POSTERS

Mapping of the Historic “1536-1669” volcanic products of Mt. Etna through Spectral Unmixing of Hyperion Hyperspectral data

Daskalopoulou V.[1], Sykioti O.[1], Koutroumbas K.[1], Rontogiannis A.[1]

[1]*Institute for Astronomy, Astrophysics, Space Applications & Remote Sensing, National Observatory of Athens, Vas. Pavlou & I. Metaxa, GR-15 236 Penteli, Greece, vdaskalop@noa.gr, sykioti@noa.gr, koutroum@noa.gr, tronto@noa.gr*

Technological advancements of the last decade, have extended our imaging capabilities to various scientific domains, such as geomorphological monitoring and planetary exploration. The identification of minerals on the composition of igneous volcanic rocks with the use of Hyperspectral Imaging (HSI), is extremely significant for the characterization of the geochemical systematics on planets. Earth’s volcanic activity deposits massive and voluminous products which are spectrally convolved, therefore mapping the latter with HSI is both challenging and intriguing. Hence the use of refined hyperspectral data, provides information on absorption spectral features that indicate the presence of minerals and an early estimation of basaltic Lava Flow (LF) alteration levels, mainly focusing on the Visible (VIS) and Near Infrared (NIR) part of the spectrum [1]. Spectral Unmixing (SU) techniques are adopted in order to identify: *i.* pure components (endmembers) present in the image and *ii.* their fractional proportions (abundances) within the pixel [2].

In the specific research, we focus on the Sicilian volcano, Mt. Etna, for an accurate estimation of the abundances of deposited volcanic products on older lava fields. The case study is intriguingly diverse, since it is an incubator of volcanological phenomena. For this purpose, a NASA EO-1 Hyperion HSI image of Etna is selected and for the sub-pixel analysis we propose **four** signal transformations that are assimilated in **Linear Least Squares Unmixing (LLSU)**. After extensive pre-processing a total of 140 bands were retained. Our approach is narrowed to the part of the Historical Eruptions (1536–1669 AD) on the sensor's FOV, where deposited products present lower correlation coefficients than those of younger lava flows. The latest geological map of Etna (Fig.1c) is used as ground truth [3] for an extensive comparison of the LFs delineation and spatial distribution of the respective abundances. The resulting abundance maps from each method are quantitatively evaluated via the Structural Similarity Index (SSIM) [4] and ultimately an efficiency assessment is given.

Mt. Etna is a large basaltic complex stratovolcano with a broad base diameter of 1.178 Km^2. Its volcanism started approximately 500 ka ago, from a submarine fissure of the Gela-Catania basin and is characterized by two major components: i) the central *summit craters* and ii) the *flank eruptions*. Summit events are consistent for many years, while flank eruptions occur every few years and are correlated with tectonic faults and shallow seismic activity [5]. Etna has the ability to change its land field rapidly, vigorously and continuously. It is capable of producing both brief paroxysmal episodes and long-standing, relatively milder eruptions. During the last 100 years Mt. Etna has produced on average 10^7 m^3 of new lava per year [6], both from its summit craters and from its flanks. The youngest active bulks of Etna are *Ellitico* and *Mongibello*. We focus our research on the persistent activity of the Mongibello volcano, which entrails the major volcanic formation of Torre del Filosofo. It contains voluminous products younger than 122 BC, with continuous temporal succession and similar lithologies. The formation is divided in *three* sub-formations formed in different time periods [3]. From the latter, the Mongibello Formation 1 (MF1) is ideal for testing unmixing processes, since it contains mostly altered lavas with high reflectance. The respective lava fields are distinct, voluminous and often do not mingle with younger lavas. Considering the Hyperion's limited swath range (Fig.1a) and spatial resolution over Etna, lava fields from 1536 – 1669 AD are contained in the data cube. Also, the initial mage is masked beyond the borders of the MF1 formation (Fig.1c).

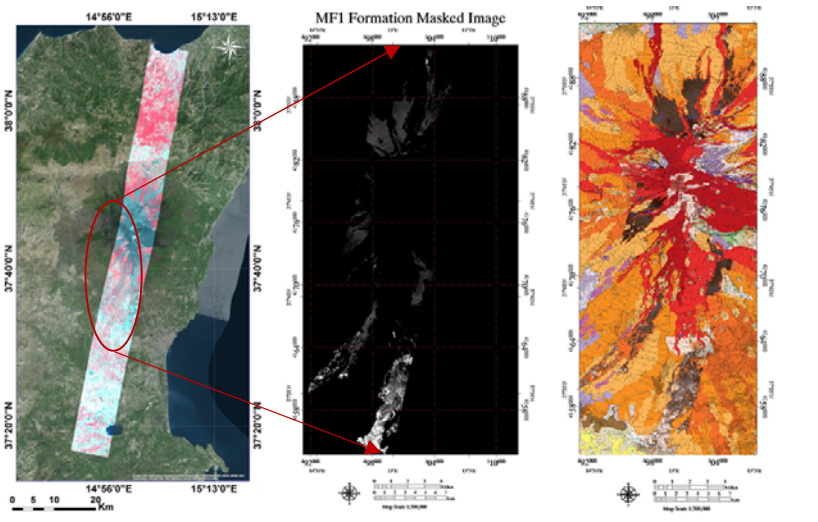

(a)	(b)	(c)

Figure 1. Location of the study area: (a) Hyperion image over Etna, (b) MF1 masked image (c) superposition of MF1 in the geological map.

Appropriate Regions of Interest (ROIs) are selected within denser lava fields and close to the eruption vents, via spectral profile examination. The endmembers were extracted from the mean pixel values for each ROI and in total 13 endmembers corresponding to 8 LFs (1536, 1537, 1566, 1610, 1614-24, 1634-36, 1646-47 & 1669 AD), two scoria cones (1610 & 1646-47 AD) and three artificial materials (industrial, semi-urban and tile rooftop areas) are selected. The determination of the number of endmembers is critical, since underestimation may result in poor

representation of the mixed HSI pixels, whereas overestimation in an overly segregated area. We assume that measured pixel spectra are linear or bilinear combinations of the 13 endmembers and implement four signal transformations [7], which are integrated on a Linear Least Squares Unmixing (LLSU) non-negativity constrained method. The resulting abundance maps indicate the fraction of each endmember on the respective lava field and they are compared against the LF's spatial distribution as shown in the geological map. Indicatively, we present the abundance maps of the first method (Fig.2) and an RGB color-composite of spatially correlated LFs, along with the extracted endmember spectral signatures (Fig.3).

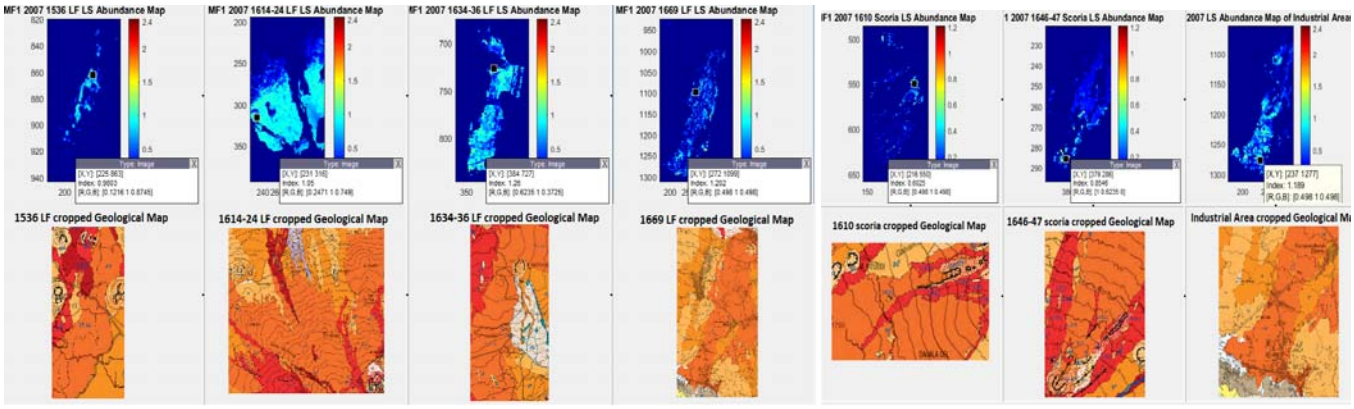

(a) (b)

Figure 2. Top row: Abundance maps resulting from method 1. Bottom row: Respective region in the geological map. (a) From left of right: LFs 1536, 1614-24, 1634-36, 1669 with similar spectral trends, (b) From left to right: scoria cones and industrial areas.

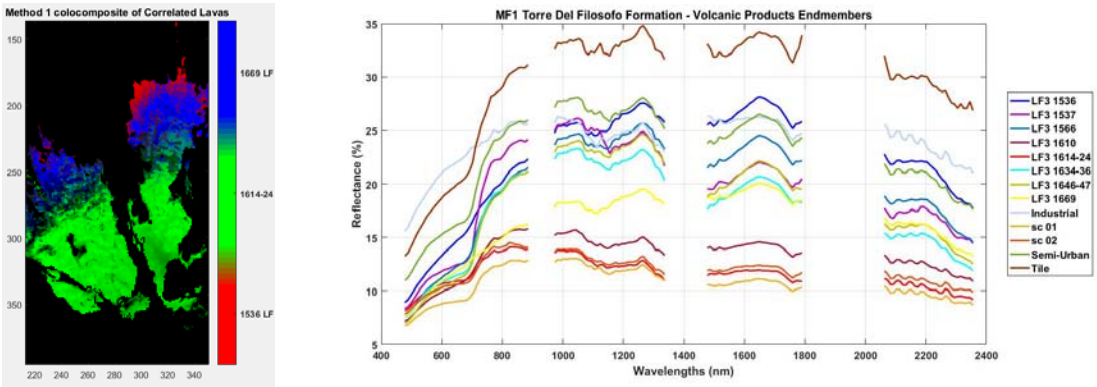

(a) (b)

Figure 3. (a) RGB color-composite of the 1536, 1614-24, 1669 correlated LF abundance maps, (b) Spectral signatures of the selected 13 endmembers

Keywords: *hyperspectral data, Etna, lava flow characterization, linear spectral unmixing, bilinear spectral unmixing, fast fourier transform, structural similarity index*

REFERENCES

[1] Keshava, N.; Mustard, J.F. Spectral Unmixing. *IEEE SPM*, **2002**, vol. 19, pg. 44-57, doi: 10.1109/79.974727

[2] Dobigeon N.; Altmann Y.; Brun N.; Moussaoui S. Linear and Nonlinear Unmixing in Hyperspectral Imaging. Chpt. 6, *Data Handling in Science and Technology Elsevier*, **2016**, Vol. 30., http://dx.doi.org/10.1016/B978-0-444-63638-6.00006-1

[3] Branca, S.; Coltelli, M. and Groppelli, G. Geological map of Etna volcano, 1:50,000 scale. *Ital.J.Geosci.*, **2011**, Vol. 130, No. 3, pp.265-291, doi: 10.3301/IJG.2011.15

[4] Zhou, W.; Bovik, A. C.; Sheikh, H. R. and Simoncelli, E. P. Image Quality Assessment: From Error Visibility to Structural Similarity. *IEEE TIP*, **2004**, Vol. 13, pp. 600–612, doi: 10.1109/TIP.2003.819861

[5] Buongiorno, M. F. et al. ETNA 2003 field campaign: Calibration and validation of spaceborne and airborne instruments for volcanic applications. ASI Projects: I/R/157/02, I/R/203/02.

[6] Allard, P.; Behncke, B.; D'Amico, S.; Neri, M. and Gambino, S . Mount Etna 1993-2005: Anatomy of an evolving eruptive cycle. *Elsevier Earth-Science Reviews*, **2006**, Vol. 78, pp. 85-114. doi: 10.1016/j.earscirev.2006.04.002

[7] Singh, K.D.; Ramakrishnan, D.A. Comparative Study of signal transformation techniques in automated spectral unmixing of infrared spectra for remote sensing applications. *IJRS*, **2017**, 1235-1257, doi: 10.1080/01431161.2017.1280625

Land cover monitoring through spectral unmixing, classification and clustering on Multispectral Sentinel-2 data of Southern Pindos

Boutsi A.Z.[1], Daskalopoulou V.[1], Bouskou E.[1]

[1]*Institute for Astronomy, Astrophysics, Space Applications & Remote Sensing, National Observatory of Athens, Vas. Pavlou & I. Metaxa, GR-15 236 Penteli, Greece, vdaskalop@noa.gr, zboutsi@noa.gr, space15013@uop.gr*

Versatile Land Cover applications such as material discrimination, resources detection and image classification require further processing of the image pixels, through spectral mixture analysis. The challenge faced here, was to implement three main techniques, Unmixing, Supervised Classification and Clustering on multispectral data acquired for a specified region of Southern Pindos. These techniques are mostly exploited in the field of Hyperspectral Imaging [1,2], where spectral information is abundant, and due to the poor thematic information of Multispectral data, bibliographic references for the latter are limited. The research was conducted on part of the Northern Pindos National Park, in the northwestern Greece, which is the largest protected forestry region, with many topographical diversities, including Natura sites and various types of vegetation. The selection of the area was based on its appropriateness concerning the distinction of basic endmember types.

In this study, we aim to perform basic methods used widely in satellite imagery, in order to unmix and, later on, classify multispectral images. Our data is Sentinel-2 products, depicting the same ground area in two different seasons, August 2015 (summer) and October 2016 (autumn), respectively, subsetted at three different spatial resolutions (10m, 20m and 30m). Then, a simplistic linearity model is assumed, suggesting that each endmember covers a defined region within the pixel area. Therefore, the measured pixel radiance, as mentioned, is a weighted average of the radiances of the pure components present and the abundances represent the percentage of each material on the pixel. Linear Least Squares Unmixing (LLSU) techniques require the a-priori knowledge of the material spectral signatures present in site [3], deeming the selection of appropriate Regions of Interest (ROIs), per general class, the first and foremost step of the followed methodology. Appropriate ROIs were selected based on gross classes Water, Vegetation and Soil on the first level of unmixing (rough unmixing) and then endmembers were extracted by averaging the pixel reflectance values per ROI. Analogously, for the refined unmixing process of the same large classes, we have identified **3** endmembers for water (Fig.1a), **4** endmembers for vegetation (Fig.1b) and **3** endmembers for soil (Fig.1c).

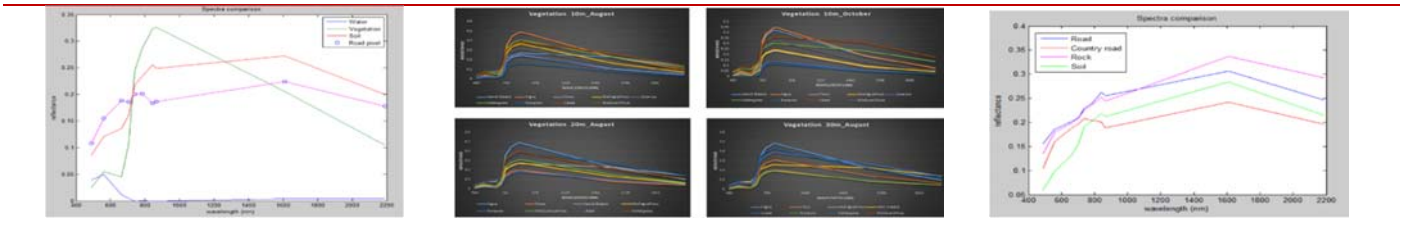

(a)	(b)	(c)

Figure 1. Endmember Spectral Signatures: (a) Water endmembers, (b) Vegetation endmembers, ultimately merged in Fagus, Crops-Grassland, Pinus-Rompolo and Low vegetation, (c) Soil and road endmembers

First, we perform **four** LLSU techniques, with and without constraints, in order to extract abundance maps. Their comparison, based on SSIM index results, allows us to decide on which one best performs the unmixing of the three basic compounds (**rough unmixing**). Thenceforth, we are able to perform further unmixing within a basic category (**fine unmixing**). Examples of the resulting abundance maps for the October-20m image are presented in Fig.2. Furthermore, we perform an NN classifier algorithm with the **11 endmembers/representative** for the two images in the three resolutions. The resulting classification map (Fig.3) is compared to the reference map and evaluated in terms of efficiency with calculated success rates, corresponding to different confusion matrices. We conclude that the classification results give slightly better results for finer resolutions, as well for the August 10m compared to the October image of the same resolution. Lastly, k-means clustering algorithm [5] six times (as many as the available images - three images per season). The algorithm is executed for several consecutive k values (number of neighbors: from 2 to 18) which correspond to clusters' number and at each execution we compute the square error. The optimum number of clusters was found to be equal to 5. Clustering results (Fig.4) are quantitatively evaluated in comparison with the classification and reference maps, while qualitatively with the computation of the degree of agreement with the reference map classes.

To conclude, it was shown that the unmixing of an image to few major categories, i.e. forestry types, water and soil, using the LS based methods works well and the problem of unexpectedly mixed endmembers (water-road) can be successfully resolved in a second level (fine) unmixing. The unmixing results were evaluated in terms of structural similarity with the initial image, compare the unmixing efficiency seasonally (per image) and with ground truth (Landsat reference map). The performance of the NN classifier was successful enough, while the relatively low success rates had to do with the smoothed out reference map. We consider that the selection of ROIs is a valuable part of the process and does definitely affect the material distribution observed (classification map). The k-means clustering algorithm (k=5,6) had remarkably good degrees of agreement when compared to the reference map, with the the August image achieving even higher values, steadily at all resolutions. Overall, all the processes used in this research for the discrimination of the various land covering materials, gave promising quantitative and qualitative results for the case of multispectral data.

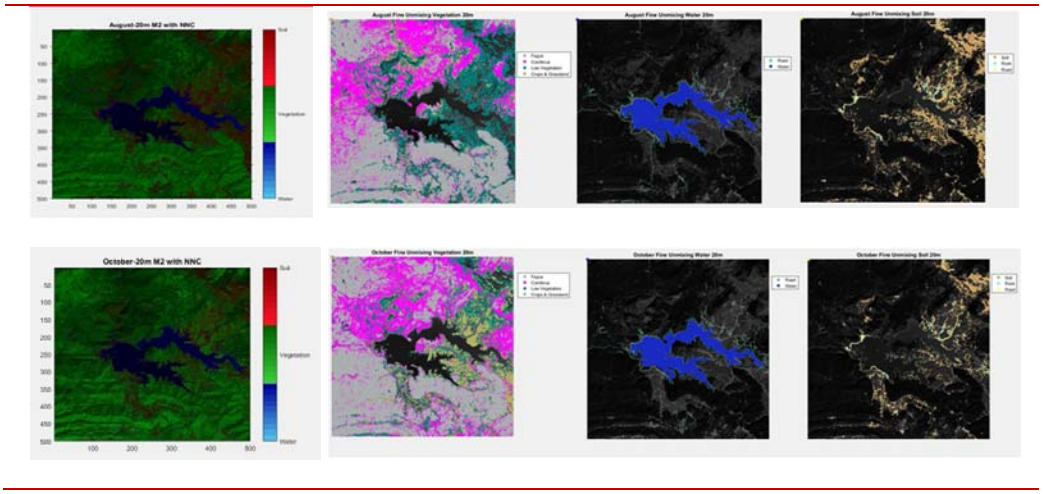

(a)	(b)

Figure 2. Abundance maps for the August and October 20m image, resulting from the most efficient LLSU method 2. (a) Rough unmixing abundance maps, (b) Fine unmixing abundance maps.

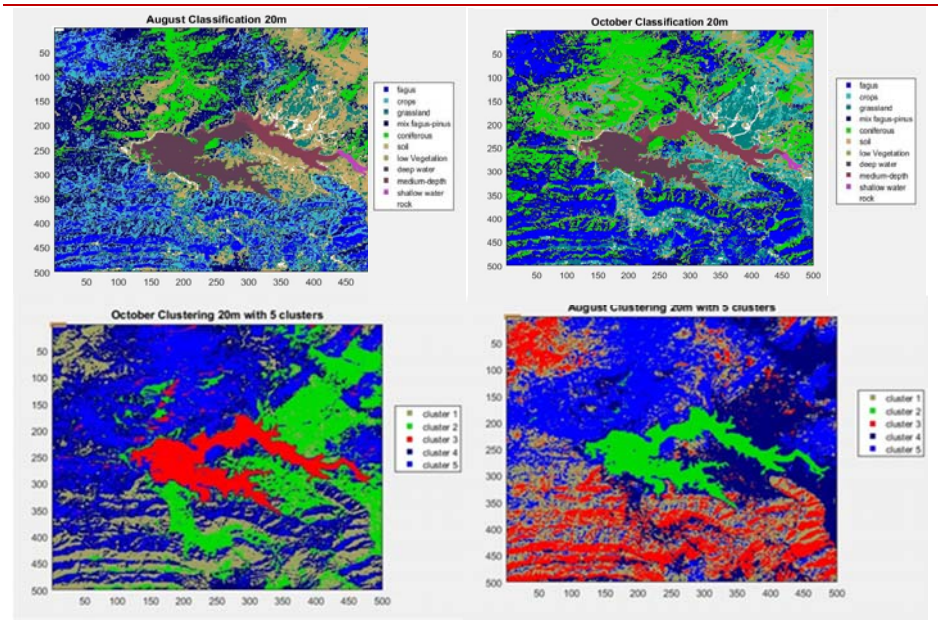

Figure 3. Top row: Classification maps for both images on the 20m spatial resolution, Bottom row: Clustering results for an optimum number of five clusters.

Keywords: *Multispectral data - Linear spectral unmixing - NN-classifier - k-means clustering - Image structural similarity - Classification map - Confusion matrix*

REFERENCES

[1] Jose M. Bioucas-Dias et al. Hyperspectral Unmixing Overview: Geometrical, Statistical, and Sparse Regression-Based Approaches, **2012**
[2] Mauro Dalla Mura et al. GIPSA-lab, Grenoble-INP, **2014**. An Overview on Hyperspectral Unmixing.
[3] Daniel C. Heinz, Student Member, IEEE, and Chein-I Chang, Senior Member, IEEE. Fully Constrained Least Squares Linear Spectral Mixture Analysis Method for Material Quantification in Hyperspectral Imagery, **2002**.
[4] Stavros Stagakis et al. Estimating forest species abundance through linear unmixing of CHRIS/ PROBA imagery, **2015**.
[5] Koutroumbas Konstantinos, Dr.. Pattern Recognition: – Feature selection – Feature generation - Clustering, **2015.**

BENCHMARKING SUPERVISED METHODS FOR HYPERSPECTRAL DATA CLASSIFICATION

Fokeas K.

NTUA, fkwstas@gmail.com

INTRODUCTION

Automatic Land cover classification from remote sensing images it's a very important issue for the Remote Sensing community. The massive amount of available data coming from national or private earth observation projects, requires an efficient yet sophisticated manner in order to analyze them properly. At the same time hyperspectral imaging has become a heated scientific discipline, which plays a significant role in remote sensing applications like precision agriculture, water quality estimation and change detection. From a methodological point of view, hyperspectral data analysis is a difficult task, mainly because of the spatial variation of spectral signatures and the well-known curse of dimensionality.

In recent years, deep learning approaches, which learn to discriminating features based on a hierarchical pattern from data, has shown greater accuracies than the shallow architectures, at tasks like image classification. In this paper, five different classification methods evaluated qualitatively and quantitatively on three widely used datasets. In particular the methods are, (1) Convolutional Neural Network, (2) Neural Network, (3) Kernel based Support Vector Machine, (4) Linear Support Vector Machine, (5) k – Nearest Neighbor.

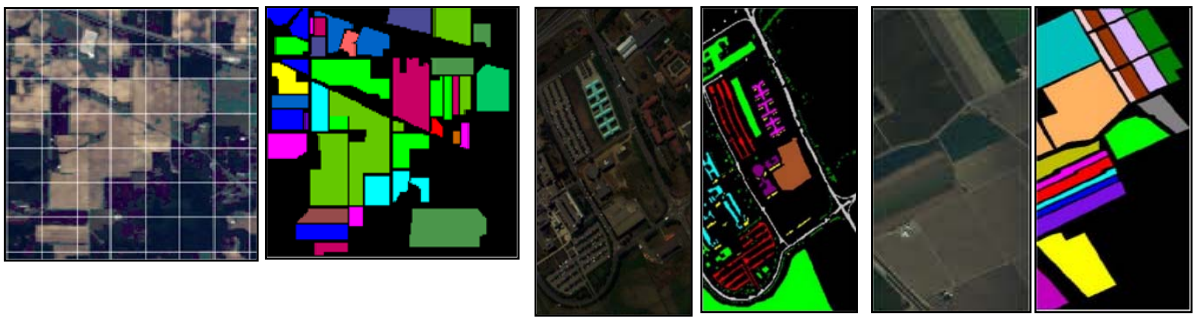

Figure 1: The three hyperspectral Images along with the ground truth matrices. Indian Pines, Pavia University and Salinas respectively.

METHODOLOGY

In this paper the classification of each pixel to a predefined number of class is based on its spectral and spatial properties. The spectral characteristics are associated with the reflectance properties at every pixel for every spectral band, while spatial information is derived by taking into consideration its neighbors. A hyperspectral image is represented as a 3D matrix of dimensions *h x w x c*, where h and w correspond to the height and width of the image and c to its channels. In order to be aligned with the nature of CNNs, a decomposition into patches, is necessary, each one of which contains spectral and spatial information for a specific pixel. More specifically, in order to classify a pixel $P_{x,y}$ at location *(x,y)* on image plane and successfully fuse spectral and spatial information, a square patch of size *s x s* centered at pixel Px,y, is used. Naming as $L_{x,y}$ the class label of the pixel at location (x,y) and as $W_{x,y}$ the patch centered at pixel Px,y, we can build a dataset D = ($W_{x,y}$, $L_{x,y}$) for x = 1, 2, …, W and y = 1, 2, …, h. Lastly for dimensionality reduction, Randomized PCA is being applied along the spectral dimension to abbreviate the image.

RESULTS

In the tables below, quantitative results are being shown. The results refer to 75% of the data being used as validation data in the Indian-Pines image, whilst 95% in the Pavia University and Salinas respectively. The first table contains the overall accuracies from the five methods without adding any noise into the image. On the contrary the second and the last table consists of the achieved accuracies, adding in the datasets a certain type of noise. The Normal noise has a standard deviation of 100 and a mean value of 0, while the Salt and Pepper noise constitutes the 10 percent of every image.

Table 2 Overall Accuracies achieved on clean datasets

Dataset	CNN	SVM-RBF	SVM-Linear	Neural Network	KNN
Indian Pines	**97.92**	91.31	90.22	89.83	86.87
Pavia university	**97.50**	96.02	88.38	93.72	95.36
Salinas	97.54	97.71	90.98	97.30	**98.94**

Table 3 Overall accuracies achieved with normal noise being infiltrated in datasets

Type of noise	**Dataset**	CNN	SVM-RBF	SVM-Linear	Neural Network	KNN
Normal Noise	Indian Pines	**97.33**	89.02	88.94	87.88	73.12
	Pavia university	**97.02**	95.48	87.29	92.64	92.61
	Salinas	96.87	96.38	86.68	94.52	**97.86**

Table 4 Overall accuracies with salt and pepper noise being infiltrated in datasets

Type of noise	**Dataset**	CNN	SVM-RBF	SVM-Linear	Neural Network	KNN
Salt and Pepper	Indian Pines	**77.73**	49.04	41.91	43.84	8.12
	Pavia university	**85.99**	81.52	67.65	79.25	61.70
	Salinas	**87.67**	80.43	45.08	70.96	49.08

CONCLUSIONS

Experimental validation shows that the deep learning approach presents superior performance for almost every dataset. Furthermore CNN is capable to maintain a great percentage of accuracy despite the noise that has been added to the data, which consequently shows the generalization capacity of deep learning architectures.

REFERENCES

[1] K. Makantasis, K. Karantzalos, A. Doulamis, and N. Doulamis, “Deep supervised learning for hyperspectral data classification through convolutional neural networks,” in Proc. IEEE IGRASS. Milan, Italy, Jul. 2015, pp. 4959-4962.

[2] Liangpei Zhang, Lefei Zhang, and Bo Du, “Advances in Machine Learning for Remote Sensing and Geosciences,” IEEE GEOSCIENCE AND REMOTE SENSING MAGAZINE, 2016.

Mapping distribution and investigation of correlation between Surface Sea Temperature and Chlorophyll-a in the Mediterranean Sea

Vasiliou N.

Open University of Cyprus, Nicosia, Cyprus, neofytos.vasou.vasiliou@gmail.com

ABSTRACT

The aim of this project, is to find the relationship between the sea surface temperature and chl-a depending on place and time in the Mediterranean sea so that we know their role and how the affect the quality at the sea environment. At the same time, we will know their influence in that area and climate trends and their effects on the place. The whole sea environment depends on the quality of sea-life, and therefore, so does the people's quality of seafood. In addition, it will operate as a mechanism which has to do with the climate and the environmental atmosphere. Our target is to show changes that take place on a monthly and yearly-basis on the areas caused by the pressure coming from the environment. Satellite data which is examined from chl-a and SST which they got from MODIS in 2003-2013, 11 years all seasons around come from the average of these ages.

METHODOLOGY

Data by satellites has been processed. More in particular, chlorophyll-a data has been obtained through SeaWIFS and the surface sea temperature from MODIS. All files were converted to shapefiles and all the pixels that belong to the sea were isolated. All in all, pixels found to belong to the sea for the area of interest is 8348. The EPSG: 4326-WGS 84 is used and the pixel number that was made by image processing is 0.175 which shows us a well-defined image.

For statistical data processing, all parameter data being examined were introduced to the SPSS program via EXCEL. There have been correlations between sea surface temperature, chlorophyll-a for each month and each date separately and with the parameters which are studied, in order to highlight the results and to draw the appropriate conclusions.

RESULTS

The linear Pearson correlation coefficient, between surface sea temperature and chlorophyll-a has been examined in its monthly and yearly intervals. A maximum absolute correlation value was found for March and minimum for June. For yearly prices, a zero to negative patient correlation values were found, all ranging from -0.207 to -0.299. The results confirm that, as mentioned above in the literature, when surface water is cold, it helps the deeper waters to surface by feeding nutrients in the sunny areas and making it easy for phytoplankton to use them. When surface water is warm, then the nutrients are trapped if they are not in mixing the vertical layers of the ocean. Streams play a role in mixing, causing puffiness. So our low surface sea temperatures offer higher concentrations of chlorophyll-a. Based on the results, the Fisheries workers can save up a lot of time and effort, but also the costs incurred during the search, making it easier and more efficient to find catches, something quite positive in times of economic crisis where the financial resources are limited to all countries bordering the Mediterranean Sea.

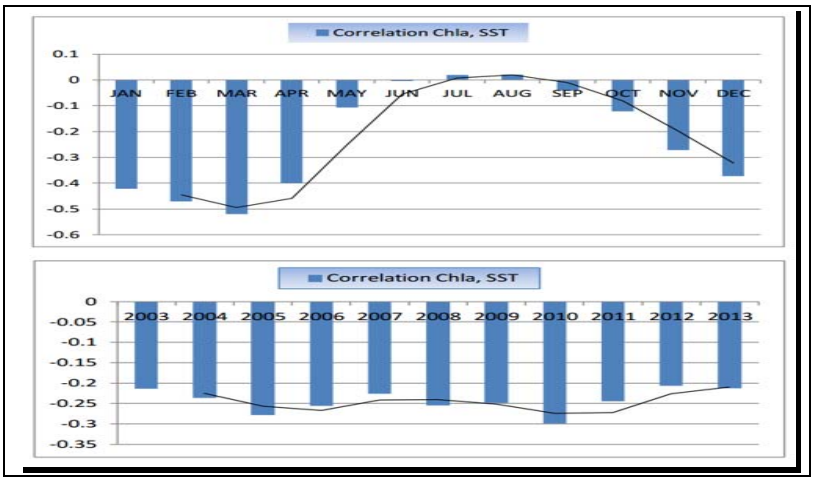

Picture 1: Graphs of the months and years correlations between chorophyll-a and SST.

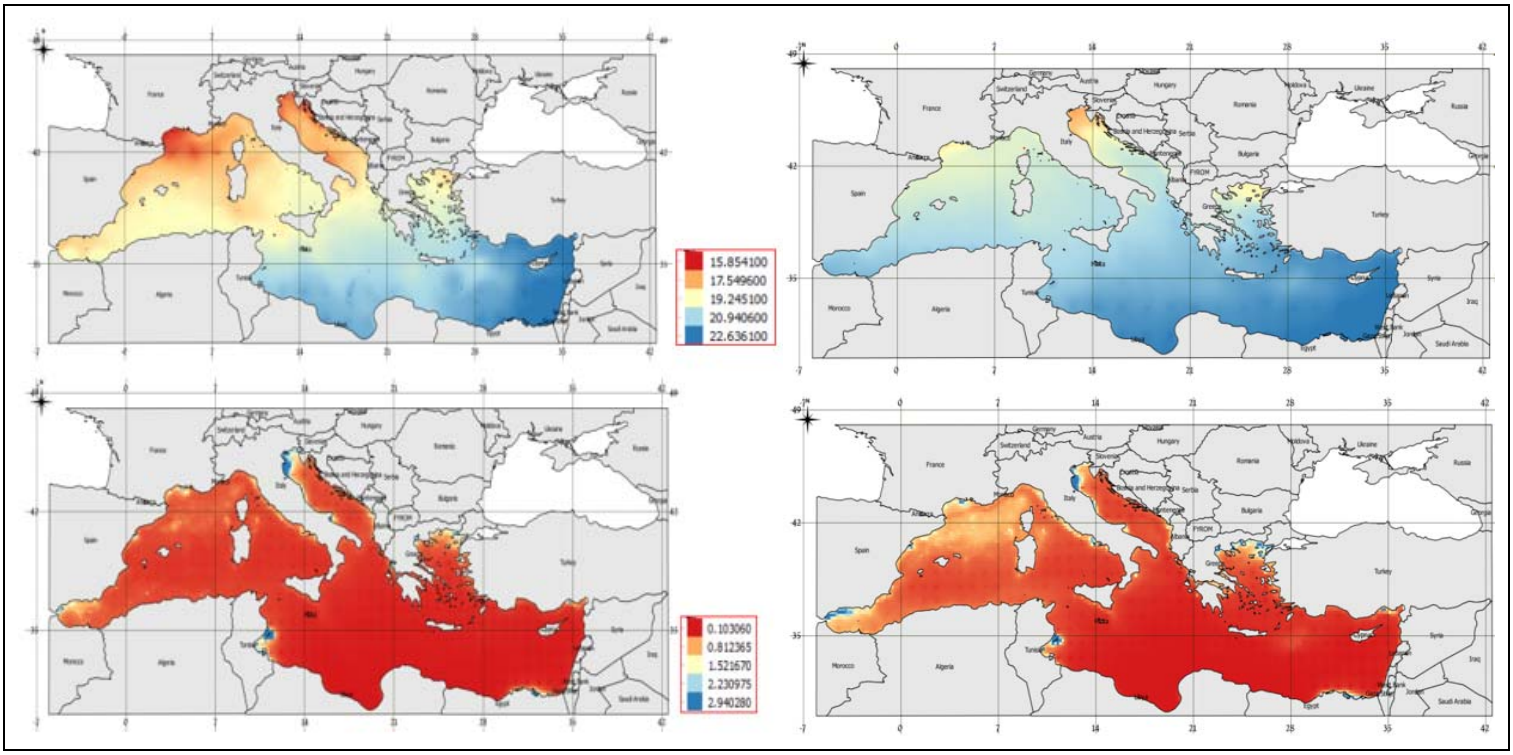

Picture 2: Maps of the chorophyll-a and SST (right:2010, left:March)

ACKNOWLEDGEMENT

Many thanks to organizers of the workshop.

REFERENCES

[1] Vasiliou, Neofytos., 2016, Mapping Distribution and Investigation of Correlation Between Surface Sea Temperature and Chlorophyll-a in the Mediterranean Sea, Faculty of Pure and Applied Sciences, Master Thesis, Open University of Cyprus, Nicosia, Cyprus, 182 p.

Lake Monitoring Using State of the Art Remote Sensing Technologies

Stefouli M.[1], Charou E.[2]

[1]*Institute of Geology and Mineral Exploration, Athens, Greece*
[2]*N.C.S.R. "Demokritos", Institute of Informatics & Telecommunications, Athens, Greece*

Lakes are valuable natural resources for water supply, food, irrigation, transportation, recreation and hydropower. They also provide a refuge for an enormous variety of flora and fauna. Some of the most valuable lakes of Europe in terms of biodiversity are located in West Macedonia. Pilot applications have been accomplished for the lakes of West Macedonia, while a special reference is made on Prespa lakes that have been studied in the framework of ESA and NATO SFP Projects and the support of LEGOS-OMP/SOI laboratory*. Traditional monitoring of lakes requires specialized instrumentation, use of personnel who can make both on site and laboratory analysis. All these refer to point measurements. However, up to date information and the total picture of the lake ecosystem along with its temporal changes are not always available. Therefore, a methodology has been applied in order to provide complementary information, essential to all aspects of lake monitoring. The poster is to present the experience gained by the application of remote sensing technologies that are related to lake monitoring. Hybrid application of remote sensing, GIS and simulation techniques have been applied for the monitoring the "environment of lakes" with automatic update of spatial databases. The application of remote sensing techniques has supported the extraction of parameters that are of importance to the lake ecosystems and its monitoring like:

- Water quality monitoring. Monitoring of total suspended sediments and chlorophyll of lakes using MERIS satellite images is supported. Remotely sensed images can support estimates of sediment load as one can identify where, when and how much sediment load occurs. These data have a temporal resolution of every 3 days, depending on cloud coverage and a spatial resolution of 300 m. These type of data are now replaced by the Copernicus Sentinel 2 & 3 data which have improved spectral and spatial resolutions.
- Geological mapping. Ground waters cannot be observed directly by existing EO satellites, however, location, orientation and length of lineaments can be derived and used as input for studies of fractured aquifers (e.g. location of sites for water harvesting.)
- Lake water level estimates. Radar Altimetry is basically a technique for measuring height. ENVISAT data provide water level reliable observations of Ochrid lake. Copernicus data can now support more accurate measurements.
- Estimates of multi-temporal land cover change. Estimates of surface lake area can be accomplished.

The GIS system supports storage and administration facilities for all data types, along with analytical methods for monitoring the lakes. TNTgis has been used for the processing, www.microimages.com. The spatial database of Prespa / Ochid lakes consists of multiple layers: Digital elevation with resolution of 100 and 30 meters, bilingual (English/ Greek) geological map** of the transnational area produced by the synthesis of maps with different scales, land cover maps, meteorological / hydrological data / lake bathymetry / water quality and quantity characteristics. These data have been obtained with remotely sensed data.

The applied technologies have the capacity to analyse a range of different types of remotely sensed and / or geological, environmental, hydrological data. Large quantities of data with very different complex interrelationships can be analysed and these makes the application interesting for lake monitoring. Also hydrogeologists / hydrologists frequently face problems characterized by uncertainties. The applied technologies assist to deal with such uncertainties as they provide useful information about different data types and map updating procedures. A combination of image processing and GIS techniques are used in order to produce efficient results concerning lake monitoring.

Earth observation techniques can be used for monitoring selected parameters of transnational lake basins. Therefore several parameters are extracted related to the description of catchments, surface areas of lakes, water level, hydrogeology and water quality characteristics (tsm, chl_conc). Uniform results on a transnational area of 4769 km2 have been used to update the GIS database. Additionally the methodology is cost effective because it can be used in conjunction with in situ observations and hydrological modelling. The remotely sensed observations have the potential to significantly improve the understanding of hydrological processes affecting lake basins in response to climate variability and anthropogenic impact. Finally results show that action should be taken in order to preserve these valuable, in terms of biodiversity lakes.

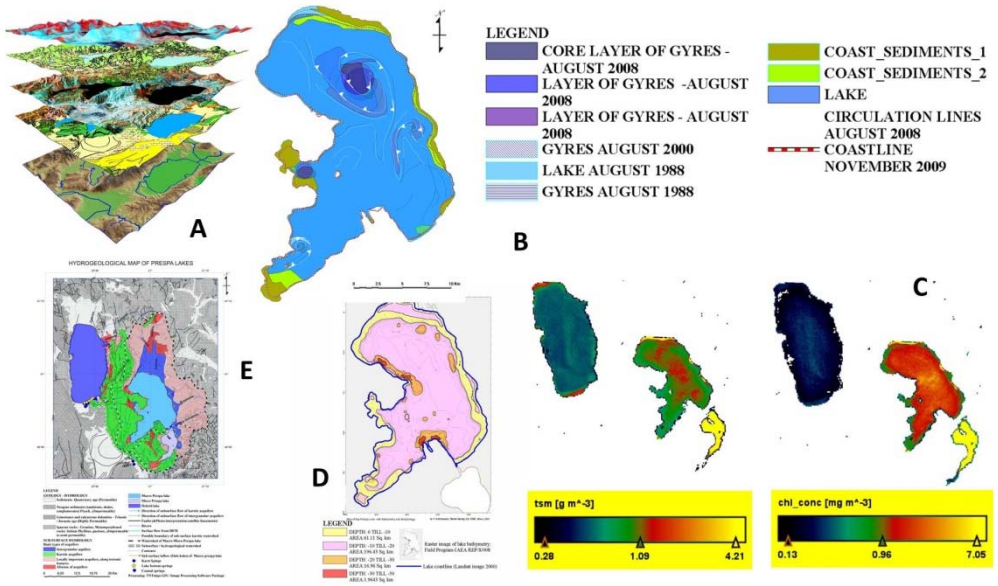

Figure 1 **A:** GIS **B:** Decadal trends of Macro Prespa lake hydraulics, circulation patterns as detected in the multi temporal VIS & TIR Landsat data **C:** Total suspended sediments & Chlorophyll **D:** Lake bathymetry **E:** Hydrogeological map

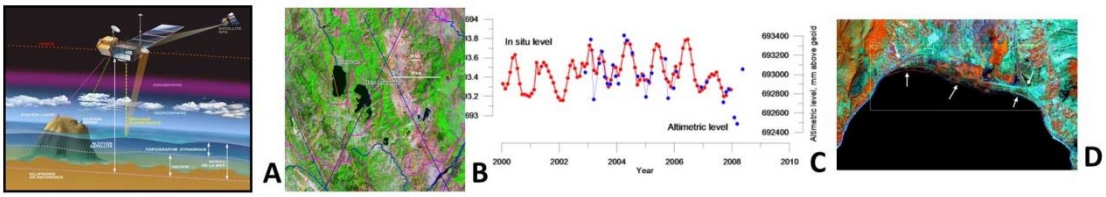

Figure 2 **A:** Radar altimetry principle **B:** Satellite ground tracks for T/P, Jason, GFO, Envisat **C:** In situ (red line and dots) and altimetric (blue line and dots) water level time series for Ochrid lake **D:** Macro Prespa lake has lost nearly 19.5 km2 of its surface in the period 1973 to 2008.

ACKNOWLEDGEMENT

*Application of Radar altimetry has been supported by A. Kouraev of LEGOS_OMP/SOI laboratory at Toulouse, France. **Aspects of the GIS system have been formulated by E. Katsimpra in the context of her M.Sc Thesis in the University of Athens – Geology Department.

UAV photogrammetry for coastal areas monitoring

Kogkas S.[1], Kozarski D.[1], Nikolakopoulos K.G.[1]

[1]*University of Patras, Department of Geology, Patras, Greece,*
stefanos.kogkas@gmail.com, dimitris.kozarski@gmail.com knikolakop@upatras.gr

INTRODUCTION

The coastal areas in the Patras Gulf suffer degradation due to the sea action and other natural and human-induced causes. Changes in beaches, ports, and other man made constructions need to be assessed, both after severe events and on a regular basis, to build models that can predict the evolution in the future. Thus, reliable spatial data acquisition is a critical process for the identification of the coastline for geologists and other scientists involved in the study of coastal morphology. High resolution satellite data, airphotos and airborne Lidar provided in the past the necessary data for the coastline monitoring. High-resolution digital surface models (DSMs) and orthophoto maps had become a necessity in order to map with accuracy all the variations in costal environments. Recently, unmanned aerial vehicles (UAV) photogrammetry offers an alternative solution to the acquisition of high accuracy spatial data [1], [2], [3], [4], [5]. This paper presents the use of UAV to map the coastline in Rio area Western Greece. Multiple photogrammetric aerial campaigns were performed. A small commercial UAV (DJI Phantom 3 Advance) was used to acquire thousands of images with spatial resolutions better than 5 cm. Different photogrammetric software's were used to orientate the images, extract point clouds, build a digital surface model and produce orthoimage mosaics. In order to achieve the best positional accuracy signalised ground control points were measured with a differential GNSS receiver. The results of this study proved that UAVs can replace many of the conventional surveys, with considerable gains in the cost of the data acquisition and without any loss in the accuracy.

STUDY AREA, DATA COLLECTION AND PROCESSING

Study area

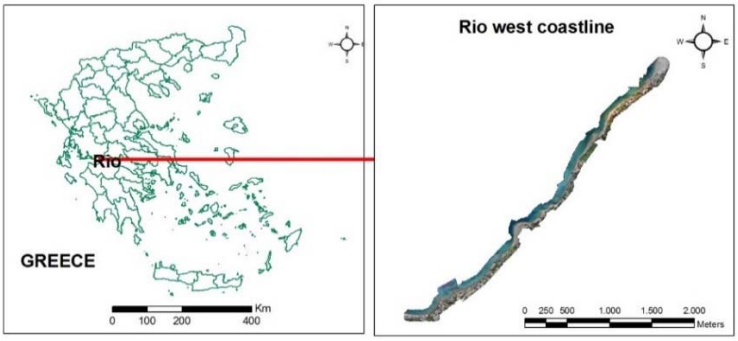

The study area is the west coastline of Rio covering an extent of 4 km in the Patraikos Gulf at the west of Rio-Antirio Bridge (Figure 1). Patraikos Gulf is located in Western Greece between Central Greece and Peloponnese. It is a relatively shallow, sea basin which communicates to the west with the Ionian Sea with a channel of 12 km width and 70m depth and to the east, with the Corinthian bay through the rib of Rio-Antirrio, which is 2 km wide and 66 m deep.

Data collection

Nine double photogrammetric grids were designed in order to cover the whole coastline in Rio, Patras (Figure 2). Every sub area was covered twice (double grid) with the camera focusing at different angle. The first flight was performed with the camera looking at 90 degrees (nadir) and the second one with the camera looking at 60 degrees (Figure 2). All the UAV missions were planned to have an 80% overlap in-track (flight direction) and a 80% cross-track sidelap. Thus, in the study area, most of the points were imaged in nine or more photos (Figure 3). Each flight was performed at 40m above ground level and a total of two thousands ninety (2090) were collected and processed with two different software as described in the next paragraph.

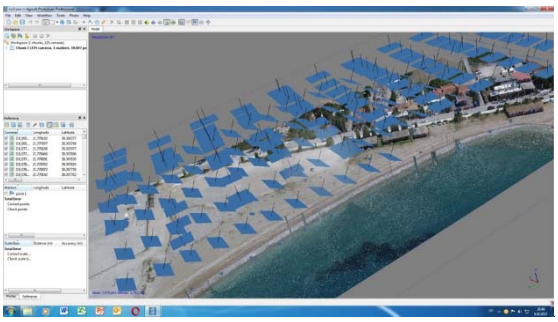

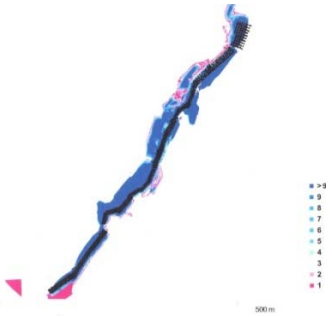

(Figure 2 & Figure 3)

Processing

Agisoft processing workflow

The nine datasets from the UAV campaigns were imported in Agisoft's Photoscan software. As described in detail in a previous study [6], the software employs computer vision techniques along with photogrammetric analysis to perform direct georeferencing or bundle adjustment with GCPs or simple similarity transformation over the whole block without GCPs. As more images are added to the block more points are taken into consideration and ensure the internal block geometry.

Pix4d workflow

The second workflow is also an automated process based on the dense image matching technology [7]. A complete automated integration of tie points measurements, camera calibration, DSM extraction and true orthomosaic production has been implemented through Pix4D Desktop.

CONCLUSIONS

The presented case study proves that the combination of photogrammetric processing of airphotos acquired by an unmanned aerial vehicle with extensive GPS measurements is highly suitable and efficient for coastline monitoring. Both Agisoft and Pix4d software have been tested for the creation of orthophotos and Digital Surface Models with satisfactory results.

REFERENCES

[1] Nikolakopoulos, K. G., Soura, K., Koukouvelas, I. K. and Argyropoulos, N. G., “UAV vs classical aerial photogrammetry for archaeological studies,” J. Archaeol. Sci. Reports 14, 758–773 (2016).

[2] Nikolakopoulos Konstantinos G., Ioannis Koukouvelas, Nikolaos Argyropoulos and Vasileios Megalooikonomou, "Quarry monitoring using GPS measurements and UAV photogrammetry", Proc. SPIE 9644, 96440J, (2015) doi:10.1117/12.2195402.

[3] Themistocleous, K., Neocleous, K., Pilakoutas, K.., Hadjimitsis, D. G., “Damage assessment using advanced non-intrusive inspection methods: integration of space, UAV, GPR, and field spectroscopy,” Proc. of SPIE, 9229, 92291O (2014).

[4] Nikolakopoulos, K. G., Kavoura, K., Depountis, N., Argyropoulos, N., Koukouvelas, I. and Sabatakakis, N., “Active landslide monitoring using remote sensing data, GPS measurements and cameras on board UAV,” Proc. SPIE - Int. Soc. Opt. Eng. 9644, 1–9 (2015).

[5] Papakonstantinou, A., Topouzelis, K. and Pavlogeorgatos, G., “Coastline Zones Identification and 3D Coastal Mapping Using UAV Spatial Data,” ISPRS Int. J. Geo-Information 5(6), 75 (2016).

[6] Skarlatos, D., Procopiou, E., Stavrou, G., Gregoriou, M., "Accuracy assessment of minimum control points for {UAV} photography and georeferencing, " Proc. SPIE 8795, First International Conference on Remote Sensing and Geoinformation of the Environment (RSCy2013), 879514 (2013) doi:10.1117/12.2028988

[7] Tola E., Lepetit V., and Fua P. Daisy, "An Efficient Dense Descriptor Applied to Wide Baseline Stereo" IEEE Transactions on Pattern Analysis and Machine Intelligence, 32(5):815– 830, (2010).

Mapping terrain changes using interferometric DSM from Sentinel-1 data.

Kyriou A [1] and Nikolakopoulos K. [1]

[1] *University of Patras, Department of Geology, Rio, Patras, Greece;; a.kyriou@upnet.gr, knikolakop@upatras.gr*

Abstract

Landslides are one of the greatest natural disasters, affecting both human life and the environment. They occur as a result of natural (earthquakes, volcanic eruptions, intense rains) and man-made (deforestation, man-made vibrations) factors, while landslide's investigation and monitoring are key aspects. Over the last years, satellite's observations have been successfully used in landslide research. One of the most promising techniques in landslide investigation is interferometry, which obtains information about Earth's surface through measurements of the phase of the backscattered radar's signal. In this context, several studies have been drawn up with the early attempts concentrating on land deformation via interferometric procedure using data from ERS-1/ERS-2 missions [1]. In respective studies, ERS data were exploited for land subsidence monitoring in Germany, Mexico and Italy [2], while ERS, Envisat ASAR data in comparison with a limited set of high resolution TerraSA-X data, covering a Czech area were interferometric processed with the same aim [3]. Over time new interferometric approaches were developed in order to achieve high accuracy results. The more widely used approach in landslide monitoring is Persistent Scatterer Interferometry (PSI), so several studies have dealt with this issue. Specifically, the key aspects of the process of monitoring the deformation after the occurrence of landslides using PSI technique have already described and applied in numerous case studies [4], [5], [6]. In this context several studies correlated the results of the PSI with data of conventional techniques such as GPS data or in situ monitoring instrumentation in order to achieve higher accuracy results or validation of the existing one [7], [8]. The newest Sentinel-1 mission and its short repeatability gave new impetus to the landslide research, leading to more systematic monitoring of areas of instability. Thus, studies have been carried out presenting the main aspects of the interferometric processing of Sentinel-1 data [9], [10], while in a respective study Sentinel-1 data were exploited in order to update inventory maps and to monitor landslide activity [11]. This work focuses on interferometric Digital Surface Model (DSM) generation using Sentinel-1 data, in order to map terrain changes after the occurrence of a landslide. In that context, many Sentinel-1 scenes were acquired covering two landslide zones located in the settlements of: a) Klepa, Aitoloakarnania Prefecture and b) Moira, Achaia Prefecture. Regarding the specific methodology, interferometric DSM accuracy has already been tested in several studies utilizing data from different missions (ERS-1/ERS-2, Envisat, TerraSAR-X, Cosmo-Skymed etc) [12], [13].

The basic idea was to evaluate Sentinel-1 data for mapping terrain changes caused by landslide by comparing two interferometric DSMs, one before the occurrence of the event and one after that. Concerning the first study area, sixteen Sentinel-1 images from both ascending and descending pass were acquired covering the period before the manifestation of the landslide (October 2014 - January 2015), while sixteen more images following the landslide event (February 2015- April 2015) were also used. Interferometric processing delivered two DSMs one before and one after the landslide occurrence. The comparison of the generated DSMs implemented through the creation of elevation profiles which were drawn across to the forehead of the slide. In all elevation profiles, a small subsidence of the terrain in the DSM after the landslide was observed, and the terrain changes were estimated around 3 meters. Regarding the second study area, a similar procedure was applied. Specifically, fifteen Sentinel-1 images covering Moira region before the landslide were acquired and processed via interferometric technique for DSM creation, while fifteen images after the manifestation of the slide (January 2017) were interferometric processed, yielding to a second DSM. However, in this case study the elevation profiles presented greater terrain changes as the elevation difference ranges between 5 to 30 meters and they are related to the actual changes.

Generally, the evaluation of the results demonstrates that the specific approach is able to give an estimation of the variations of Earth's surface after the occurrence of the landslide. It was proven that terrain changes may be mapped using interferometric DSMs, however the results are more qualitative due to the reduced accuracy of Sentinel-1 DSMs.

References

[1] Gens, R. & Van Genderen, J.L., 1996. SAR interferometry—issues, techniques, applications, International Journal of Remote Sensing (17), pp. 1803–1835.

[2] Strozzi T., Wegmiiller U., Tosl L., Bitelli G. & Spreckels V., 2001. Land Subsidence Monitoring with Differential SAR Interferometry, Photogrammetric Engineering & Remote Sensing, Vol. 67, No. 11, pp. 1261-1270.

[3] Lazecký M., Rapanta P., Perissinb D. & Bakoň M., 2014. Deformations of highway over undermined Ostrava-Svinov area monitored by InSAR using limited set of SAR images, Proceedings of CENTERIS 2014 conference.

[4] Crosetto M., Gili J.A., Monserrat O., Cuevas-Gonz´alez M., Corominas J., Serral D., 2013. Interferometric SAR monitoring of the Vallcebre landslide (Spain) using corner reflectors, Nat. Hazards Earth Syst. Sci., 13, 923–933, doi:10.5194/nhess-13-923-201

[5] Fu W., Guo H., Tian Q., Guo X., 2010. Landslide monitoring by corner reflectors differential interferometry SAR, International Journal of Remote Sensing, 31:24, 6387-6400, DOI: 10.1080/01431160903413713

[6] Wasowski J. & Bovenga F., 2014. Investigating landslides and unstable slopes with satellite Multi Temporal Interferometry: Current issues and future perspectives, Engineering Geology, Volume 174, Pages 103-138, https://doi.org/10.1016/j.enggeo.2014.03.003

[7] Fan J., Xia Y., Zhao H., Li M., Wang Y., Guo X., Tu P., Liu G., Lin H., 2014. Monitoring of landslide deformation based on the coherent targets of high resolution InSAR data, Remote Sensing of the Environment: 18th National Symposium on Remote Sensing of China, Proc. of SPIE Vol. 9158, 91580K, doi: 10.1117/12.2064013

[8] Tofani V., Raspini F., Catani F., Casagli N., 2013. Persistent Scatterer Interferometry (PSI) Technique for Landslide Characterization and Monitoring, Remote Sensing, 5, 1045-1065; doi:10.3390/rs5031045

[9] Devanthérya N., Crosetto M., Cuevas-González M., Monserrat O., Barra A., Crippa B., 2016. Deformation monitoring using Persistent Scatterer Interferometry and Sentinel-1 SAR data, Procedia Computer Science, Volume 100, 2016, Pages 1121-1126, https://doi.org/10.1016/j.procs.2016.09.263

[10] Yague-Martinez N., Prats-Iraola P., Rodriguez Gonzalez F., Brcic R., Shau R., Geudtner D., Eineder M., Bamler R., 2016. Interferometric Processing of Sentinel-1 TOPS Data, IEEE Transactions on Geoscience and Remote Sensing 54(04):1-15, doi: 10.1109/TGRS.2015.2497902

[11] Barra A., Monserrat O., Mazzanti P., Esposito C., Crosetto M., Scarascia Mugnozza G., 2016. First insights on the potential of Sentinel-1 for landslides detection, Geomatics, Natural Hazards and Risk, 7:6, 1874-1883, DOI: 10.1080/19475705.2016.1171258

[12] Crosetto, M., Monserrat, O., Cuevas, M. & Crippa, B., 2011. Spaceborne differential SAR interferometry: Data analysis tools for deformation measurement. Remote Sensing (3), pp. 305–318.

[13] Jiang, H., Zhang, L., Wang, Y. & Liao, 2014. Fusion of high-resolution DEMs derived from COSMO-SkyMed and TerraSAR-X InSAR datasets. J. Geod. (88). pp. 587–599.

Assessment of landslide susceptibility using geospatial analysis and interferometry data, in the mountainous municipalities of Nafpaktia and Karpenisi

Krassakis P. [1], Loupasakis C. [2,1]

[1]*School of Science and Technology , Hellenic Open University, Patra, Greece.*
[2] *School of Mining and Metallurgical Engineering, National Technical University of Athens, Athens, Greece.*
krassakis@certh.gr, cloupasakis@metal.ntua.gr

ABSTRACT

Landslides globally have caused major socioeconomic and environmental impact annually. Climate change and occasional extreme weather events combined with human activities have increased the number of observed landslides in global scale. According to the Emergency Disasters Data Base (EM-DAT), landslides events per continent, have killed totally over 60000 people and produced over 3500 million US$ in damage in the period between 1903 and 2004 (Fig. 1).

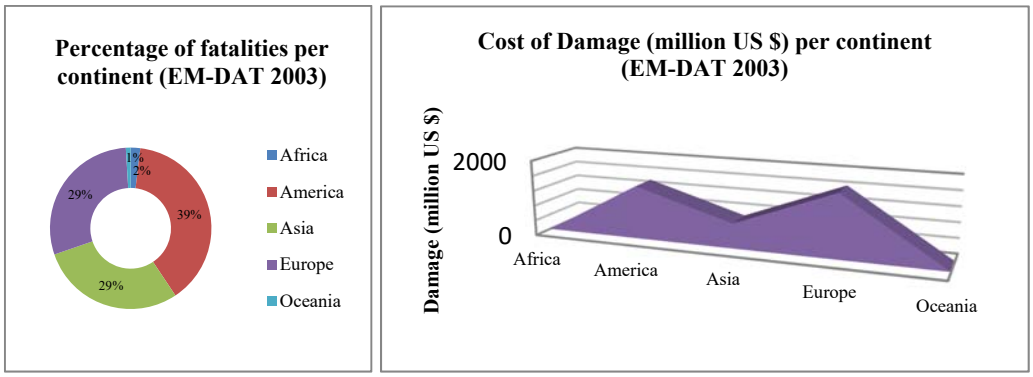

***Fig. 1** : Number of fatalities and cost of damage from landslides during 1903 to 2004, sorted by continents (Source: EM-DAT: The OFDA/CRED International Disaster database)*

The main purpose of the current study, was to examine the assessment of landslide susceptibility in the mountainous Municipalities of Nafpaktia and Karpenisi (Central Greece) by using geospatial analysis and interferometry data.

These areas suffer from multiple landslide events because of its tectonic and geological settings (East Pindos flysch, argillites and siltstones), while high intensity and long lasting rainfall episodes have been most of the times the triggering factor. In fact, the landslide events evaluated in the current study took place during a high precipitation three days episode of the first quarter of 2015.

The applied method for the landslide susceptibility mapping was based on the combination of Rock Engineering System (RES) (semi-quantitative methodology) and persistent scatterers interferometry (PSI) technique.

The base methodology for developing the map of landslide susceptibility was based on semi-quantitative implementation of Rock Engineering System (RES), in order to identify the prone areas. Landslide susceptibility assessment forms the basis of any hazard mapping, which is one of the essential parts of quantitative risk mapping.

First step of the process, was the identification of the events and construction of the landslide inventory map. For this purpose 159 landslide events were recorded in the study area. The locations of the landslide phenomena were identified from various scientific publications, technical reports, public sources and satellite image processing using Landsat 8, Sentinel, as long as E.S.R.I. Imagery.

Next step, was the evaluation of ten critical factors, including altitude, slope, aspect, lithology, NDVI, land cover, distance to drainage, precipitation, distance to fault, and distance to road. The following step was the creation of the 10x10 Interaction Matrix, a basic tool for RES approach as long as Matrix coding, a semi - quantitative method to rate the influence of a particular parameter on all the other parameters, based on experts judgment.

Therefore, classification of all 10 factors in 5 values from 0 to 4 (range of stable to unstable slopes) was the final step of the procedure for the preparation and construction of the landslide susceptibility map (Fig. 2). Finally, interferometry data of persistent scatterers (PSI) was analyzed for monitoring slope deformations with millimetric precision. Produced results show areas with ground deformations that could correspond with landsliding area.

Examining the output of the RES method, very high percentage of landslide events (> 74%) were located in zones of very high and high landslide susceptibility. 15.72% and 26.86% of the total area corresponds to high and very high landslide susceptibility areas. Additionally, 116 landslide events out of 159 have been located in very short distance from road network (up to 10 meters). This result indicating how strong is the spatial relationship between a landslide occurrence and road network, validating that a produced susceptibility map could be an efficient tool for the landslide risk management of the examined area.

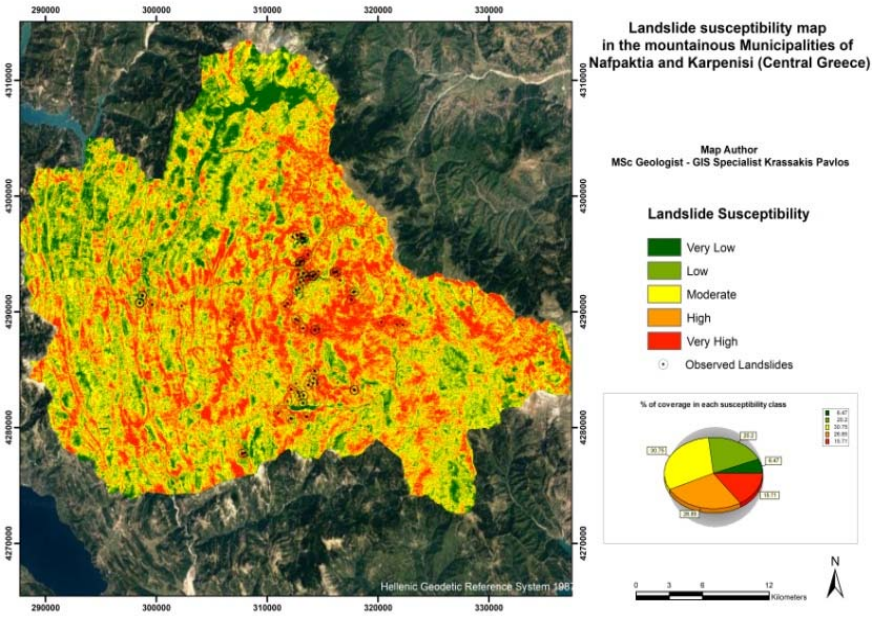

***Fig. 2** : Landslide susceptibility map of the study area*

REFERENCES

Tsangaratos, P., 2012. Research on the engineering geological behavior of the geological formations by the use of information systems. PhD Thesis, NTUA, Athens, pp. 363 (in Greek with extensive summary in English)

Rozos, D., Bathrellos, G., Skillodimou, H., 2011. Comparison of the implementation of rock engineering system and analytic hierarchy process methods, upon landslide susceptibility mapping, using GIS: a case study from the Eastern Achaia Country of Peloponnesus, Greece.

Investigating land subsidence phenomena by using remote sensing techniques and ground truth engineering geology investigation methods.

Tsangaratos P.[1], Loupasakis C.[1], and Ilia I.[1]

[1] *National Technical University of Athens, School of Mining and Metallurgical Engineering, Department of Geological Studies, Zografou Campus, Heroon Polytechniou 9, 15780 Zografou, Greece; ptsag@metal.ntua.gr, cloupasakis@metal.ntua.gr, gilia@metal.ntua.gr*

ABSTRACT

Land subsidence is a geological hazardous phenomenon that mainly occurs as a consequence of a number of physical and human related activities [1]. During the past decades numerous studies have been conducted concerning areas that experience ground subsidence phenomena especially due to aquifers over-exploitation within the territory of Greece. Thessaly Plain is among the areas in which land subsidence has been related to reservoir compaction with cases observed since the early 90's [2, 3, 4, 5, 6, 7]. The main objective of the present study was to investigate land subsidence in the wider area of Farkadona Municipality in the Trikala regional unit, Thessaly, Greece, by utilizing remote sensing techniques and conventional engineering geology investigation methods. This involved defining the geological, hydrogeological and tectonic settings of the wider research area and analyzing a set of Synthetic Aperture Radar images processed with the Persistent Scatterer Interferometry (PSI) technique. Concerning the PSI data, they were derived from a descending data set provided by the German Space Agency acquired in 1995–2003 by the European Space Agency satellites ERS1 and ERS2 [8]. From the conducted PSI analysis, 13,895 PSs were identified in the data set acquired at the descending orbit of ERS1/2 from 29/4/1995 to 05/10/2003, within the municipality of Farkadona. The Line of Sight displacement rates vary from +15.48 to −14.13 mm/year. The analysis of the velocity of the PSI data showed that with a threshold of ±1.50 mm/yr, the stable PSs are 94.86 % of the total number of PSs. About 3.61 % of the PSs shows a downwards velocity greater than -1.50 mm/yr, indicating subsiding movement (Fig.1).

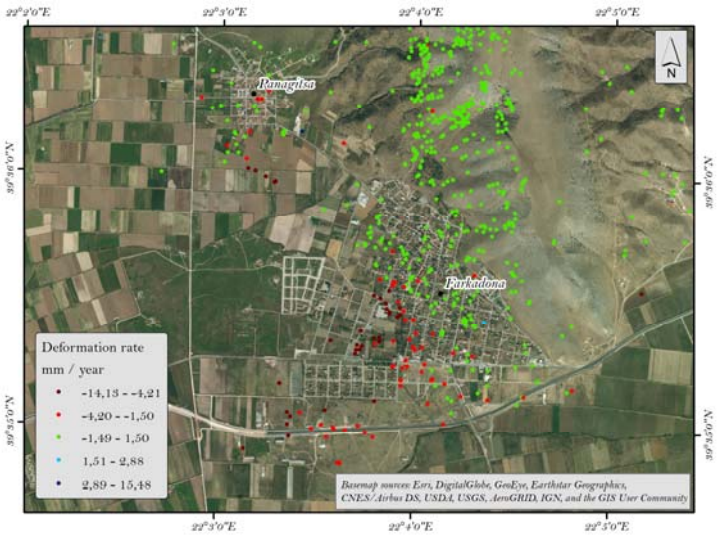

Fig.1. PSI deformation rate measurements

Concerning the water table from the nearby monitoring wells, and based on measurements that refer to a period between 1995 and 2003, it appears that there is a temporal trend in the fluctuation of the water table. During each year a drawdown and upward motion of the water table level takes place between the dry and wet season, reaching up to 16 m, whereas after 2009 a clear decline is obvious (Fig.2).

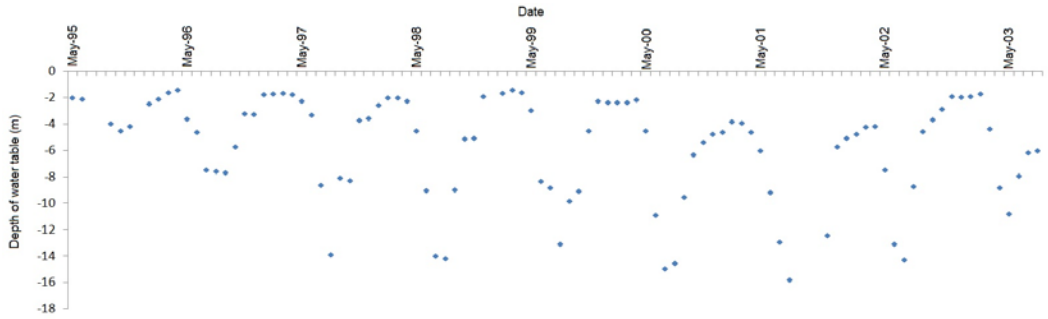

Fig 2. Piezometric level variation (1995–2003) for water well D27

The results of the study indicated a clear trend between the thickness of the loose Quaternary deposits and the deformation rate. Areas that the loose Quaternary deposits have thickness greater than 50 m are more likely to have deformation rate less than -3.00 mm/year. Moreover, areas that are covered with highly compressible Quaternary geological formations have also high deformation rates. Increasing subsidence rates are observed at almost the entire area within the city complex of Farkadona, which is covered by loose Quaternary sediments of considerable depth. In most cases, the increased deformation rates have caused damages in the form of tensile cracks, mainly along the road network and adjacent buildings.

REFERENCES

[1] Loupasakis, C., Agelitsa, V., Rozos, D. and Spanou, N. Mining geohazards—land subsidence caused by the dewatering of opencast coal mines: The case study of the Amyntaio coal mine, Florina, Greece. Natural Hazards, Springer, 70, 675–691 (2014).

[2] Soulios, G. Subsidence de terrains alluviaux dans le sud-est de la plaine de Thessalie, Grèce. Proceedings International Symposium on Engineering Geology and the Environment. Balkema, Rotterdam (1997).

[3] Ganas, A., Salvi, S., Atzori, S. and Tolomei, C. Ground deformation in Thessaly, Central Greece, retrieved from Differential Interferometric analysis of ERS-SAR data, 11th International Symposium on Natural and Human Induced Hazards & 2nd Workshop on Earthquake Prediction, Patras, Greece, 41, 22–25 (2006)

[4] Rozos, D., Sideri, D., Loupasakis, C. and Aposolidis, E. Land subsidence due to excessive ground water withdrawal. A Case Study from Stavros—Farsala Site, West Thessaly Greece. In: Proceedings of the 12th International Congress, Patras, Greece (2010).

[5] Vassilopoulou, S., Sakkas, V., Wegmuller, U. and Capes, R. Long term and seasonal ground deformation monitoring of Larissa plain (central Greece) by Persistent Scattering Inferferometry, Central European Journal of Geoscience, 5, 61-76 (2013).

[6] Modis, K. and Sideri, D. Spatiotemporal estimation of land subsidence and ground water level decline in West Thessaly basin, Greece, Natural Hazards, 76, 939-954 (2015).

[7] Ilia, I., Loupasakis, C. and Tsangaratos, P. Assesing ground subsidence phenomena with Persistent Scatterer Interferometry data in Western Thessaly, Greece. 14th International Congress of the Geological Society of Greece, At Thessaloniki, Greece, Volume: Volume L (2016).

[8] Adam, N., Rodriguez Gonzalez, F., Parizzi, A. and Liebhart, W. Wide area persistent scatterer Interferometry, Proceedings of IGARSS, Vancouver, Canada (2011).

A FEASABILITY STUDY TO ESTIMATE VERTICAL DEFORMATION IN THE CENTRAL SOUTHERN MARGIN OF THE GULF OF CORINTH USING DIGITAL ELEVATION MODELS

Panoutsopoulos G.[1], Sykioti O.[2], Kranis H.[1], Skourtsos Em.[1], Elias P.[2]

1 Department of Geology and Geoenvironment, National and Kapodistrian University of Athens, Panepistimioupolis 15784 Zografou, Athens, Greece. geopanoutsop@geol.uoa.gr, hkranis@geol.uoa.gr, eskourt@geol.uoa.gr

2 Institute for Astronomy, Astrophysics, Space Applications & Remote Sensing, National Observatory of Athens, 15236 Penteli, Greece. sykioti@noa.gr, pelias@noa.gr

ABSTRACT

This study is a first effort to estimate the potential of Digital Elevation or Terrain Models (DEM, DTM), to measure the vertical axis deformation in the Central Southern margin of the Gulf of Corinth (Greece) in a period of 40 years. This is the period that separates the production year of the topographic maps of the Hellenic Military Geographical Service (HMGS) (1967) from the production year of the National Cadastre & Mapping Agency S.A. (NCMA S.A.) orthophotomaps (2007). The area is known to present a general maximum uplift rate of the order of ~3 mm/yr during the Holocene (Pirazzoli *et al.* 2004).

The study area is located along the coast of the central southern part of the Gulf of Corinth, aiming to the residual marine terraces between the towns of Xylokastro (east) and Derveni (west). It is dominated by Plio-Pleistocene syn-rift deposits, which consist of fluvio-lacustrine facies and Gilbert type fan deltas and have been uncoformably deposited on the alpine basement of Pindos and Tripolis Units. The major faults that control the area are the active onshore normal faults of Derveni – Lykoporia and the East Xylokastro and the inactive offshore normal West Xylokastro Fault (Fig. 1).

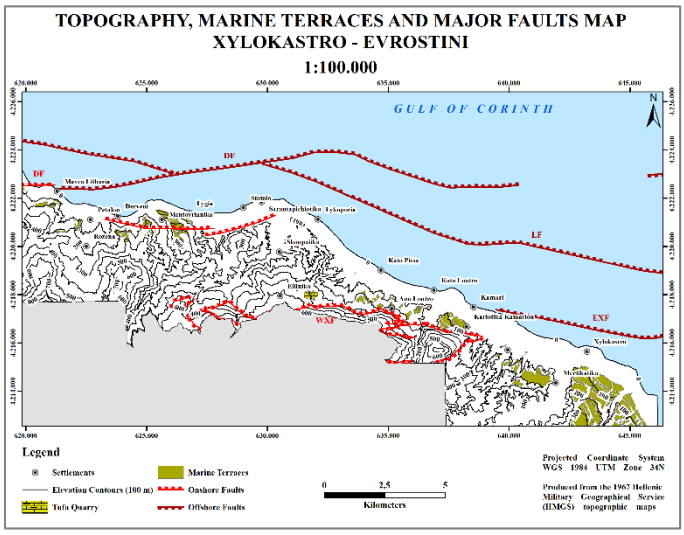

Figure 1. Topography, marine terrace and major faults map of the study area (Armijo *et al.* 1996, Nixon *et al.* 2016).

The main data set consisted of the 5 m cell size DTM, produced by the digitization of the 1:5.000 scale HMGS topographic maps of the area (Fig. 2a), and the 5 m cell size DEM of the NCMA S.A. (Fig. 2b) both projected in WGS 1984 UTM Zone 34N coordinate system. A set of more than 300 stable Geographic Control Points (GCPs) was selected for the co-registration of the two digital models. (Fig. 2). Following, the DEM of Difference ($DoD_{HMGS-NCMA.}$) was calculated by subtracting the two co-registered DEMs (James *et al.* 2012).

Using the same approach, two additional DoDs were produced, one using the ASTER GDEM and one using the SRTM DEM of the area ($DoD_{HMGS-ASTER}$ and $DoD_{HMGS-SRTM,}$ correspondingly). The cell size of these two DoDs is ~28m (Miliaresis & Paraschou, 2005).

The comparison of the three calculated DoDs showed the DoD issued from the subtraction of HMGS and NCMA provided more accurate and detailed results despite the observed NCMA DEM production errors that were difficult to correct (Fig. 3). Additional errors are also induced by the combined use of both DEM (NCMA, ASTER GDEM and SRTM DEM) and DTM (HMGS).

All three DoDs present extreme altitude difference values. This is mainly observed in areas of highly unstable relief. For the other areas, the calculated altitude differences are within reasonable and expected limits.

As reported in previous studies, in the last 40 years a Holocene uplift rate of the order of 3 mm/yr produces a total vertical uplift of 12 cm. This means that it is difficultly detected by the DoD. This value is ~4 times less than the average difference value of $DoD_{HMGS-SRTM.}$ and ~7 times less than the $DoD_{HMGS-NCMA}$ one.

Furthermore, the total observed vertical altitude changes are the result of the combination of several factors, including tectonics, land cover/use changes, human interferences etc. The results of this feasibility study show that the landscape dynamics is a complex phenomenon where tectonic deformation is one component. For this purpose, additional measurements and other auxiliary multisource data have to be utilized and combined in order to calculate the tectonic component from the overall observed vertical altitude differences.

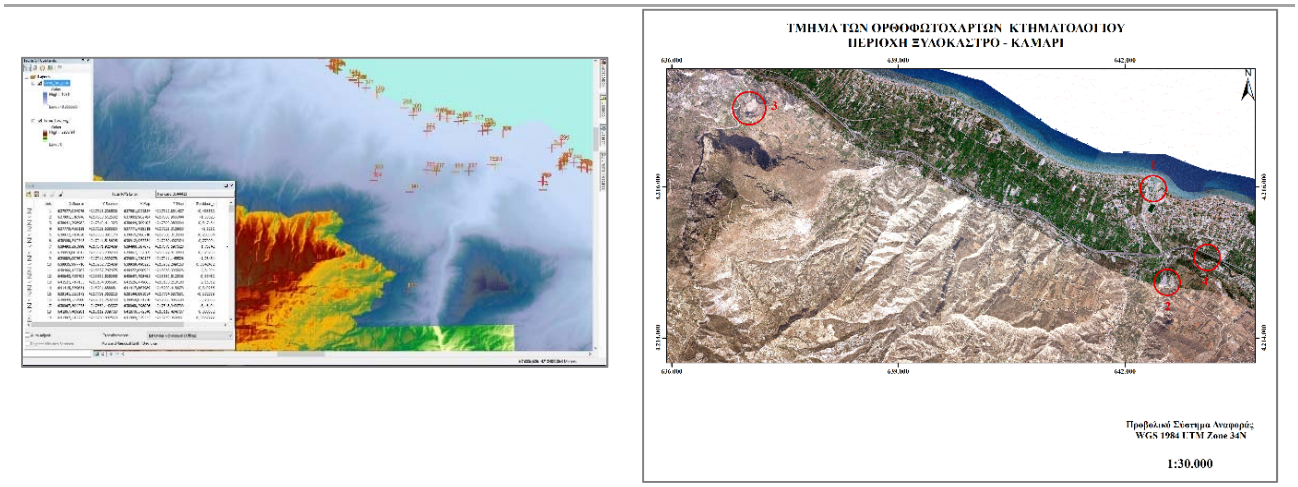

Figure 2. (a) Hill-shaded DTM produced by the digitization of the HMGS topographic maps (blue color) and of the NCMA S.A. DEM. The symbols (red and green crosses) correspond to the GCPs selected (red and green crosses). The bottom left table, shows information on a part of the GCPs. The total RMS error is shown at the bottom left of the table; (b) NCMA orthophotomap (left) at the region of Xylokastro – Kamari. The red circles No. 1, 2 and 3 show areas of human intervention while the circle No. 4 shows vegetation effects. All values in the before mentioned circles and their surrounding areas, occur within the expected and reasonable range. Although not highly visible in the NCMA orthophotomap, the vegetation's expansion is quite distinguishable.

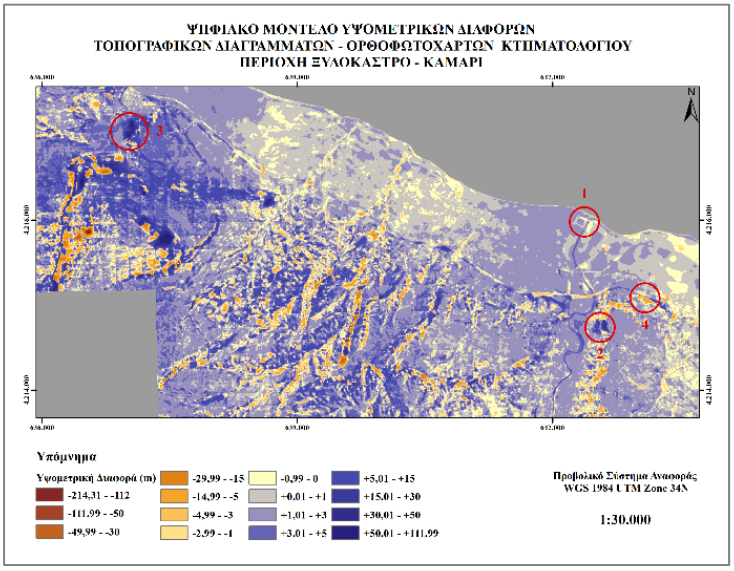

Figure 3. $DoD_{HMGS\ -\ NCMA}$ at the region of Xylokastro – Kamari. The red circles No. 1, 2 and 3 show areas of human intervention while the circle No. 4 shows vegetation effects. Red circles and surrounding areas values, as in fig. 2b.

REFERENCES

Armijo R., Meyer B., King G.C.P., Rigo A. and Papanastassiou D. (1996). Quaternary evolution of the Corinth Rift and its implications for the Late Cenozoic evolution of the Aegean, Geophys. J. Int., 126, 11–53.

James L.A., Hodgson M.E., Ghoshal S. and Megison Latiolais M. (2012). Geomorphic change detection using historic maps and DEM differencing: The temporal dimension of geospatial analysis. Geomorphology 137 (2012), 181–198.

Miliaresis G.Ch. and Paraschou Ch.V.E. (2005). Vertical accuracy of the SRTM DTED level 1 of Crete. International Journal of Applied Earth Observation and Geoinformation, 7 (2005), 49–59.

Nixon C.W., McNeill L.C., Bull J.M., Bell R.E., Gawthorpe R.L., Henstock T.J., Christodoulou D., Ford M., Taylor B., Sakellariou D., Ferentinos G., Papatheodorou G., Leeder M.R., Collier R.E.L., Goodlife A.M., Sachpazi M. and Kranis H. (2016). Rapid spatio-temporal variations in rift structure during development of the Corinth Rift, central Greece. Tectonics, 35, 1225–1248.

Panoutsopoulos, G. (2017). Morphotectonic study of the central southern margin of the Gulf of Corinth. MSc thesis, National and Kapodistrian University of Athens. Faculty of Geology and Geoenvironment, Department of Dynamic, Tectonic and Applied Geology.

Pirazzoli P.A., Stiros S.C., Fontugne M. and Arnold M. (2004). Holocene and Quaternary uplift in the central part of the southern coast of the Corinth Gulf (Greece). Mar. Geol., 212, 35–44.

Ionospheric Anomalies prior to Recent Strong Earthquakes in Greece observed by CGPS Data

Vlachou K.[1]

[1] *Department of Geography, Harokopeio University, Athens, Greece, kvlachou@hua.gr*

ABSTRACT

The relationship between strong earthquakes (Mw>6) which have recently occurred in Greece and the observed ionospheric anomalies is investigated. The applied methodology is based on the propagation effect of the Global Positioning System (GPS) satellite transmitted signal through Ionosphere as defined in Electromagnetic Wave Propagation and Plasma Theory. Time-series of vertical total electron content (VTEC) were extracted over continuously recording GPS ground stations located inside each earthquake preparation zone. A statistical analysis of VTEC values, as estimated over each CGPS station, was additionally carried out during earthquake periods to identify ionospheric disturbances. The present research revealed anomalous ionospheric variations a few days prior to the examined seismic events: i) the Mw=6.1 (January 26th, 2014) and Mw=5.9 (February 3rd, 2014) Cephalonia Earthquakes and ii) the Mw=6.8 (May 24th, 2014) North Aegean Earthquake. Positive deviations lasting up to 12 hours, that account for 40-80% enhancement of the daily measured VTEC values relative to non-disturbed conditions, were clearly detected at the nearest to the seismic epicenters stations. Considering the prevailing quiet geomagnetic conditions, it is concluded that the observed ionospheric anomalies may constitute precursors associated with the Cephalonia and the North Aegean Earthquakes.

ACKNOWLEDGEMENT

Author would like to thank: i) the Geodynamic Institute of National Observatory of Athens for providing CGPS data (http://www.gein.noa.gr/services/GPS/noa_gps.html) and ii) the German Research Center for Geosciences in Potsdam (http://www.gfz-potsdam.de) and the World Data Center for Geomagnetism in Kyoto (http://wdc.kugi.kyoto-u.ac.jp) for providing geomagnetic indices.

The algorithm used in the present study for TEC estimation has been developed as part of author's PhD research at Geophysics & Geothermics Department of National & Kapodistrian University of Athens that was co-financed by the European Union (European Social Fund – ESF) and Greek national funds through the Operational Program "Education and Lifelong Learning" of the National Strategic Reference Framework (NSRF) - Research Funding Program: Heracleitus II. Investing in knowledge society through the European Social Fund.

REFERENCES

Baran L.W., Shagimuratov I.I. & Tepenitzyna N.Y., 1997. The use of GPS for ionospheric studies. Artif. Satellites, J. Planet. Geode., 32(1), pp. 49-60.

Dach R., Hugentobler U., Fridez P. & Meindl M., 2007. Bernese GPS Software Version 5.0. Astronomical Institute, University of Bern, Bern, Switzerland, pp. 612.

Dobrovolsky I.P., Zubkov S. I. & Miachkin V. I., 1979. Estimation of the size of earthquake preparation zones. Pure Appl. Geophys., 117(5), pp. 1025-1044.

Ouzounov D.P., Pulinets S.A., Davidenko D.A., Kafatos M. & Taylor P.G., 2013. Space-borne observations of atmospheric pre-earthquake signals in seismically active areas. Case study for Greece 2008-2009. Thales, Special issue in honor of Prof. Emeritus Michael E. Contadakis, 1, pp. 259-265.

Pulinets S.A., Leyva Contreras A., Bisiacchi-Giraldi G. & Ciraolo L., 2005. Total electron content variations in the ionosphere before the Colima, Mexico, earthquake of 21 January 2003. Geofis. Int., 44(4), pp. 369-377.

Pulinets S. & Davidenko D., 2014. Ionospheric precursors of earthquakes and Global Electric Circuit. Adv. Space Res., 53(5), pp. 709-723. doi:10.1016/j.asr.2013.12.035.

Ruzhin Y.Y. & Depueva A.K., 1996. Seismoprecursors in space as plasma and wave anomalies. J. Atmos. Electr., 16(3), pp. 271-288.

Investigation Land Subsidence Phenomena of the Thriassio Basin using Radar Interferometry Techniques

Kaitantzian A.[1], Loupasakis C.[1], Parcharidis I.[2]

[1]*School of Mining and Metallurgical Engineering, National Technical University of Athens, ankait@metal.ntua.gr, cloupasakis@metal.ntua.gr*
[2]*Department of Geography, Harokopio University of Athens, parchar@hua.gr*

ABSTRACT

The identification of geohazard potential in large plane areas, subject to rapid urban and industrial growth, is important for the urban and infrastructures planning as well as for the risk management. Land subsidence phenomenon has been identified as one the most severe geological hazards affecting these areas. Numerous studies have been contacted during the last decades worldwide concerning areas that experience this phenomenon. Some examples include Italy [1], USA [2], China [3] and Mexico [4]. In Greece, this phenomenon has been observed in areas such as the Kalochori region [5], the Anthemounta plain [6], the Thessaly plain [7], the Amyntaio basin [8-9] and has caused significant damage to buildings and infrastructure.

The main objective of the current study is to employ state of the art Synthetic Aperture Radar Interferometry (SAR) techniques to monitor ground deformations in the Thriassio basin in the western part of the city of Athens. A dataset of ERS1&2 and ENVISAT ASAR images have been processed with the Persistent Scatterer Interferometry (PSI) analysis and hybrid interferometric technique (Singular Value Decomposition algorithm). The interferometric results have been correlated with the geological, geotechnical and hydrogeological conditions of the study area in order to interpret the land subsidence mechanism and to detect its causal factors.

In the 1992–2001 period, LOS deformation rates between -3 and -10 mm/yr have been observed at the entire area extending northwest of the Aspropyrgos town, where the thickest layer of loose Quaternary sediments occur. On the contrary, from the period 2002-2010 in the northern west part of the Thriassio basin and in the Elefsis town LOS deformation rates reaches the up to -3mm/yr were observed (Fig.1a,b).

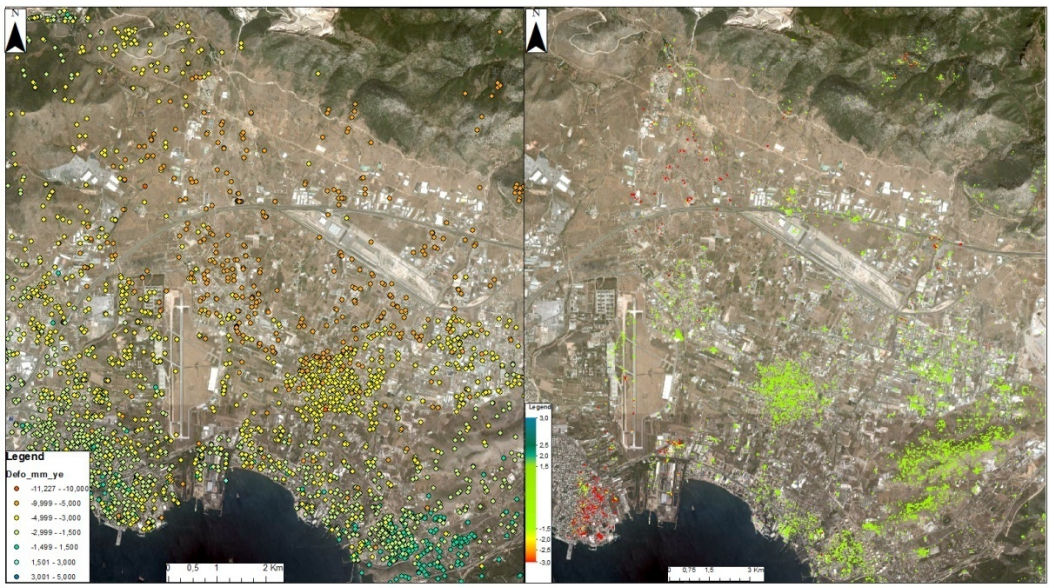

Fig.1. a) Velocities from 1992 to 2001 as derived by the PSI analysis of ERS1&2 data. b) Velocities from 2002 to 2010 as derived by the SVD analysis of ENVISAT data.

Considering the isopiezometric curves map of October 1999 (Fig 2a), it can be easily identified that the depression cones caused by the private industrial drills are related with the areas affected by land subsidence. In addition, comparing the isopiezometric curves of 1999 and 2016, a ground water drawdown that reaches 16m northwest of the study area is observed (Fig.2b). The level of the piezometric surface in the Thriassio basin presented significant rise at the entire basin during the time period 2006 to 2008.

The outcomes of the performed analysis indicated that the land subsidence phenomena must be attributed primarily to the exploitation of groundwater reservoir, resulting to the consolidation fine-grain Quaternary formations.

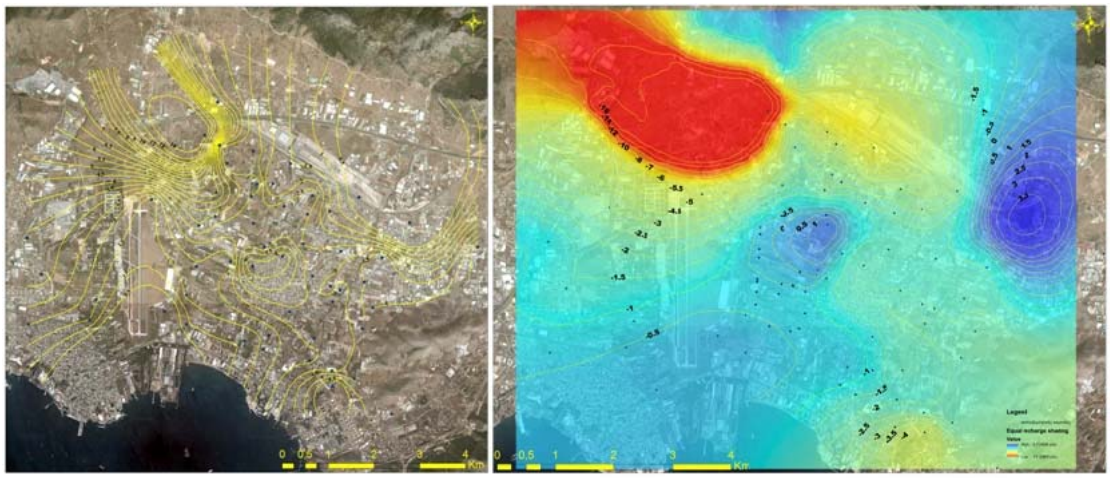

Fig. 2. a) Isopiezometric map October 1999. b) Equal drawdown contours between September 2016 and October 1999.

REFERENCES

[1] Stramondo S., Bozzano F., Marra F., Wegmuller U., Cinti FR., Moro M., Saroli M., 2008. Subsidence induced by urbanisation in the city of Rome detected by advanced InSAR technique and geotechnical investigations, Remote Sens. Environ., 112(6), 3160–3172.

[2] Galloway DL., Hudnut KW., Ingebritsen SE., Phillips SP., Peltzer G., Rogez F., Rosen PA., 1998. Detection of aquifer system compaction and land subsidence using interferometric synthetic aperture radar, Antelope Valley, Mojave Desert, California, Water Resou.r Res, 34(10), 2573–2585.

[3] Yang HL., Peng JH., Wang BC., Song YZ., Zhang DX., Li L., 2015. Ground deformation monitoring of Zhengzhou city from 2012 to 2013 using an improved IPTA, Nat. Hazards, http://doi:10.1007/s11069-0151953-x .

[4] Siles GL., Alcerreca-Huerta JC., Lopez-Quiroz P., Hernandez JC., 2015. On the potential of time series InSAR for subsidence and ground rupture evaluation: application to Texcoco and Cuautitlan–Pachuca sub-basins, northern Valley of Mexico, Nat. Hazards, 79(2), 1091–1110.

[5] Svigkas N., Papoutsis I., Loupasakis C., Tsangaratos P., Kiratzi A., Kontoes C., 2016. Land subsidence rebound detected via multi-temporal InSAR and ground truth data in Kalochori and Sindos regions, Northern Greece, Eng. Geol., 209,175–186.

[6] Raspini F., Bianchini S., Moretti S., Loupasakis C., Rozos D., Duro J., Garcia M., 2016. Advanced interpretation of interferometric SAR data to detect, monitor and model ground subsidence: outcomes from the ESA-GMES Terrafirma project, Nat. Hazards, 83, 155–181.

[7] Vassilopoulou S., Sakkas V., Wegmuller U., Capes R., 2013. Long term and seasonal ground deformation monitoring of Larissa Plain (Central Greece) by persistent scattering interferometry, Cent Eur J Geosci, 5, 61–76.

[8] Loupasakis C., Angelitsa V., Rozos D., Spanou N., 2014. Mining geohazards—land subsidence caused by the dewatering of opencast coal mines: the case study of the Amyntaio coal mine, Florina, Greece, Nat, Hazards, 70, 675–691.

[9] Tzampoglou P. and Loupasakis C., 2017. Evaluating geological and geotechnical data for the study of land subsidence phenomena at the perimeter of the Amyntaio coalmine, Greece, Int. J. of Mining Sci. Technology, https://doi.org/10.1016/j.ijmst.2017.11.002 .

Flood Susceptibility Index (FSI)

(A new Index for mapping Flood Susceptibility via RS & GIS)

Stathopoulos N.[1], Kalogeropoulos K.[2], Polykretis Ch.[2], Skrimizeas P.[3], Louka P.[4], Karymbalis E.[2], Chalkias Ch.[2]

[1] School of Mining and Metallurgical Engineering, Sector of Geological Sciences, Laboratory of Technical Geology and Hydrogeology, National Technical University of Athens, Greece, nstath@metal.ntua.gr

[2] Department of Geography, Harokopio University, Athens, Greece, kalogeropoulos@hua.gr, chpolycretis@hua.gr, karymbalis@hua.gr, xalkias@hua.gr

[3] Hellenic National Meteorological Service, Forecasting and Research Division, Greece, panagiotis.skrimizeas@hnms.gr

[4] Department of Natural Resources Development and Agricultural Engineering, Agricultural University of Athens, Greece, p.louka@aua.gr

Abstract

Natural disasters have important impacts in many countries worldwide, with a large number of deaths, destructions in technical works and infrastructure, and dislocations of population. Moreover, due to the significant effects of climate change, these impacts are expected to rise in the upcoming years for a lot of countries. Although, technology and science have developed significantly nowadays, natural disasters keep having disastrous economic, environmental, and human results at a global scale. The study of these phenomena is constant during the last decades and presents augmentation trends (Smith and Petley, 2009). In order to manage adequately their effects, it is of high importance to synthesize risk and hazard maps for both natural and artificial environments (Smith, 2014). Flood mapping is a useful tool for improving short- and long-term assistance in the affected areas directly after the event. The flood danger/risk can be defined at many scales, from universal to local ones. This work describes a new index for mapping the susceptibility of flooding. This index is called Flood Susceptibility Index (FSI) and is based on the use of Remote Sensing (RS) data, GIS modeling and statistical analysis (Stathopoulos et al., 2018). The implementation of the proposed method requires two main categories of spatial data: geographical background data related to flooding and floods inventory. The general research strategy is to calculate the density of floods within classes of each background factor, and then to use these values for the estimation of integrated flood susceptibility index. Accordingly, the mapping of this index can be used for the flood susceptibility zonation. Thus, the research framework includes (a) spatial database creation of the flood-related factors, (b) categorization of these factors, (c) extraction of the flooded areas by analyzing RS imagery, (d) calculation of the flooded areas within each factor category, by using GIS techniques (the output of this step is the calculation of the FSI for each category), (e) integration of FSI values in order to calculate Total FSI for each mapping unit and finally (f) mapping/zonation of the Total FSI in the study area. The flood inventory was extracted from RS imagery. Afterwards, the flood inventory was split into a testing dataset 70% for training the FSI model and the remaining 30%, which was used for validation.

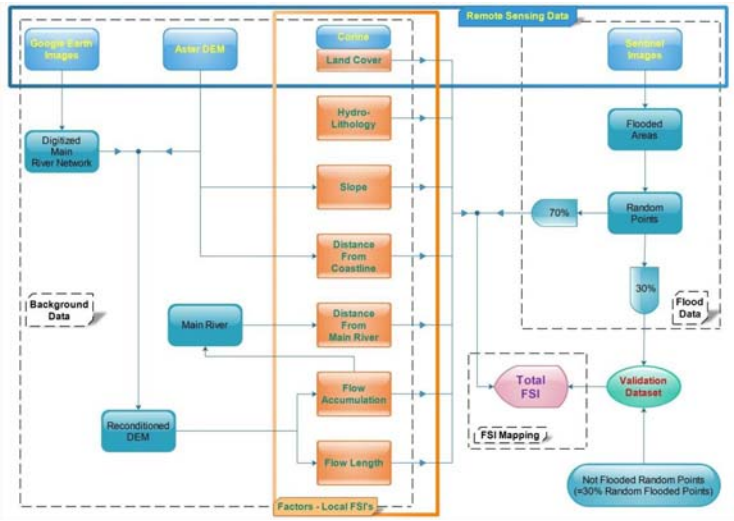

Fig. 1. Flowchart of the methodology

This approach was used to produce flood susceptibility maps of Sperchios river basin, in central Greece. Factors implemented in the proposed analysis include slope, land cover, hydrolithology, flow accumulation, flow length, distance from main river network, and distance from coastline. The primary data used in this work is a) Aster GDEM, b) SENTINEL-1 images, c) Corine Land Cover, d) Google Earth Images,

e) Geological maps and f) Watershed shape file. Flood Susceptibility Index (FSI) defines the importance of a factor category on flood occurrence according to spatial distribution of the pixels of the considered factors and the flooded pixels. This method calculates the FSI for each category of all factors (e.g. land cover, lithology, slope, etc.), which are selected for the case study. Thus, the FSI for the factor category j (FSIj) is defined as follows:

$$FSI_j = \ln\left[\frac{\left(\frac{Npix(S_j)}{Npix(N_j)}\right)}{\left(\frac{\sum Npix(S_j)}{\sum Npix(N_j)}\right)}\right] \quad (1)$$

where Npix (Sj) is the number of flooded pixels in factor category j, and Npix (Nj) is the total number of pixels in the same factor category. Thus, the FSI presents the relative susceptibility to flood occurrence. If a category is highly correlated to flooding, the area associated with this category will have a high positive FSI value. A negative FSI value for a specific category is an indicator of low flooding density in this class. Thus, high positive FSI values indicate FS density in this class much higher than the average and high negative FSI values, indicate FS density much lower than the average. Consequently, for a causal factor to be useful for flood susceptibility mapping, its categories should provide a range of FSI values. The overall susceptibility S for each pixel is defined as:

$$S = \frac{1}{n}\sum_{i=1}^{n} FSI_i \quad (2)$$

where FSIi is the susceptibility for the factor i, and n is the total number of the factors. A typical FSI mapping is presented below, where the map is classified into five classes ("Very Low", "Low", "Moderate", "High" and "Very High" susceptibility) based on "Natural Breaks (Jenks)" classification method. The accuracy was found to be 96.5% indicating an excellent prediction capability for the proposed model.

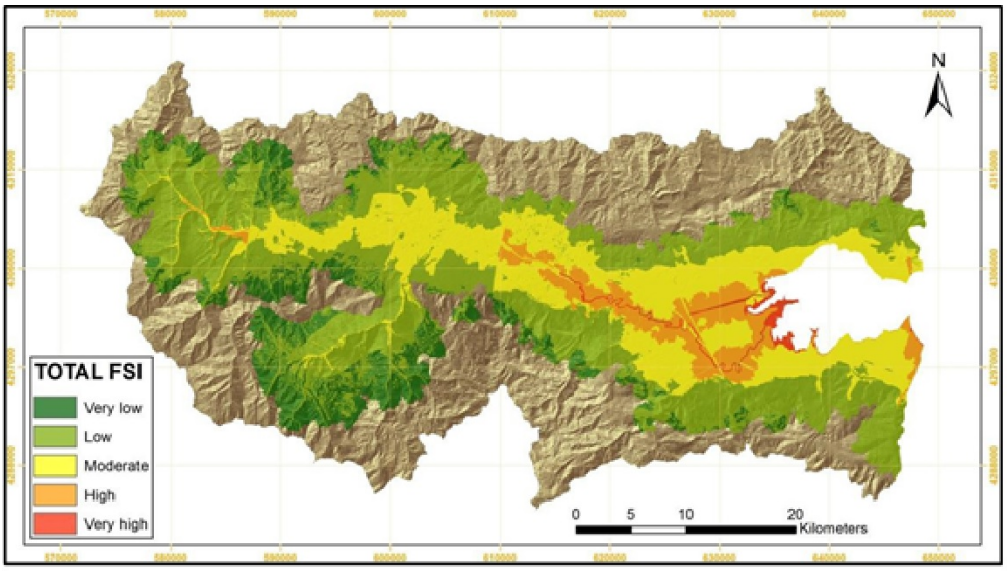

Fig. 2. Total FSI mapping

Keywords: Floods, Remote Sensing, GIS, Flood Susceptibility Index

References

Smith, K., 2014. Regions of Risk: A Geographical Introduction to Disasters, 1st ed. Routledge, Abingdon, UK.

Smith, K., Petley, D. N. 2009. Environmental Hazards: Assessing risk and reducing disaster, 5th ed. Routledge, Abingdon, UK.

Stathopoulos, N., Kalogeropoulos, K., Polykretis, Ch., Skrimizeas, P., Louka, P., Karymbalis, E., Chalkias, Ch., 2018. Introducing Flood Susceptibility Index Using Remote-Sensing Data and Geographic Information Systems: Empirical Analysis in Sperchios River Basin, Greece. In: Petropoulos, G. P. (Eds.), Islam, T. (Ed.). (2018). Remote Sensing of Hydrometeorological Hazards, Boca Raton: CRC Press, 381-400.

Synergy of Sentinel-2 satellite data with an Unmanned Aircraft System (UAS) for precision farming: A pilot vineyard in Greece

Vlachopoulos O.[1]

[1]*National Observatory of Athens, Vas. Pavlou & I. Metaxa, GR-15 236 Penteli, Greece,*

The recent leaps in technological advancements and the capabilities for low cost and high quality equipment has provided the agricultural and scientific community with tools and analytical methodologies that enable rapid, easy and consistent data acquisition for farming purposes.

Site-specific agricultural analysis has been performed for a pilot vineyard in the region of Attiki, Greece, during the important cultivation period of summer (June to August 2017) in regard to possible stress factors, irrigation issues, crop vigor, hydrological behavior etc., utilizing **airborne and space-borne remote sensing techniques**, while developing the **zonal approach** as a potent strategy to address those issues and consequently optimize the cultivation practices.

The current study exercises precision agriculture for vineyards, otherwise called **precision viticulture**. The methodology and the instrumentation utilized have been chosen and engineered in regard to crops specific **spectral reflectance and emissivity characteristics**, employing an **Unmanned Aircraft Systems (UAS)** with thermal and multispectral monitoring capabilities.

A commercial four-band and panchromatic sensor array, the **Parrot SEQUOIA multispectral sensor** and the **radiometric Flir Vue Pro R thermal camera** comprised the remote sensing UAS payloads, performing flights over the ~20ha vineyard area. The specific pilot site has been due to its **high internal variability** .

The multispectral, panchromatic and thermal datasets were processed through a **photogrammetric pipeline** to create orthomosaics of the surveyed area. These orthomaps were employed to extract **Vegetation Indices** like the Normalized Difference Vegetation Index (NDVI), the Red Edge Chlorophyll Index (CI-RedEdge) and others.

The pilot vineyard is also examined for the **temporal variation** of its several characteristics through the open **Sentinel-2 satellite images**, atmospherically corrected, in order to provide a holistic and consistent approach to the remotely sensed vineyards.

The whole procedure has been labored through the open Geographic Information System platform **QGIS** utilizing where needed **Python** and **R** programming languages and the commercial **Pix4D software**.

The **UAS orthomosaic products** and the **satellite multispectral images** of the vineyard were assessed for their information capacity and PV contemporary value. The overall results were highly rich in their information qualities and quantities, highlighting the spatiotemporal variation within the vineyard and providing indications for stress evaluation and optimization strategies through the interpretation of the grapevines specific characteristics, while illustrating the potential of advanced techniques like hyperspectral monitoring, very high resolution satellite imaging and the inseparable in situ components.

Keywords*: vineyard; unmanned aerial vehicle; UAV; unmanned aircraft system; UAS; precision farming; agriculture; viticulture; multispectral; thermal; photogrammetry; vegetation index; Sentinel 2; remote sensing; earth observation*